DEVELOPMENT OF MULTI-LAYERED GRADIENT CERAMIC MEMBRANE

BY

MIRZA AQEEL BAIG

A Thesis Presented to the

DEANSHIP OF GRADUATE STUDIES

KING FAHD UNIVERSITY OF PETROLEUM & MINERALS

DHAHRAN, SAUDI ARABIA

In Partial Fulfillment of the
Requirements for the Degree of

MASTER OF SCIENCE

In

MECHANICAL ENGINEERING

APRIL 2011

KING FAHD UNIVERSITY OF PETROLEUM & MINERALS

DHAHRAN 31261, SAUDI ARABIA

DEANSHIP OF GRADUATE STUDIES

This thesis, written by Mirza Aqeel Baig under the direction of his thesis advisor and approved by his thesis committee, has been presented to and accepted by the Dean of Graduate Studies, in partial fulfillment of the requirements for the degree of **MASTER OF SCIENCE IN MECHANICAL ENGINEERING**.

Thesis Committee

Dr. Tahar Laoui (Advisor)

11/05/2011

Dr. Syed Fida Hassan (Member)

Dr. Khalid Al Hooshani (Member)

Dr. Amro M. Al- Qutub
Department Chairman

Dr. Salam A. Zummo
Dean of Graduate Studies

3/7/11

Date

Dedicated to

My beloved parents for their prayers, sacrifices, love,

encouragement and everything they did for me throughout my life.

ACKNOWLEDGEMENTS

First and above all, I praise Allah (S.W.T), the Almighty for providing me this opportunity and granting me the capability to proceed this work and successful completion of my M.S at King Fahd University of Petroleum and Minerals (KFUPM). I gratefully acknowledge KFUPM and Deanship for Scientific Research Collaboration with M.I.T for their financial support during my M.S.

Mechanical Engineering Department, Physics department, Chemistry department, Centre of Excellence in Nano Technology and Centre for Petroleum and Minerals are gratefully acknowledged for providing the facilities to carry out the experimental work.

I would like to express my deepest gratitude to my advisor Dr. Tahar Laoui, for his valuable time and also for giving me encouragement, guidance, support and inspiration throughout this research work. He is an outstanding advisor, mentor and friend. I would also like to thank Dr. Syed Fida Hassan for all the fruitful discussions, thoughtful advices and guidance. My sincere thanks to Dr. Khalid Al-Hooshani for his great support during the maximum part of my thesis work by giving me access to Chemistry labs as well as his warm encouragement in difficult times and I will never forget the early morning coffee from him during the research work in his lab.

Special thanks to Mr. Faheemuddin Patel for his friendly discussions, valuable advice and continuous support especially during the hard times of research work. Thank you Mr. Faheem for making my research atmosphere friendly and jolly. Thanks to Dr. Zuhair for

allowing me to work on SEM whenever required. Mr. Saleh and Lab Engr. Mr. Hashmi were very supportive during the SEM and XRD analysis. I would like to thank Dr. Oki and Fareed who were very helpful and supportive. Thanks to all KFUPM-MIT project team members Dr.Shakeel, Dr. Faiz-ur-Rehman and Dr. Muataz for their valuable help from time to time.

Thanks are also due to all the graduate students and faculty with whom I interacted during my Masters namely Dr. Mukhaimer who always encouraged me, Mr.Sarfaraz for his support time to time as well as Zabi, Awad, Abdullahi, Azhar, Mr. Murtuza, Najam, Rakhibul Hasan, Salman, Pervez, Riyaz, Mr. Rizwan Farooqui, Mr. Kareem and my unpredictable roommates Mr.Naser and Mr. Momin.

Last but not least, I would like to thank my parents for their unconditional support and duas throughout my life. In particular, the patience and understanding shown by my mum, dad, brother and sisters during my M.S is greatly appreciated.

TABLE OF CONTENTS

ACKNOWLEDGMENT ..... **iv**

LIST OF TABLES ..... **ix**

LIST OF FIGURES ..... **x**

THESIS ABSTRACT (ENGLISH) ..... **xv**

THESIS ABSTRACT (ARABIC) ..... **xvii**

CHAPTER 1 INTRODUCTION **1**

1.1 Distillation process 1

1.2 Membrane technology 2

1.3 Membranes 3

1.3.1 Membrane characteristics 4

1.4 Aim and objectives 5

CHAPTER 2 LITERATURE REVIEW **6**

2.1 Ceramic Membranes 6

2.2 Ceramic support 9

2.2.1 Pressing or Compaction method 10

2.2.2 Extrusion process 13

2.3 Intermediate layer 17

2.3.1 Sol-gel technique 17

2.3.2 Effect of hydrolysis ratio 19

2.3.3 Membrane layer deposition 21
2.3.4 Drying 23
2.3.5 Thermal treatment 23
2.3.6 Synthesis procedures for titania layer using Sol-gel technique 23

2.4 Top or Active layer 27
2.4.1 Zeolites 28
2.4.2 Hydrothermal synthesis 29
2.4.3 Microwave Synthesis 31
2.4.4 Microwave Synthesis of Zeolite Membranes 32
2.4.5 Linde Type A (LTA) Zeolite 33
2.4.6 LTA Zeolite Membrane 35

2.5 Characteristics 38
2.5.1 Scanning Electron Microscope 39
2.5.2 X-Ray Diffraction 40
2.5.3 Mercury Porosimetry 41

CHAPTER 3 EXPERIMENTAL PROCEDURE 43

3.1 Preparation of macro-porous ceramic support 43
3.1.1 Powder Compaction 43
3.1.2 Sintering 45
3.1.3 Porosimetry 45
3.1.4 Diametral Compression test 46

3.2 Preparation of mesoporous layer on macroporous support 47
3.2.1 Preparation of TiO_2 colloidal sol solution 47
3.2.2 Deposition of titania layer using manual dip-coating technique 48

3.2.3 Deposition of titania layer using automated dip coating method 49

3.3 Preparation of microporous layer on mesoporous TiO_2 layer..... 51

3.3.1 Synthesis of LTA zeolite membrane using multiple MH synthesis method 52

3.3.2 Synthesis of LTA zeolite using in-situ aging microwave heating synthesis 54

3.4 Characterization 56

CHAPTER 4 RESULTS AND DISCUSSION 57

4.1 Preparation of macro-porous support..... 57

4.1.1 As-received α-alumina powder..... 57

4.1.2 Powder compaction..... 59

4.1.3 Sintering of the compact 60

4.1.4 Strength test 63

4.2 Deposition of meso-porous TiO_2 layer 65

4.2.1 SEM analysis for manually and automated coated titania layer 65

4.2.2 X-Ray Diffraction results for mesoporous TiO_2 layer..... 70

4.3 Porosimetry measurements 71

4.4 Synthesis of micro-porous LTA Zeolite layer 74

4.4.1 SEM and XRD Analysis for multiple microwave synthesis..... 75

4.4.2 In-situ aging microwave heating synthesis 77

4.4.3 Effect of in-situ aging time 78

4.4.4 Effect of microwave heating synthesis time 83

CHAPTER 5 CONCLUSIONS AND FUTURE SCOPE..... 91

References ……93

Vita……..103

LIST OF TABLES

Table 2.1 LTA structure type..... 34

Table 3.1 Green densities of the compacts at different compaction pressures 44

LIST OF FIGURES

Figure 2.1 Schematic representation of a multilayer membrane consisting of grains, grain boundaries and pores [15]. 7

Figure 2.2 Range of nominal pore diameters for commercially available membranes [17]. 8

Figure 2.3 Uni-axial Press [8]. 10

Figure 2.4 SEM micrographs of particles of the α-Al_2O_3 powders [27]..... 11

Figure 2.5 SEM micrographs of α-Al_2O_3 ceramics sintered at (a) 1350, (b) 1400, (c) 1450°C for 4 h [27]. 12

Figure 2.6 Extrusion Process [8]..... 13

Figure 2.7 SEM micrograph of alumina support (a) Plate (b) tube after sintering at 1400°C for 2h [22]. 15

Figure 2.8 Comparison on the (a) flexural strength and (b) % porosity for F500, F600 and F2000 at different sintering temperatures [30]. 16

Figure 2.9 Sol-gel method [8]. 18

Figure 2.10 Dip coating [8]..... 22

Figure 2.11 FE-SEM cross-sections (20,000×) pictures of (a) titania and (b) mixed, colloidal sol–gel membrane layers on (a) α-Al_2O_3 and (b) RBAO support [44]. 24

Figure 2.12 Preparation steps of TiO_2 oxide powder. $Ti(OiPr)_4$: titanium isopropoxide = $Ti(OC_3H_7)_4$ [47]. 27

Figure 2.13 Hydrothermal zeolite synthesis. The starting materials (Si-O and Al-O bonds) are converted by an aqueous mineralizing medium (OH-and/or F-) into the crystalline product (Si-O-Al bonds) whose microporosity is defined by the crystal structure [58]... 30

Figure 2.14 (a) Sodalite cage and (b) LTA framework formed by linking sodalite cages through double four – rings[51]. 34

Figure 2.15 (a) Channel system and (b) cages in LTA [51]. 35

Figure 2.16 Comparison of synthesis model of zeolite membrane prepare by microwave heating and conventional heating [68]. 36

Figure 2.17 Schematic diagram for scanning electron microscope [73]. 40

Figure 2.18 Cumulative volume of mercury as a function of the applied pressure [8]. ... 42

Figure 3.1 Compaction steel die with upper and lower punch 43

Figure 3.2 Carver Auto pellet press 44

Figure 3.3 MTI high temperature furnace..... 45

Figure 3.4 Diametral test..... 46

Figure 3.5 Preparation steps of Colloidal TiO_2 sol solution 47

Figure 3.6 Flow diagram for manual dip coating process 49

Figure 3.7 Flow diagram for automated dip coating method..... 50

Figure 3.8 Teflon holder with fitted substrate placing in Teflon reactor vessel. 52

Figure 3.9 Microwave Oven (synthos 3000, Anton Paar) 53

Figure 3.10 Synthesis reactor vessel for Microwave oven 53

Figure 3.11 Autoclave reactor with Teflon tube and Teflon holder fitted with support coated with TiO_2 54

Figure 3.12 Schematic diagram for the fabrication of multi-layered membrane..... 55

Figure 4.1 SEM micrographs of as the received α - alumina powder taken at (a) low magnification, (b) higher magnification 58

Figure 4.2 XRD pattern of the as-received α-alumina powder..... 58

Figure 4.3 Green α-alumina compact pressed at 620 MPa..... 59

Figure 4.4 Variation of green density with applied compaction pressure 60

Figure 4.5 Sintered α-alumina substrate initially compacted at 620 MPa..... 61

Figure 4.6 XRD pattern of the sintered α-alumina substrate 61

Figure 4.7 SEM micrographs of the sintered α-alumina substrate at different magnification 62

Figure 4.8 Alumina substrates used for structural testing..... 63

Figure 4.9 Fractured sample after being subjected to diametral compression test 64

Figure 4.10 Diametral compression test curve 64

Figure 4.11 SEM images of TiO2 colloidal sol single coating on alumina substrate at different magnifications (a) × 25,000 (b) ×150,000. 65

Figure 4.12 SEM images of TiO_2 colloidal sol double coating on alumina substrate at different magnifications (a) × 22,000 (b) ×45,000. 67

Figure 4.13 SEM image of cross-section of triple coated titania layer on α-alumina substrate at two different magnification (a) × 4,300 (b) ×6,500. 67

Figure 4.14 SEM images of TiO_2 triple coating on Al_2O_3 substrate (dipping time 15min, heat treated at 500C, 1h), at magnification (a) × 550 (b) ×10,000 68

Figure 4.15 SEM image of triple coated TiO_2 film on glass substrate. 69

Figure 4.16 SEM images of TiO_2 double coated film on 316 stainless steel substrate at different magnifications (a, b, c, d). 69

Figure 4.17 XRD pattern of anatase- TiO_2 powder obtained by Sol-Gel method and heat treated at 450°C, 1h. 70

Figure 4.18 XRD patterns of anatase patterns of double (a) and triple (b) coated titania layer on α-alumina substrate 71

Figure 4.19 Mecruty Porosimeter 72

Figure 4.20 Pore size analysis and its distribution of alumina substrate 72

Figure 4.21 Pore size analysis and its distribution of TiO_2 coated alumina substrate 73

Figure 4.22 XRD patter for prepared LTA zeolites layer by Multiple MH synthesis method..... 75

Figure 4.23 SEM images of LTA zeolite membrane on mesoporous TiO_2 layer using multiple MH synthesis method at different magnification (a) ×1,800 (b) ×5,500..... 76

Figure 4.24 SEM image after 4hrs of in-situ aging on titania/Alumina substrate at different magnification..... 78

Figure 4.25 XRD pattern after 4hrs of in-situ aging on titania/Alumina substrate..... 79

Figure 4.26 (a,b) SEM images of the gel layer formed on the titania-alumina substrate after in-situ aging for 7hr at 50°C. 79

Figure 4.27 XRD patterns of the TiO_2 coated Al_2O_3 support after in-situ aging for 7hr in autoclave reactor at 50°C. 80

Figure 4.28 SEM image after 12hrs of in-situ aging on Titania/Alumina support surface at different magnification..... 81

Figure 4.29 XRD pattern after 12hrs of in-situ aging on Titania/Alumina support 81

Figure 4.30 SEM images of in-situ aging on TiO_2 coated Al_2O_3 substrate after(a) 4hrs, (b) 7hrs, and (c) 12hrs of aging time. 82

Figure 4.31 SEM images of the as-synthesized membranes prepared by in-situ aging method, 7hr at 50°C 83

Figure 4.32 SEM images of LTA zeolite layer formed at different synthesis time using in-situ MH synthesis. (a) 5min (b) 10min synthesis time 84

Figure 4.33 XRD images of LTA zeolite layer formed using in-situ aging (for 7hr at 50°C) and 10min of MH synthesis time. 85

Figure 4.34 XRD patterns of in-situ aging MH synthesized (at 90°C for 15min) layer of LTA zeolite on titania coated alumina substrate..... 86

Figure 4.35 (a&b) SEM images of the continuous and dense layer of LTA zeolite membrane synthesized at 90°C for 15min using in-situ aging MH synthesis method at different magnification..... 87

Figure 4.36 SEM image of LTA zeolite layer formed by using in-situ aging MH synthesis at 90°C for 15 min synthesis time [67]. 87

Figure 4.37 SEM images of cross-section of LTA zeolite membrane synthesized at 90°C for 15min using in-situ aging MH synthesis method at different magnification. 88

Figure 4.38 Pore size analysis and its distribution of LTA zeolite layer on titania coated alumina substrate. 89

Figure 4.39 Pore size analysis and porosity of multilayer membrane overlapped. 89

THESIS ABSTRACT (ENGLISH)

NAME: MIRZA AQEEL BAIG

TITLE: DEVELOPMENT OF MULTI-LAYERED GRADIENT CERAMIC MEMBRANE

MAJOR: MECHANICAL ENGINEERING

DATE: APRIL 2011

Ceramic membranes are the permselective barriers usually made from ceramic materials such as Al2O3, TiO2, ZrO2, SiO2 and zeolites. Layer thickness, pore size and amount of porosity are the key elements that govern the fabrication of ceramic membranes. The aim of this research is to explore the development of ceramic based multilayer membrane of porous structure with gradient porosity for potential filtration and purification applications. Disc shaped macro-porous alumina support was fabricated by powder metallurgy technique with α-alumina particle size of 0.3 μm and compacting pressure of 620 MPa followed by sintering at 1400°C for 2h. An average pore size of 0.25 μm with 50% porosity and thickness of 2mm were obtained as determined by scanning electron microscopy and mercury porosimetry technique. Further research was carried out for the preparation of meso- and micro-porous layers which were deposited on top of the macro-porous α-alumina support. The intermediate meso-porous TiO2 layer was deposited on top of α-Al2O3 support using sol-gel dip coating technique followed by drying and heat treatment. The average pore size obtained was approximately 0.08μm with porosity of 30% and thickness of approximately 1 μm.

The micro-porous zeolite A (LTA) layer was synthesized on the deposited meso-porous TiO2 layer, after being subjected to UV irradiation. The intermediate meso-porous layer of titania was applied to bridge the pore size gap between the α-alumina support and micro-porous LTA zeolite layer (possessing sub-nanometer pore size), thus forming a multi-layered ceramic membrane with a porosity gradient. The pre-treatment of meso-porous titania layer with UV photons played a major role to improve the surface hydrophilicity of the substrate. In-situ aging microwave heating synthesis method was utilized to synthesize LTA zeolite layer. During the synthesis, the effect of such

parameters, like in-situ aging time and synthesis time, on the formation of LTA zeolite layer was investigated. Crystals of 1-3 µm were grown on the substrate surface yielding a continuous and dense layer of LTA zeolite. The measured thickness of the formed zeolite layer was 2-3 µm.

The developed multilayer membrane with graded (macro-, meso- and micro) porous structure will have the potential to allow selective passage of a particular species (solvents such as water molecules), while other species i.e, solutes (such as heavy metals, hydrated ions) are retained partially or completely during filtration/purification/desalination process. The next phase of this project is to evaluate the filtration performance of these developed membranes using dedicated flow test cell.

MASTER OF SCIENCE DEGREE
KING FAHD UNIVERSITY OF PETROLEUM & MINERALS
Dhahran, Saudi Arabia

THESIS ABSTRACT (ARABIC)

الاسم: **ميرزا عقيل بيك**

العنوان: **تطوير الأغشية السيراميكية متعددة الطبقات**

التخصص: **الهندسة الميكانيكية**

التاريخ: **أبريل 2011**

تستعمل الأغشية السراميكية كعوائق للمرور الأجسام غير المرغوبة في عملية التحلية وتنقية الموائع وغالبا ماتصنع هذه الأغشية من مواد مثل: Al_2O_3, TiO_2, ZrO_2, SiO_2 and zeolites وتشكل كلا من سماكة الطبقة وحجم المسامات ونسبة المسامية أهمية كبرى في تصنيع وتحسين الأغسية السيراميكية. الهدف من هذا البحث هو إكتشاف وتطوير الأغشية السيراميكية المنفذة متعددة الطبقات والمسامية من أجل تطبيقات التنقية. من خلال إستخدام تقنية *powder metallurgy* تم تصنيع الطبقة الأساسية من حبيبات مادة الألومينا على شكل أقراص بحجم 0.3 مايكرومتر وبضغط 620 ميجا باسكال ثم تم تسخينها إلى 1400 درجة مئوية لساعتين. بإستخدام جهاز *scanning electron microscopy* وتقنية *mercury porosimetry technique* تم تحديد متوسط حجم المسام في الطبقة وهو مايقارب 0.25 مايكرومتر وتشكل المسامية 50% من الطبقة بسماكة قدرها 2 ميلليمتر. بعد ذلك تم تصنيع الطبقة الثانية من خلال ترسيب حبيبات TiO_2 على سطح الطبقة الأساسية من خلال إستخدام تقنية واعدة وهي تقنية *sol-gel dip coating* وبعد تدراسة وإختبار السطح 30% من السطح تشكل نسبة المسامية وحجم المسامات 0.08 مايكرومتروسماكة 1 مايكرومتر تقريبا تشكل طبقة *zeolite A (LTA)* اخر طبقة في هذا البحث وتم تصنيعها من خلال تقنية نمو حبيبات الزيولايت على سطح الطبقة التي قبلها ومن أجل تحسين عملية الترسيب والنمو تمت عملية تحسين وتهيئة السطح لتكون مستوية ومقدار الترابط والتلاصق بين الطبقتين أقوى وأفضل.حجم الكريستال يقع في المدى بين1-3 مايكرومتر وكذلك سمك الطبقة يقع بين 2-3 مايكرومتر. تطوير ودراسة هذه الأغشية السيراميكية متعددة الطبقات والمسامات لديها المستقبل الواعد في فلترة وتنقية الموائع. الخطوة الثانية في هذا المشروع سيهتم بالتقييم المختبري لأداء هذه الأغشية.

درجة الماجستير في العلوم

جامعة الملك فهد للبترول و المعادن

الظهران المملكة العربية السعودية

CHAPTER 1 INTRODUCTION

The increase in growing world population has necessitated the use of desalination to meet their needs for fresh water resources. More than one billion people are without clean drinking water and approximately 2.3 billion people (41% of world population) lives in regions with water shortages [1]. Conventional fresh water resources such as lakes, rivers, and groundwater are misused; as a result, these resources are either diminishing or becoming saline. Therefore solution such as water reuse and salt water desalination has emerged as the keys to supporting future generations across the globe. Desalination in general is a process of removing salt from water to produce fresh water. Desalination has become an important source of drinking water production, with thermal desalination processes developing over the past 60 years and membrane processes developing over past 40 years [2].

The two basic categories of water purification technologies that are used for desalination: Distillation process (Thermal Technologies) and Membrane Technologies.

1.1 Distillation process

Distillation is the technique in which distilled water is heated to the boiling point (100 degrees Centigrade) and converted to steam. The steam obtained is then cooled and condensed back into liquid form to get pure water. Distillation kills biological contaminants such as bacteria, parasites, and viruses, and removes organic and inorganic

chemicals, heavy metals, volatile gases, and other contaminants. Distillation does not remove substances that have boiling points at a lower temperature than water [3].

Thermal distillation process has been used for hundreds of years to produce fresh water, but large-scale municipal drinking water distillation plants began to operate during the 1950s. Middle East countries has pioneered the design and implementation of seawater thermal desalination by using the first process called multi-effect distillation (MED) and later using a process called multi-stage flash (MSF) distillation. Today, the Middle East collectively holds 50% of the world's desalination capacity and primarily uses MSF technology. While thermal desalination has remained the primary technology of choice in the Middle East, membrane processes have rapidly developed since the 1960s and now surpass thermal processes in new plant installations. Outside of the Middle East, new RO desalination installations have been steadily increasing; in 2001, 51% of new installed desalination capacity used RO desalination, and in 2003, RO desalination accounted for 75% of new production capacity [4].

1.2 Membrane technology

Membrane technologies are the most common technology of desalination in which membranes are made from wide variety of materials such as polymeric materials that include cellulose, acetate and nylon and non polymeric materials such as ceramics, metals and composites. Polymeric membranes are dominating in the membrane market and the ceramic membranes are used mainly in special cases where polymeric cannot be used. Major problems associated with polymeric RO/NF membranes are: (1) excessive fouling due to poor feed flow hydrodynamics; (2) low resistance to chlorine and other oxidants;

(3) extensive pretreatment/chemical usage and associated waste generation and (4) lack of desirable surface charge to reduce fouling potential [5]. Development of alternative nano-structured ceramic membranes represents a novel technology area with possibilities to offer high permeates flux, high salt rejection and improved biofouling. Ceramic membranes are especially suitable for processes with high temperatures and harsh chemical environments or for processes were sterilizability of the membrane is important. Because of this, the ceramic membranes have found many applications in the food, beverage, biotechnological and pharmaceutical industries as well as in the petrochemical industry, environmental control, electronic industry, gas separation and other process industries.

1.3 Membranes

A membrane is a thin film of porous material that allows water molecules to pass through it, but simultaneously prevents the passage of larger and undesirable molecules such as viruses, bacteria, metals, and salts [1]. The most important function of a membrane is to act as a selective barrier, allowing the passage of certain components and the retention of others from a determined mixture, implying the concentration of one or more components both in the permeate and in the retentate. The selectivity of membrane is related to the dimensions of the molecule or particle of interest for separation and the pore size [6]. The performance of a membrane in separation is influenced by its chemical composition, temperature, pressure, feed flow and interactions between components in the feed flow and the membrane surface [7].

1.3.1 Membrane characteristics

The separation performance of ceramic membranes is directly associated with the overall membrane morphology. Information about the pore size, shape, density, distribution and membrane surface properties for porous ceramic membranes and gas tightness, crystal structures and permeation characteristics of specific gases for dense ceramic membranes are therefore of importance to both membrane manufacturers and users, so as to allow a meaningful prediction of separation performances of the membranes [8]. Membranes are classified on the basis of their structure as symmetrical or asymmetrical. An asymmetric membrane has larger pore size whereas symmetric has uniform pore size in cross-section [6]. Defect-free surface layers with narrow pore size distributions as well as required porosity of support and supporting layers are the desirable properties of ceramic membranes. The most important characteristics of membranes that govern the fabrication of membranes are: thickness, pore diameter, solvent permeability and porosity. Other important parameters for membrane characteristics are: permeate flow rate, heat, chemical and mechanical resistance [9].

1.4 Aim and objectives

The aim of this project is:

- To develop ceramic based multilayer membrane (Al_2O_3, TiO_2 and LTA zeolite) of porous structure with gradient porosity to allow selective passage of particular species for potential filtration and water purification.

To achieve the above aim, it is proposed:

- To fabricate macro-porous α-alumina support using powder compaction and sintering.
- To deposit meso-porous TiO_2 layers on macro-porous support using sol-gel dip coating technique followed by drying and heat treatment.
- To synthesize micro-porous LTA zeolite layer using in-situ aging MH synthesis method on the top of mesoporous TiO_2 layer coated alumina substrate.
- To study the effect of in-situ aging time and MH synthesis time on the formation of microporous LTA zeolite layer.
- To characterize the surface morphology, phases, crystallinity, pore size, porosity and strength of the membrane using SEM, XRD, EDS, mercury porosimetry and diametral compression test method.

CHAPTER 2 LITERATURE REVIEW

2.1 Ceramic Membranes

Ceramic or inorganic membrane refers to a supported porous multi-layer system made from inorganic materials such as metals, ceramics, glasses and inorganic polymers. Ceramic membrane is the membrane made by ceramic material [10]. Because of many advantageous characteristics such as high chemical, mechanical and thermal stability and microbial degradation resistance, due to these properties ceramic membranes are used in more harsh environments than polymeric membranes. Therefore, ceramic membranes are expected to replace the organic membranes which are still used mostly in current industrial separation and purification processing [11].

Ceramic membranes have found many applications for separation and catalysis in the field of food processing [9], beverage, biotechnological [12] and pharmaceutical industries as well as in the petrochemical industry [13], environmental control, electronic industry and other process industries. This application depends on membrane pore structure and chemical features. In filtration for example pore size determines which level of separation can be achieved [14]. In order to combine a high permeability with the wanted selectivity, all commercially available porous ceramic membranes, and most of the laboratory-made membranes, are asymmetric. Therefore the support consists of a very open pore structure, and on top of the support one or more thin layers with smaller pores are deposited. The top layer or actual separation layer contains the smallest pores and

defines the real selectivity of the porous membrane. The support of the membrane is used to enhance the mechanical strength. The intermediate layers are used to gradually decrease the pore size and the surface roughness of the membrane [15]. A schematic picture of the multilayer membrane with grains, grain boundaries and pores is shown in Figure 2.1. In membrane desalination, water is transported across a membrane, while salts are almost completely retained. In addition to the dissolved ions found in seawater, the seawater includes a wide variety of fine suspended matter that include sand, clay, microorganisms, viruses, and colloidal matter. The size of these compounds varies over a range of $5x10^{-2}$ to 0.15 μm [16].

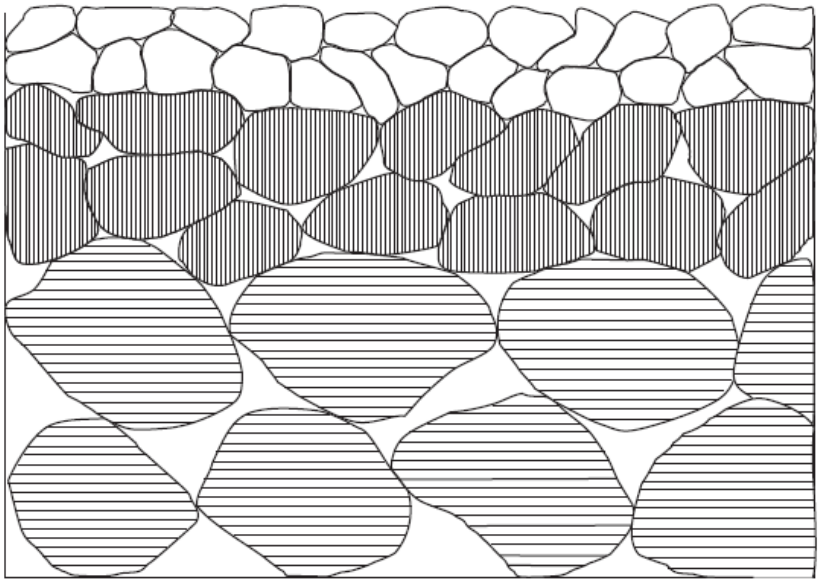

Figure 2.1 Schematic representation of a multilayer membrane consisting of grains, grain boundaries and pores [15].

In the context of filtration, reverse osmosis (RO) and nanofiltration (NF) processes allow selective passage of a particular species (solvent), while other membranes, including ultrafiltration (UF), and microfiltration (MF), are designed to remove materials of

increasing size, as indicated in Figure 2.2. The macro and micro filtration for removal of sand, pollens, particles and bacteria requires 100-1000nm pores. Ultrafiltration which tends to separate micro-molecules, viruses and large proteins in solution requires a pore size 10-100 nm. Nanofiltration and reverse osmosis capable of separating solvents or desalting sea water which requires a pore size smaller than 1 nm [17]. The RO and NF processes are being recognized as key technologies to address the global challenges with the scarcity of clean water.

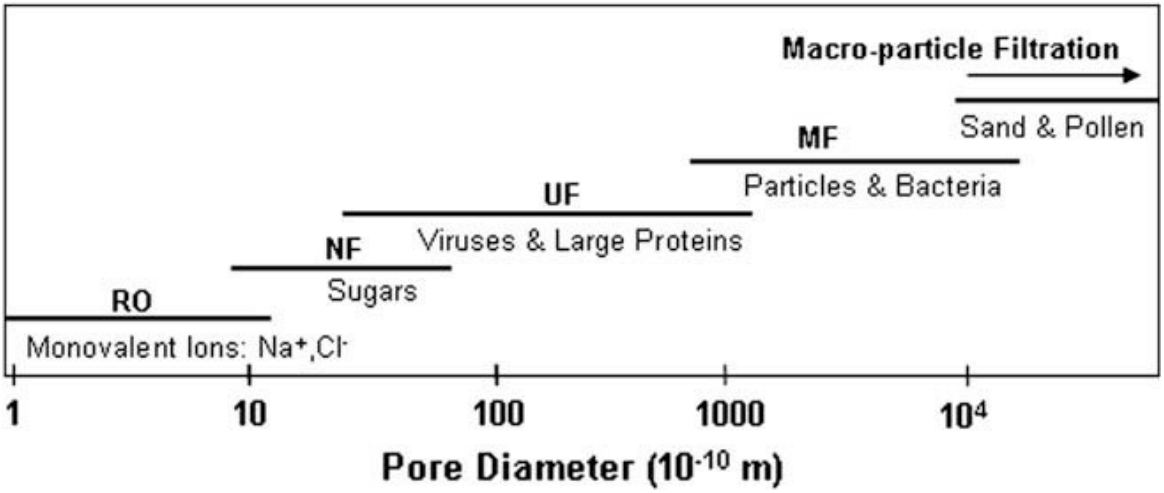

Figure 2.2 Range of nominal pore diameters for commercially available membranes [17].

Typically, asymmetric porous ceramic membranes are used with a support thickness of about 1- 3 mm. The most common oxides used for membranes are alumina (Al_2O_3) and zirconia (ZrO_2) for microfiltration layer which are 10-30μm thick. Ultrafiltration membranes are a few micrometers thick and typical materials are alumina (Al_2O_3), zirconia (ZrO_2), titania (TiO_2) and ceria (CeO_2). Nanofiltration membranes are less than 1μm thick, generally made of zirconia, titania and zeolites [18].

Membrane supports are mainly produced by slip casting, tape casting, extrusion and pressing. The main method for the preparation of metal oxide intermediate and top layers is the sol–gel technique [19]. Mesoporous intermediate layers are made by colloidal sol gel process whereas microporous top layers by polymeric sol gel process. These sols are prepared either from metal salts or from metal organic precursors [20]. The layers are deposited on the supports or on the previous multilayer structure by dip coating or spin coating. The porosity of the supports or the structure of multilayer prepared earlier leads to the gelling of the sols on that surface. The formed gel layers are further dried and heat treated to form the final membrane layers. This thermal treatment process is called calcination or sintering [21]. The purpose of heat treatment is to stabilize the crystallographic and morphological structure of the dried layer.

2.2 Ceramic support

Ceramic support need to have certain characteristics to allow thin membrane layers on top of it. They should have high porosity for high permeability, good mechanical strength in order not to get cracks or breakage during handling and installing, smooth surface to allow other layers on top of it [22]. Porosity, flexural strength and pore sizes of the supports strongly depend on the particle sizes of the raw materials as well as on the sintering temperatures of the supports. The particle sizes of the powder determine the pore sizes of the support whereas the sintering temperatures strongly affect porosity and flexural strength of the supports [23].Currently, most of the ceramic supports are made from alumina powder, due to its high mechanical strength and it can be formed into very

porous structure. For the fabrication of ceramic support the most commonly used processes are compaction and extrusion [24].

2.2.1 Pressing or Compaction method

Compaction is the most common method for preparing the compacted support. In this the powders are pressed into required shapes using dies and presses that are either hydraulically or mechanically actuated. This compaction is done in order to get required shape, density, and particle to particle contact and to make the part sufficiently strong to be handled and processed further [25]. This pressing is done in two ways either by

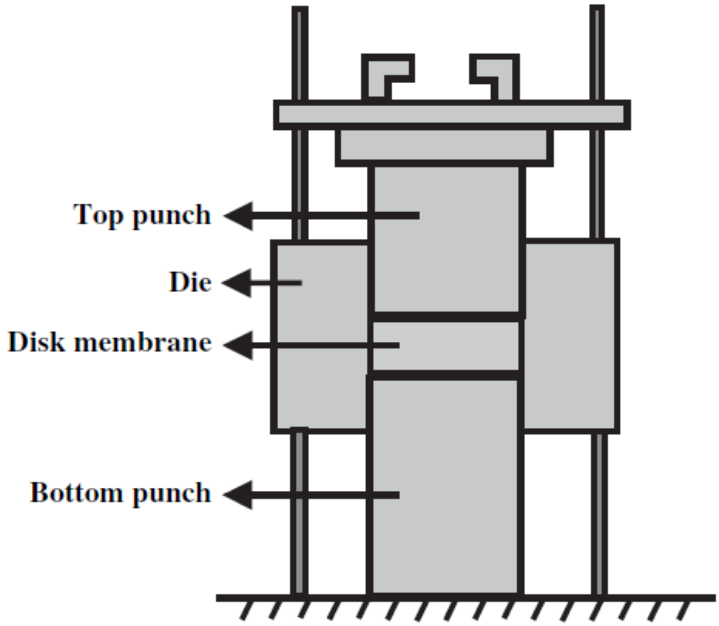

Figure 2.3 Uni-axial Press [8].

uniaxial Pressing (Figure 2.3) or by hot isostatic pressing. The as-pressed powder is known as green compact. The density after compaction depends on the compaction pressure, powder composition and hardness of the powder. Prior to sintering, the compact

is brittle and its strength, known as green strength is low [26]. After sintering the compacts become strong and with better mechanical properties. Cheng-Liang Huang et al used this compaction method to prepare the alpha alumina support and to know its microstructure and microwave dielectric properties by studying the effect of sintering temperature. The particle size of alpha alumina powder used was of 0.14 μm (Figure 2.4). The relative density of the green sample reached 53% at a pressing pressure of 400MPa. These pellets were then sintered at temperatures from 1350 to 1550°C for 4h in air [27].

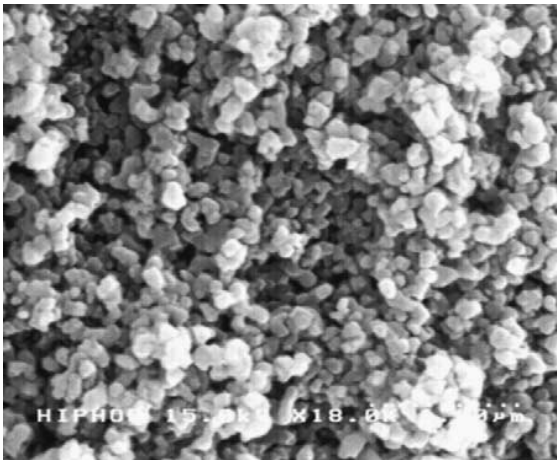

Figure 2.4 SEM micrographs of particles of the α-Al_2O_3 powders [27]

At different sintering temperatures XRD patterns were recorded and no second phase was observed. The as sintered surfaces were porous and the samples exhibited small grain size when sintered at 1350°C (Figure 2.5a). With the increase in sintering temperature the number of pores decreased and the rate of grain growth decreased. The pores were almost eliminated at 1450°C (Figure 2.5c). Therefore the author concluded from the result that a low relative density of 88.28% was obtained at 1350°C due to the porous specimen. However, the relative density increased and started to saturate at 1450°C (relative density= 97.58%) with increasing sintering temperature[27].

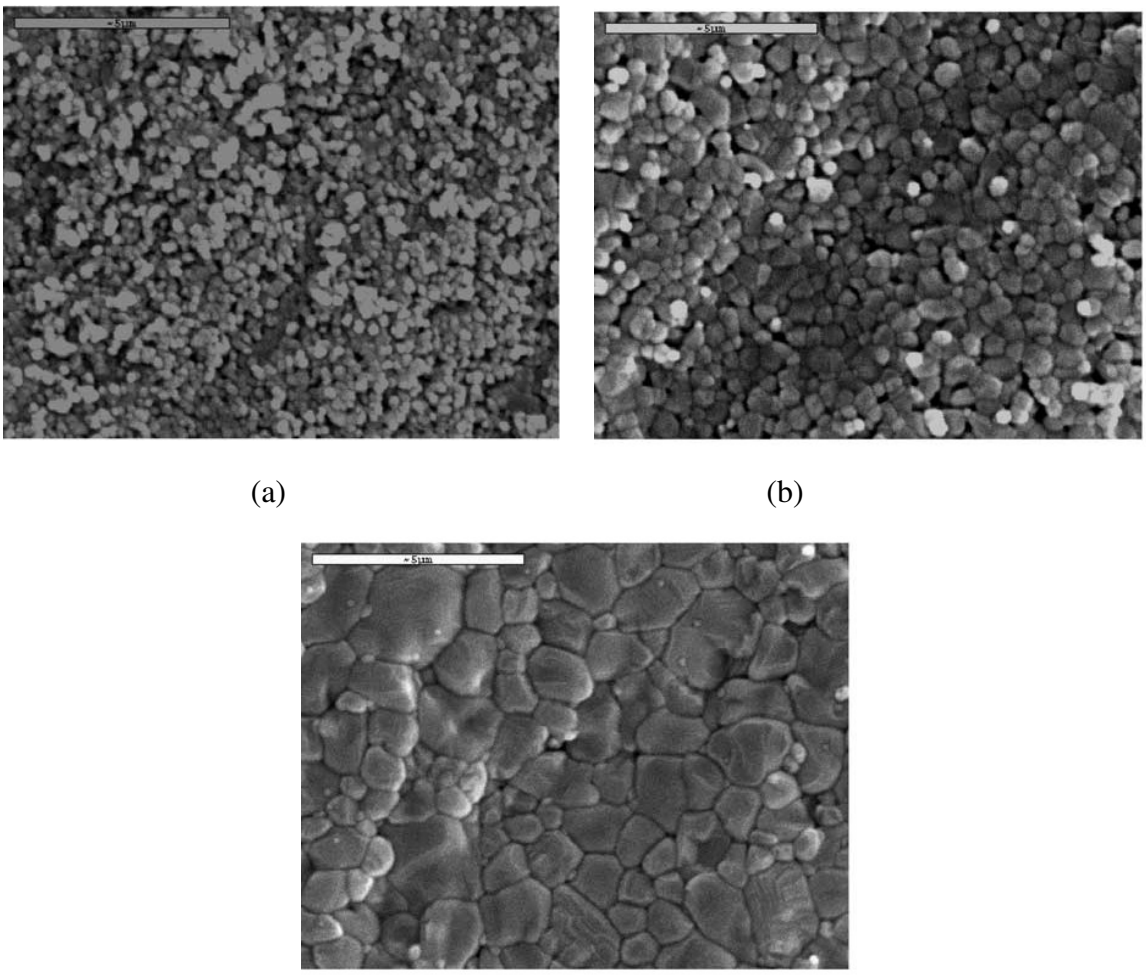

(a) (b)

(c)

Figure 2.5 SEM micrographs of α-Al_2O_3 ceramics sintered at (a) 1350, (b) 1400, (c) 1450°C for 4 h [27].

Zhijian Huanga et al, also used compaction method to study the property of sinterability of ceramics using hybrid microwave heating. High purity alumina powder with a particle size of 1μm with MgO–Al_2O_3–SiO_2 system sintering additives, which consist of 21.5 wt.% MgO, 61 wt.% SiO_2, and 17.5 wt.% Al_2O_3, were employed to control the microstructure and decrease the sintering temperature. Al_2O_3 powder and sintering additives were mixed with organic binder, and consolidated by uni-axial pressing into disks (35mm diameter×15mm thickness) at 130MPa. The prepared green compacts had a

density of approximately 60%. At sintering temperature of 700°C the pore size obtained was about 4 µm [28]. Ali Alem et al studied on the multilayer titania membranes which has the alumina support. The alumina support was prepared by using the compaction method. For the preparation of support, Al_2O_3 granulate powder was shaped into a disk of 15mm in diameter and 2mm in thickness using a uni-axial press. The alumina disks were pressed by applying a pressure of 31 MPa. The sintering process was then performed at 1350°C for 1 h in order to get good bonding and mechanical strength such that other layers can be applied on it. [29].

2.2.2 Extrusion process

Extrusion process is another technique to fabricate the support structure is a very productive forming technique that is used for both large products ranging up to 1 ton and small products weighing only a few grams [8]. In extrusion, a stiff paste is compacted and shaped by forcing it through a nozzle as shown in Figure 2.6.

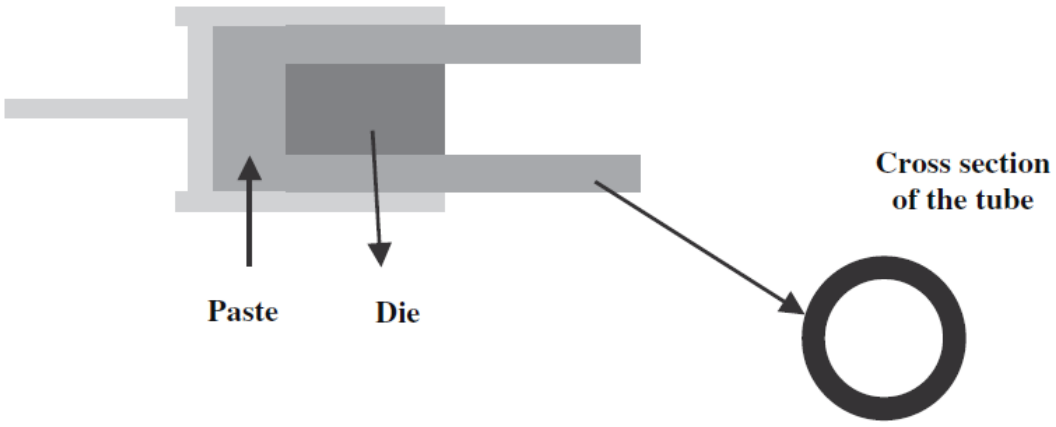

Figure 2.6 Extrusion Process [8]

A requirement is that the precursor should exhibit plastic behaviour, that is at lower stresses behave like a rigid solid and deform only when the stress reaches a certain value called the yield stress. A.Kritikaki et al used extrusion process to fabricate porous alumina substrates which were processed by employing a commercial alpha-alumina powder of an average particle size of 5 μm with a specific surface area of 1 m^2/g. The powder was mixed with 1 wt.% of surfactant, 6wt% of binder propyl-methoxy cellulose and deionized water (20%) in a shear mixer and was extruded in rod of 1cm diameter using a piston extruder. The green rods were dried at 110°C and sintered either at 1500°C or at 1600°C for 2h with a heating rate of 3°C /min [19]. Another author Khanthima Hemra et al fabricated the alumina support by using extrusion process. Alumina powder (AL-45) was mixed with an organic binder and water to achieve the possible homogeneity and consistency, and then homogenized in a high speed mixture and subjected to a triple roller mill for shear condition, in order to obtain the homogeneous alumina dough.

To completely dissolve organic binder into water, the alumina dough were wrapped in plastic bag and stored under temperature below 10°C and then kept in extruder to extrude the alumina support in the form of tubes. The extruded support samples were dried at room temperature and then heated at 3°C/min to 500°C and held at this temperature for 2h before raising the temperature to 1400°C for 2h at same heating rate. The apparent density and porosity of alumina supports were measured by water immersion technique while the microstructure by SEM [22].

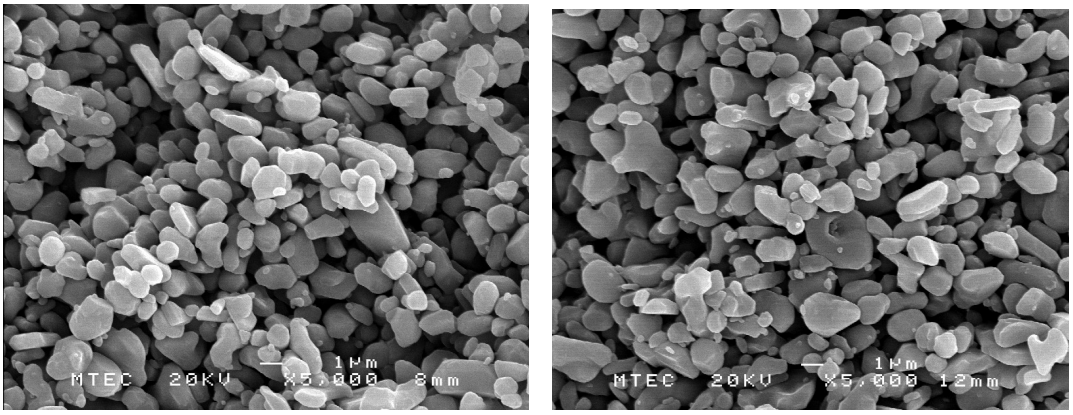

(a) (b)

Figure 2.7 SEM micrograph of alumina support (a) Plate (b) tube after sintering at 1400°C for 2h [22].

From the SEM images shown in Figure 2.7 for both plate and tube, and by using mercury porosimetry the author concluded that the alumina support prepared consisted of large pore to provide the permeability for using as a membrane. The author found that the pore size obtained was 0.4 μm with a density of 2.4 g/cm^3 and porosity of 40 %.

Zarina Abdul Wahid et al studied on the performance of ceramic supports and the process used for fabricating was extrusion. Fused alpha alumina powders of three different sizes were used 20 μm (F500), 10 μm (F600), 1 μm (F2000). Binders such as sodium carbonyl methyl cellulose were used to bind the alumina particles together by organic bonds and to give good strength after shaping and drying. Bentonite clay was used as additive to give plasticity to alumina body so that it can be easily shaped into tubular form. The sintering temperature for the alumina supports were in the range of 1100 to 1500°C. Characterization was done using Bubble Point test for Porosity and pore size, Universal Testing Machine for flexural strength and SEM for Microstructure [30].

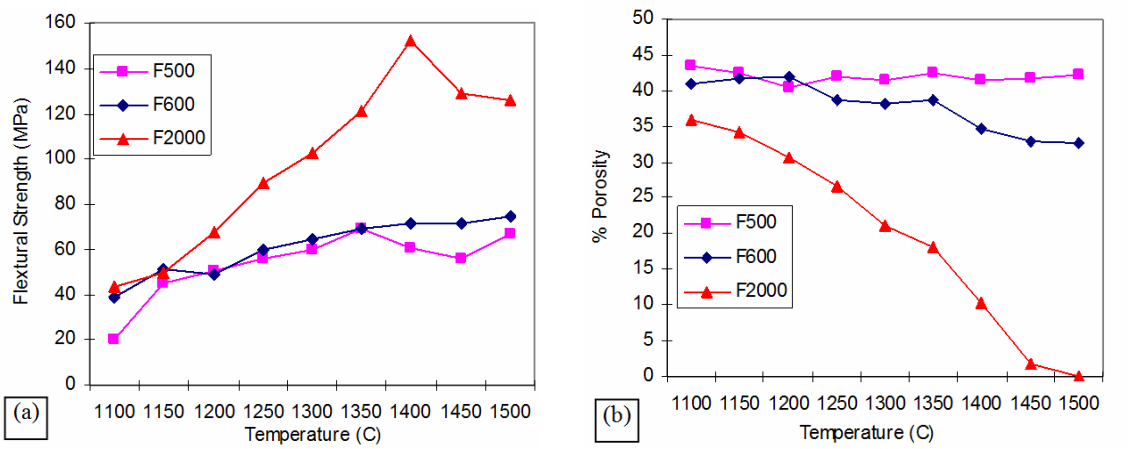

Figure 2.8 Comparison on the (a) flexural strength and (b) % porosity for F500, F600 and F2000 at different sintering temperatures [30].

Figures 2.8(a) and (b) demonstrate the flexural strength and percent porosity for all the samples respectively. F2000 shows increasing sintering temperatures, resulted in tremendous increase in strength and decrease in porosity. F500 and F600 indicated a slight increase in strength and a slight decrease in porosity. In fact, F600 exhibited very small differences compared to F500. This shows that tubes with smaller particle sizes exhibit drastic changes in strength and porosity with increasing temperatures than larger particle size tubes.

Results obtained for alumina support with particle size of F500 (20µm) was 6 µm pore size with 40-50% porosity (sintering temp-1350°C) and flexural Strength of 60 – 70 MPa. For the particle size of F600 (10µm) pore size obtained was 3.5µm with a porosity of 30-50% (sintering temp-1300°C) and for particle size of F2000 (1µm) pore size obtained was <1 µm and porosity of 30-50% (Sintering temp-1200°C). From the results it has been concluded that smaller particle size need lower optimum sintering temperature

compared to larger one and increase in sintering temperature resulted in increasing flexural strength but decrease in porosity.

2.3 Intermediate layer

The mesoporous intermediate layer was synthesized by using sol-gel process, which includes the preparation of sol solution, deposition of layer, drying and heat treatment. The preparation of sol solution is mainly depends on sol-gel chemistry of transition metal alkoxide precursors, controlled hydrolysis and condensation reactions during sol preparation by optimization of synthesis parameters.

2.3.1 Sol-gel technique

Sol-gel is a chemical process that converts colloidal or polymeric sol solution to a gelatinous substance as shown in a Figure 2.9 a schematic diagram of sol to gel in both the routes. [31]. Sol gel process is most commonly used for layer formation for different materials. The sol-gel method was first applied for development of ceramic ultrafiltration membranes by Leenaars et al. [32]. It extensively studied and has a great interest because of its simplicity and application for layer formation with improved properties such as synthesis of glasses, ceramics and glass ceramic materials with high purity, homogeneity and controlled microstructure. However for the preparation of membrane it includes sol preparation, deposition of layer, drying and heat treatment. This sol-gel process was most widely used in the preparation of silica membranes [33]. Sol-gel process consists of two different routes for the membrane layer preparation, colloidal or particulate route and the other is polymeric route as shown in Figure 2.9. The colloidal route is made by

dispersing small particles in an aqueous medium where it is prevented from agglomeration by repulsion of similar charges at the surface of particle. In this metal alkoxide precursor is mixed with water to form a sol and then this sol is coated on a membrane support, where it forms a colloidal gel. In the second route i.e, the polymeric route is formed by polymerizing the molecular species in a homogenous solution [34]. In this process metal organic precursors are reacted with alcoholic media where the polymeric particles separated because of their small size. The sol prepared using polymeric route is mainly controlled by hydrolysis and condensation of metal alkoxide in non-aqueous solvents [35].

Overall in both the routes of colloidal and polymeric, stable sols are formed by controlling the hydrolysis and condensation rate which has the great effect on sol preparation.

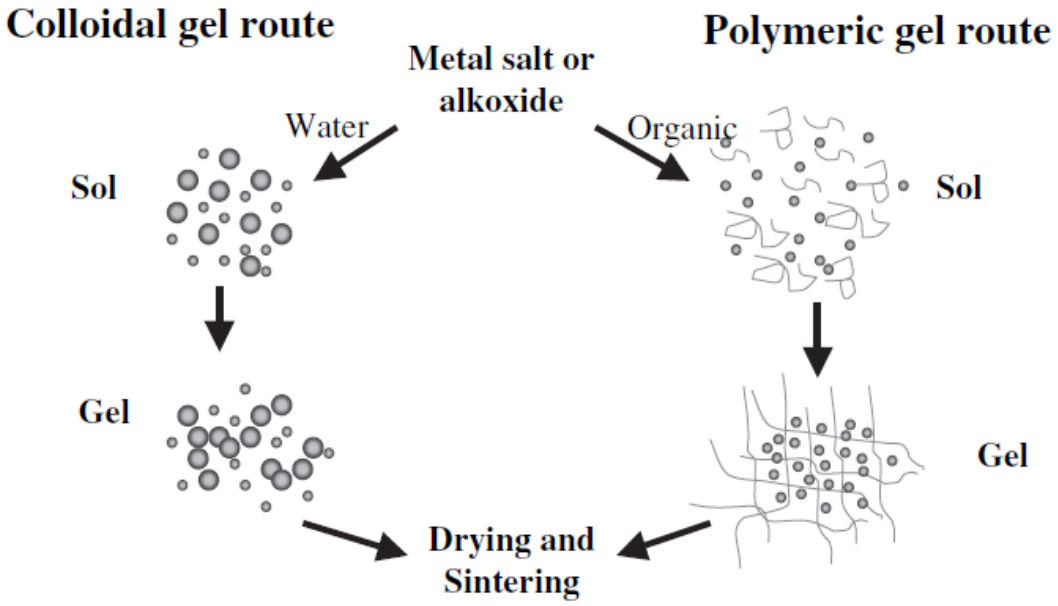

Figure 2.9 Sol-gel method [8].

The sol-gel chemistry of metal alkoxide is based on inorganic polymerization. Hydrolysis and condensation reactions of metal alkoxide precursors in an organic solvent which leads to the formation of metal-oxo-based macromolecular network. He precursors which are usually used for metallo-organic compounds are $M(OR)_n$ – (M=Si, Ti, Zr, Al) [36].

The overall hydrolysis and condensation reactions as reported by sekulic et al can be written as:

Hydrolysis: M-OR + H_2O → M-OH + R-OH.

Condensation: M-OH + M-OX → M-O-M +X-OH (Oxolation)

M-OH + M-XOH → M-OH-M + X-OH (olation) Where X=H, or X=R)

In the hydrolysis reaction alkoxide groups are replaced with hydroxyl groups. Whereas in the condensation reaction, there is formation of OH bridges via olation and oxygen bridge formation via oxolation [36].

2.3.2 Effect of hydrolysis ratio

The hydrolysis ratio is one of the important parameter in preparation of stable sol solution. The hydrolysis ratio is defined as the ratio of molar concentration of water and metal alkoxide (for our case Ti) [37].

$$r_w = \frac{[H_2O]}{[Ti]}$$ Where Metal Alkoxide = Ti, Al, Zr…..

Sekulic et al defined two major factors in the case of titania alkoxide hydrolysis, based on the stoechiometrically needed number of molecules of water per molecule of titania for complete hydrolysis [36].

i.e, if $r_w <= 4$,

For this case if rw vale is less than or equals to 4 which satisfy the condition to process of polymeric sol-gel in which network of partially hydrolysed and polycondensed oligomers diluted in the solvent are formed.

Whereas, if $r_w > 4$,

In this condition if r_w is greater than 4 which results in the formation of cross-linked polymers i.e, particulate sols are formed. In this case excess water is used for colloidal sol preparation.

The chemical reaction during the hydrolysis and condensation of titanium(IV) iso-propoxide is given below:

(A)

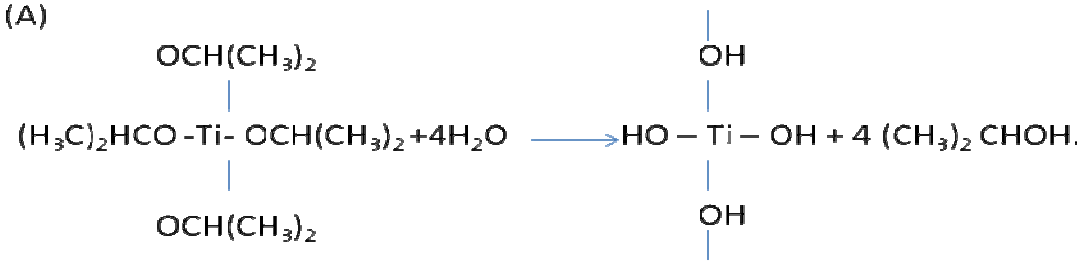

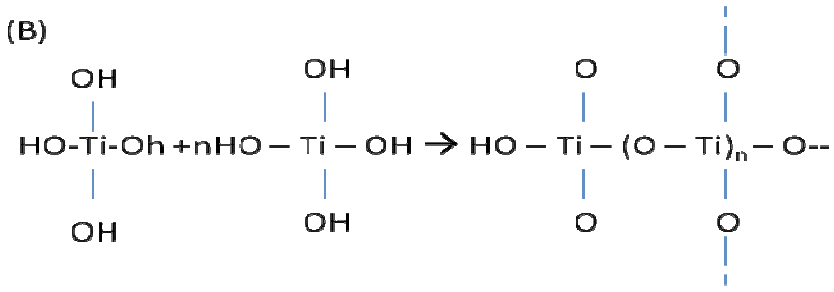

2.3.3 Membrane layer deposition

Once the required stable sol is prepared by controlled process, the remaining steps include deposition of layer, drying and calcination. For the layer deposition or coating, different techniques are used like dip coating, spin coating, slip casting and spraying.

Dip-coating technique is a very simple technique which involves dipping a substrate into the prepared sol-solution for required time and then withdrawn it at a specific coating speed or time [38, 39, and 40]. The film coating mechanism generally occurs when the dipping time is short and the viscosity of suspension is high. This is because adhering dispersion layer is retained as a result of drag force exerted by substrate during withdrawal from dispersion. Figure 2.10 gives the schematic diagram of dip coating technique.

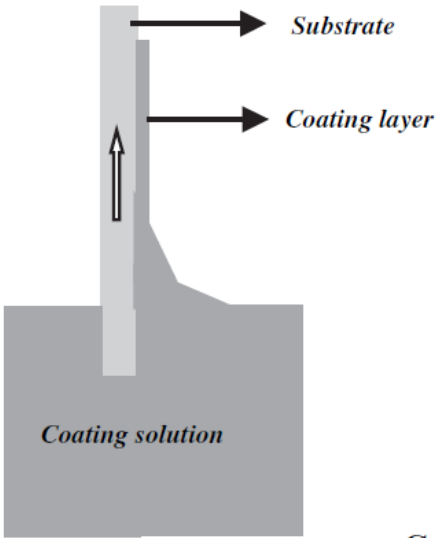

Figure 2.10 Dip coating [8]

The thickness of the layer of liquid on a vertical moving wall is proportional to speed of withdrawal and viscoity of suspension [34]. The spraying technique is used to spray the sol-solution through the spray guns while the substrate moves at a desired speed. In this technique it is difficult to get a uniform and homogeneous coating [34].

Whereas, spinning or spin coating technique in which the substrate rotates and the liquid sol is spread uniformlyby pouring the solution. The factors like spinning rate, viscosity of sol, the thinner film formed. The mechanism by which the layer is formed on the susbtarte is that there is a cappillary force that drives the dispersion medium through support. In the current study dip coating technique was used to deposit the mesoporous titania layer uniformily [41].

2.3.4 Drying

After the application of layer, then comes the drying process. It is one of the most important factors because in this step large stresses develop due to capillary force of pore liquid that cannot be relaxed by shrinkage because of existence of rigid support [36]. If this developed stress increases to a certain limit the layer gets cracks and sometimes it peels it off from the support.

2.3.5 Thermal treatment

The final step for the membrane layer formation is the heat treatment by sintering the samples or substrates. Using this process it gives microstructure, mechanical and chemical integrity to the system [42 and 43]. During this heat treatment all the solvents and other residual organic matters and nitrides are removed. The heating and cooling process which develops stresses due the coefficient of thermal expansion, there will be a mismatch between the support and the layer applied which results in cracking or delaminating of the surface. So this has to be controlled by gradually heating and cooling during the sintering process.

2.3.6 Synthesis procedures for titania layer using Sol-gel technique

Tim Van et al studied the characteristics of multilayer TiO_2 membrane consisting of two mesoporous anatase inter layer and a microporous anatase top layer. The multilayer TiO_2 membranes were developed via a multiple sol–gel dip-coating procedure. As support material, tubular membrane supports consisting of alpha-Al_2O_3 with a TiO_2 inner layer. First, mesoporous membrane layers are applied on the membrane support by colloidal

sol–gel dip-coating: two dip-coating cycles are applied in order to produce mesoporous membrane layers with a thickness of ca. 1 μm. Secondly, a very thin microporous top-layer is applied via a polymeric sol–gel dip-coating technique are used. To prepare the colloidal and polymeric sols, a metal alkoxide precursor ($Ti(OC_3H_7)_4$, TTI; Acros) is hydrolyzed, the essential parameter being the rate of hydrolysis. To obtain the colloidal sol, suspensions of larger nanometer-sized particles (35 nm) are prepared by reacting the precursor with an excess water ($[H_2O]/[TTI] = 25$). Polymeric sols containing oligomers (<5 nm) are obtained by a strictly controlled hydrolysis with a small amount of water ($[H_2O]/[TTI]<4$) [44].

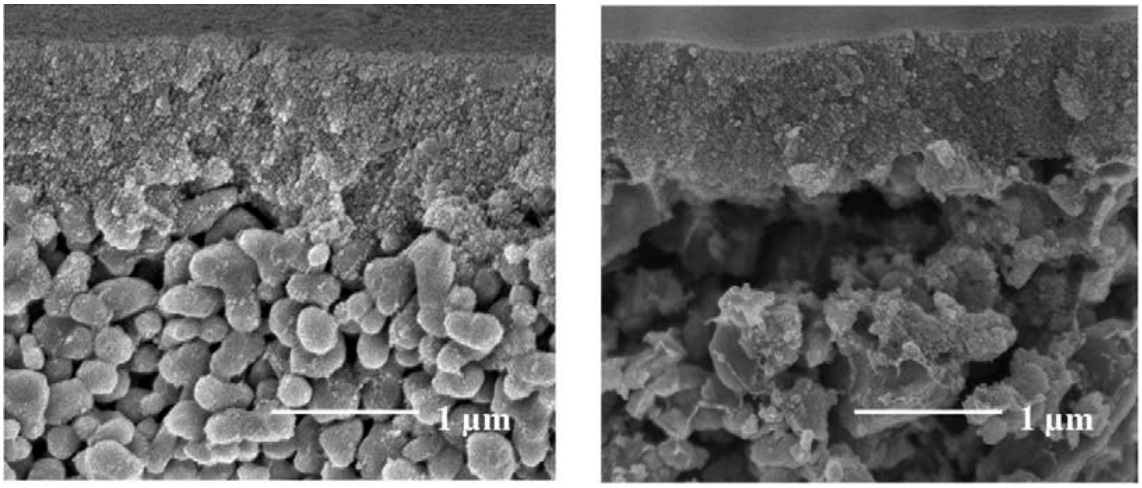

Figure 2.11 FE-SEM cross-sections (20,000×) pictures of (a) titania and (b) mixed, colloidal sol–gel membrane layers on (a) α-Al_2O_3 and (b) RBAO support [44].

The multilayer membrane structure was visualized with field emission scanning electron microscopy as shown in Figure 2.13 for titania and mixed colloidal sol-gel membrane layer. The microstructure of the membrane layers was characterized by X-ray diffraction,

Hg-porosimetry and N_2- adsorption/desorption measurements. Alumina layer could be formed easily with an average thickness above 2 μm and then properly smoothing the surface of the support. Titania layers deposited by a single dip-coating procedure resulted in an average thickness of 0.5 μm. Therefore, a second dipping procedure had to be used to increase the thickness of the membrane up to 1 μm (Figure 2.11a). By applying an Al_2O_3–TiO_2 combination as intermediate layer a thickness of ca. 1 μm was obtained (Figure 2.11b).

The membrane layer of colloidal-TiO_2 with anatase phase has obtained a pore size of 4nm and porosity of 35% and the layer of polymer-TiO_2 with anatase phase structure has a pore size of 2nm and porosity of 35% [44].

P.Puhlar et al studied on microporous TiO_2 membranes coated on the top of tubular ceramic multi layer support. Polymeric sol-gel technique has been used and during the coating is applied the conditions maintained are 50% humidity and 22°C temperature. The control of humidity during the coating and drying process was essential for producing the high quality NF-membrane because humidity influences the hydrolysis and condensation of the gel network. Polymeric gel coating applied and dried for 1hr at room temperature and sintered at 450° C for 1h. The results obtained for the TiO_2 top layer with a thickness of 250nm and pore size of 5nm [45]. Ali Alem et al studied on the titania ultrafiltration membrane, its preparation and characterization. The titania mesoporous layer was prepared by sol-gel dip coating technique.

The method used to prepare the titania colloidal sol and consequently to prepare the membrane layer, was the sol–gel technique.TiO_2 sol was obtained by hydrolysis of tetra

isopropyl orthotitanate ($Ti(OC_3H_7)_4$) via the addition of an excess H_2O ($[H_2O]/[Ti] > 4$). A solution of tetra isopropyl orthotitanate in isopropanol was added drop wise to a solution of water in isopropanol while stirring at high speed. The obtained hydrolysis product was filtered and then washed with water to remove the alcohol. The washed filtrate was redispersed in water to have Ti concentration of 5×10^{-4} mol/cm^3. The mixture was then electrostatically stabilized by HNO_3 and then was peptized at 50°C for 1.5h to create a stable titania sol. The sol was treated ultrasonically for 2h to break the weakly agglomerated particles. Finally a stable titania sol was obtained through this processing method. The layer was formed by dip-coating the support in the prepared sol [46].

N. Agoudjil, T. Benkacem et al investigated on the synthesis of porous titania membranes. The Titanium dioxide was prepared by the hydrolysis and condensation of titanium isopropoxide $Ti(OC_3H_7)_4$ and was used as precursor; nitric acid (solution 65%) was employed as an acid catalyst to promote the formation of polymeric sols and ethanol as solvent. A specific amount of $Ti(OC_3H_7)_4$ was dissolved in an equal volume of ethanol and mixed with deionized water. In this study a procedure for the preparation of titania membranes by sol-gel technique was reported. The influence of several processing parameters on particle size and on stability of sol was investigated. For a given titanium concentration, the hydrolysis condensation reactions were mainly governed by two parameters, namely the initial hydrolysis ratio, $[H_2O]/[Ti]$, and the inhibitor ratio, $[H^+]/[Ti]$ [47].

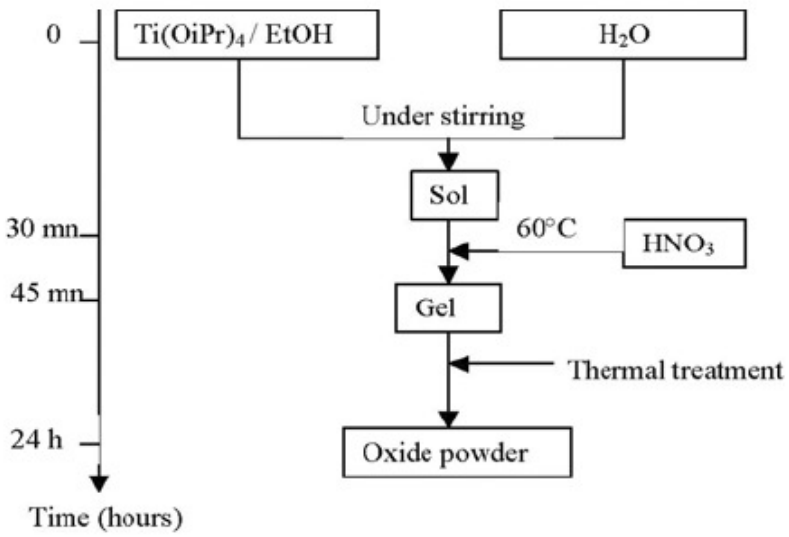

Figure 2.12 Preparation steps of TiO_2 oxide powder. $Ti(OiPr)_4$: titanium isopropoxide = $Ti(OC_3H_7)_4$ [47].

Controlled hydrolysis of alkoxide precursors is the key parameter in formation of thin films using the sol-gel process. The results showed that as the calcination temperature increased, the number of pores decreased as a result of sintering while at the same time the pore size increased [47].

2.4 Top or Active layer

The top layer which is the actual separation layer of the membrane for the removal hydrated sodium and chlorine ions from water which are in sub nano-meter pore size. Most commonly used material for the active layer with sub nano-meter pore size are zeolites. Zeolites have a great attention due to their uniform micro-porous structure, good thermal stability, high mechanical strength and high resistance to relatively extreme chemical environment [48].

2.4.1 Zeolites

Zeolites are the crystalline aluminosilicates with an open structure of three dimensional framework built from SiO_4 and AlO_4 tetrahedral sharing all the corners with each other linked through oxygen atoms with periodic arrangements of cages and uniform channels of nanometer dimensions. Crystal structure defines the pores of the molecular dimensions. The general formula for the chemical composition of zeolites may be expressed as:

$$(M+, 0.5M2+)_m[Al_mSi_{x-m}O_{2x}].nH_2O$$

Where, M is the extra frame work cation. When there is an exchange of the silicon for aluminum in the frame work, results in a net negative charge which will be compensated by extra framework cations. The framework structure consists of interconnected voids or intracrystalline channels that are occupied by cations and water molecules. Currently over 190 zeolite framework structures are available which are registered to the structure Commission of International Zeolite Association (IZA) [49] and new ones are discovered frequently. From those which are produced synthetically and are of commercial interest are only about 17. They are AEL, AFY, BEA, CHA, EDI, FAU, FER, GIS, LTA, LTL, MER, MFI, MOR, MTT, MWW, TON, and RHO [50]. Zeolites can perform as a "molecular sieves", rejecting molecules larger than their pore windows. They exhibit pore sizes from 0.3 to 1.0 nm and pore volumes from about 0.10 to 0.35 cm^3/gm. Typical zeolite pore sizes include: (i) small pore zeolites with eight - ring pores, free diameters of 0.30 – 0.45 nm (e.g., zeolite A), (ii) medium pore zeolites with 10 – ring pores, 0.45 – 0.60 nm in free diameter (ZSM - 5), (iii) large pore zeolites with 12 - ring pores of 0.6 –

0.8 nm (e.g., zeolites X, Y) and (iv) extra - large pore zeolites with 14 - ring pores (e.g., UTD - 1)[51].

Several types of zeolites are widely used in the (petro) chemical industry as catalysts, adsorbents, ion-exchangers, water desalination and show a great potential in membrane synthesis. [52] Zeolite membranes are the thin polycrystalline zeolite layers deposited on porous in-organic supports. As they have high crystallinity, zeolites have a well-defined pore size, and are chemically and thermally stable which makes them suitable for gas separation [53], water separation and membrane reactors [54-56]. Zeolite membranes have several advantages over polymeric membranes and other inorganic membranes [56]. Zeolites show an increased chemical stability compared to polymers and amorphous silica. Zeolites are more thermally stable, allowing significantly higher driving forces (temperatures and pressures) and potential in separations. Because of the well defined pore size, true molecular sieving can be achieved resulting in high selectivities [57]. The synthesis of zeolites can be done by either using hydrothermal synthesis or microwave synthesis.

2.4.2 Hydrothermal synthesis

The origin of zeolite synthesis as known today was pioneered by the work of Richard barrer and Robert Milton in late 1940's. Robert Milton used more reactive starting materials i.e, freshly precipitated aluminosilicate gels, enabling reactions to be carried out under the milder condition which leads to the discovery of zeolite X and zeolite A. Zeolite synthesis under hydrothermal synthesis are formed from the solutions of sodium aluminate, sodium silicate or sodium hydroxide.

In brief a typical hydrothermal synthesis can be described as follows [58]:

(a) Silica and alumina are mixed together which are amorphous reactants with a cation source preferably in a highly basic medium.

(b) Now the solution of aqueous reaction mixture was heated usually at reaction temperature above 100°C in a sealed autoclave.

(c) Once the synthesis temperature has reached, the reactants remain amorphous for some time.

(d) After the induction period (i.e, the time between notional start of the reaction and the point at which crystalline product is first observed) was finished crystalline zeolites are formed.

(e) These are then washed several times, filtered and then dried.

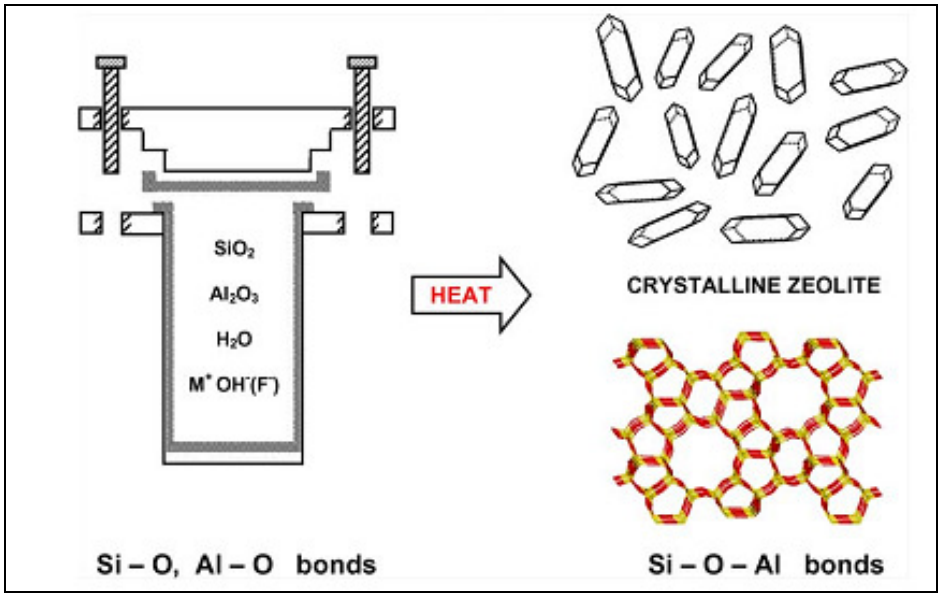

Figure 2.13 Hydrothermal zeolite synthesis. The starting materials (Si-O and Al-O bonds) are converted by an aqueous mineralizing medium (OH-and/or F-) into the crystalline product (Si-O-Al bonds) whose microporosity is defined by the crystal structure [58]

In the Figure 2.13, it shows a schematic diagram of hydrothermal zeolite synthesis. The Si, Al elements which makes up the microporous framework are imported in an oxide form. These amorphous precursors and oxides contain Si-O and Al-O bonds. During the hydrothermal reaction in presence of alkali metal hydroxide crystalline zeolite products are formed containing the Si-O-Al linkages. Therefore the transformation of an amorphous aqueous aluminosilicate gel under the action of heat turns in to a crystalline zeolite product.

2.4.3 Microwave Synthesis

Since last one decade microwave heating has been widely used in many chemical reactions, such as organic and inorganic synthesis, oxidation-reduction, and polymerization as well as in the fields of zeolite synthesis. For microwave synthesis of zeolite, the first report was given in an U.S patent by Mobil oil Corp. in 1988 for the LTA Zeolite synthesis and MFI (ZSM-5) [59]. By using microwave heating, crystallization was increased significantly by exposing the synthesis gels to the radiations of microwave. Therefore, after this microwave heating synthesis was used for different number of zeolites including Zeolite-A (LTA) [60, 61], Faujasite (FAU) [62], Beta (BEA) [63], ZSM-5 (MFI) [65], Silicate-1 (MFI) and so on. Thereafter number of publications has been increased year by year on microwave heating synthesis of zeolites.

When Conventional heating is compared M.H synthesis is much faster, cleaner and more energy efficient. Cundy in 1998 has studied the possible influences of microwave heating on the synthesis of zeolites which mainly focuses on (i) uniform heating of the synthesis

mixture (ii) Increase of the reaction rate and (iii) Changing the association between species within the synthesis mixture [66]. The temperature lower than 100°C is applied for the crystallization of some of the zeolite structures like types LTA, and FAU (Zeolite X and Y). For steel, since it is not transparent for microwave therefore either full-teflon or full ceramic autoclave was used. Many companies worldwide use a standard frequency for microwave oven i.e, 2.45 GHz.

2.4.4 Microwave Synthesis of Zeolite Membranes

Usually Zeolite powders are synthesized, apart from it there is a great interest for supported zeolite layers because of their potential application in separations [61], reactors [54], sensors and electrical insulators. Supported zeolite layers are potential because of their excellent properties such as uniform pore structure, high thermal stability and high mechanical strength. Different types of zeolite membranes were used on different substrates for liquid or gas separation. The first zeolite membrane prepared for industrial application is for dewatering of bio-ethanol by using LTA Zeolite membrane [64]. Several other methods were developed for the fabrication of supported zeolite membranes or layers, including in-situ hydrothermal synthesis, secondary seeded growth synthesis method, multi synthesis and ex-situ hydrothermal synthesis. From all these techniques in-situ hydrothermal synthesis was best and mostly used because in this the surface of the porous support is directly in contact with synthesis precursor solution and keep the complete system under controlled conditions in order to nucleate and grow a thin conditions in order to nucleate and grow a thin continuous zeolite film on the surface of the support. When quality of the membrane is considered in-situ hydrothermal synthesis is not suitable because of it is very sensitive to certain conditions. In this case

seeded secondary growth is considered as the flexible and attractive for formation of high quality zeolite membranes because of its better control over microstructure of the membrane i.e, thickness of the membrane layer and orientation of the membrane.

For preparation of zeolite membranes by using microwave heating with full teflon autoclave and setting the standard frequency at 2.45 GHz crystallization of zeolites is carried out. Microwave synthesis is a simple, fast and energy efficient method which in turn reduces the synthesis time and cost for zeolite preparation. During synthesis in the autoclave it forms heterogeneous nucleation on the walls of the autoclave or on the support on which the layer of zeolite is formed. Whereas the bulk amount is formed due to homogenous nucleation. The zeolite membranes are prepared and are supported by the macroporous supports such as alpha alumina, titania or zirconia. Up to now different types of zeolite membranes were prepared successfully like LTA, FAU, MFI, SOD, AFI, CHA and Zeolite T as well as MOF's by using microwave synthesis heating.

2.4.5 Linde Type A (LTA) Zeolite

"Table 2.1 lists the type material (the common name for the material for which the three letter code was established), the chemical formula representative of the unit cell contents for the type material, the space group and lattice parameters, the pore structure and known mineral and synthetic forms. From the Figure 2.14, it shows the LTA framework type which can be build by linking sodalite cages through double four-rings which creates a cavity called alpha cavity accessible to molecules larger than water via a three-dimensional eight-ring channel system.

Table 2.1 LTA structure type

Type material	Linde type A (zeolite A)
Chemical formula	$\|Na_{12}(H_2O)_{27}\|_8[Al_{12}Si_{12}O_{48}]_8$– LTA
Space group	Pseudo cell: cubic, Pm3m, a = 12.30Å. Super cell (8×volume of pseudo cell): cubic, Fm-3c, a=24.61 Å.
Pore structure	Three - dimensional eight - ring
Synthetic forms	Alpha, ITQ - 29, Linde type A, 3A, 4A, 5A, LZ - 215, N – A, SAPO - 42, ZK - 21, ZK - 22, ZK - 4, UZM – 9

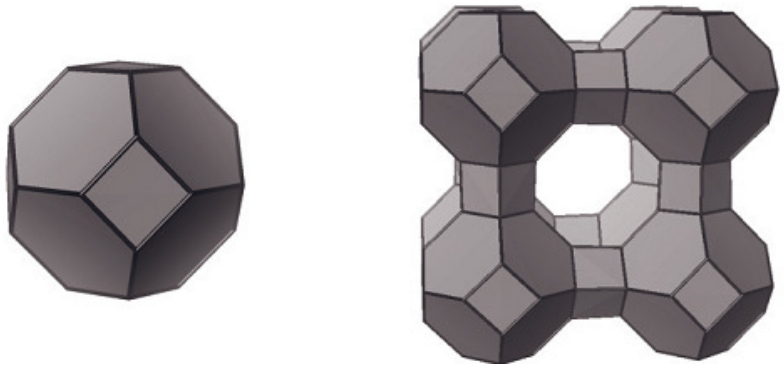

(a) (b)

Figure 2.14 (a) Sodalite cage and (b) LTA framework formed by linking sodalite cages through double four – rings[51].

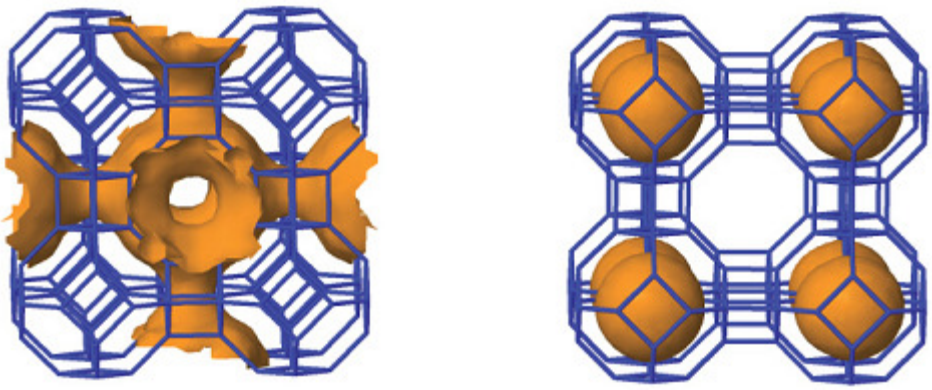

(a) (b)

Figure 2.15 (a) Channel system and (b) cages in LTA [51].

The shape of the channel system in LTA is shown in Figure 2.15a, and the cages in the structures which do not allow molecules larger than water is shown in Figure 2.15b. The Si/Al ration for commonly synthesized LTA is 1, which allows for strict alternation of the Si and Al atoms in the structure and a doubling of the unit cell lattice parameter leading to a super cell with eight times the volume of the smaller cell. Si/Al ratio generally varies from 1 to about 6'' [51].

2.4.6 LTA Zeolite Membrane

As discussed above LTA has a cubic unit cell and the pore size can be tuned by cation exchange. Synthesis of LTA zeolite membranes has been a great interest due to its strong hydrophilicity along with small pore size about 0.4nm. Among the other zeolites, LTA was the first one to use in industrial application for dewatering of bioethanol. Synthesis of LTA zeolite is relatively simple, template free and low temperature is used for crystallization i.e, less than 100°C when compared to other types of zeolites. Other than this it is one of most widely studied zeolite (LTA) by using microwave synthesis.

Han prepared the first LTA zeolite membrane in 1999 by using microwave synthesis heating. During this he found that the microwave heating increased crystallization rate and reduced the time for synthesis i.e, from several hours to 15 to 20 min. When microwave heating is compared to conventional heating, it is 10 to 12 times shorter in crystallization time which in turn reduces the thickness by minimizing the growth and there is good permeation characteristics are formed. Below is the schematic diagram (Figure 2.16) which shows the differences between conventional and microwave heating process.

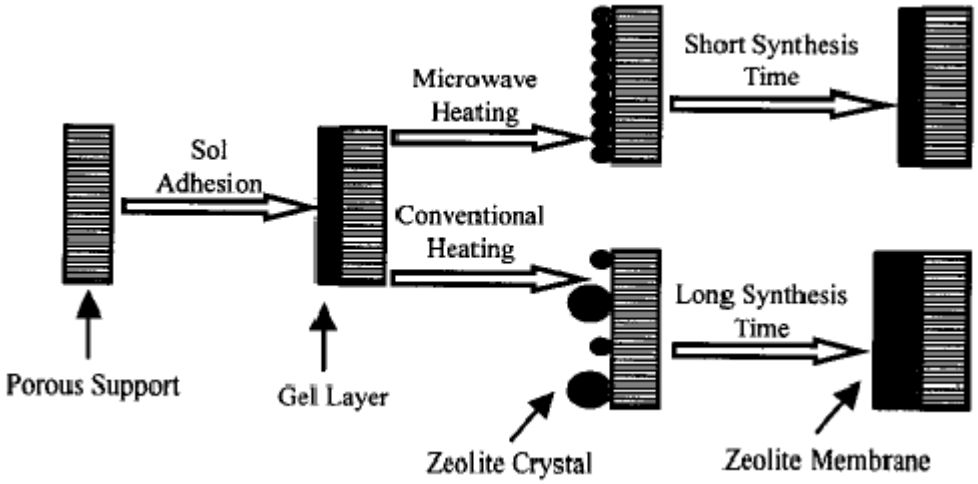

Figure 2.16 Comparison of synthesis model of zeolite membrane prepare by microwave heating and conventional heating [68].

In the current study for the preparation of micro-porous layer zeolite-A of frame LTA was selected because of its great interest in selectivity in separation and has potential to sieve out molecules in a continuous process due to its hydrophilicity. The intercrystalline pore size of LTA zeolites is about 0.41nm with Si/Al ratio of 1. The small pore size of LTA zeolite helps to reject the hydrated sodium and chlorine ions of size 0.7nm during the filtration process. For the application in separation processes the membrane must be

defect free and continuous. The synthesis of defect free membrane is still challenging although different methods have developed to improve the quality of the membrane. In general for the preparation of zeolites membrane are formed in three stages as shown in Figure 2.16. After the preparation of support on which zeolites layer is applied follows with (i) sol-gel adhesion on the substrate to form the gel layer (ii) nucleation and (iii) crystallization and the coating formation [70].

In this study, macro-porous alumina substrate was coated with an intermediate meso-porous layer which helps to increase the adhesion to the initial gel layer formed during synthesis. As discussed earlier, different methods were developed to synthesize zeolites membrane. The widely used technique for the synthesis of zeolites membranes are in-situ synthesis and secondary growth. During in-situ synthesis there is an abundant heterogeneous nucleation was formed which helped in forming good quality membrane. Previously many experiments were done on in-situ synthesis to optimize the synthesis composition of solution of ZSM-5 zeolites membrane [67]. Van den berg at al used in situ synthesis for LTA zeolite membrane which was supported by titania. The titania supports were U.V irradiated to increase the population of LTA zeolites nuclei on the support surface [69]. Whereas in secondary growth method, nucleation will be done by pre-seeding the support layer. By controlling the seed layer, uniform molecular sieving membrane was synthesized. However to obtain a continuous layer of seed is very difficult with full coverage. Therefore for the industrial mass production, in-situ synthesis is simpler and more preferable than secondary growth.

By using microwave synthesis, the energy from the microwave is directly supplied by an electromagnetic field to the synthesis material. Because of this, it results n a rapid

heating throughout the material with reduced thermal gradient. Therefore microwave synthesis has many advantages like small zeolite particles, short synthesis time and high purity. Because of these characteristics it has great interest for quick preparation of high performance zeolite membrane [72]. Present study also reports that continuous zeolite membrane cannot be microwave synthesized without seeding which was also reported elsewhere.[71] After that we tried to synthesize using in-situ synthesis method to get a uniform and continuous layer of LTA zeolite layer without seeding which was successfully done on titania coated alumina substrate. In this some parameters like synthesis time and aging time play major role in getting a continuous layer. During aging, the synthesis mixture was aged with the titania coated alumina substrate fitted to a Teflon holder in the reactor. This process is called in-situ aging. In this first it forms an amorphous gel layer during aging process on the surface of the support which contains nuclei in order to increase the surface concentration. Afterwards microwave heating synthesis was carried out at different synthesis time to convert the formed amorphous gel into crystalline zeolite layer [67].

2.5 Characteristics

For porous ceramic membranes, separation properties are directly determined by characteristics of the porous structure such as pore size, shape, connectivity, particle packing, surface area, etc. Therefore, proper characterization of the porous structures is important for the development of commercial ceramic membranes. Characterization techniques for ceramic membranes can generally be classified according to the nature of obtained parameters: (1) morphology/structure related parameters and (2) permeation

related parameters. Therefore, the characterization techniques such as scanning electron microscopy (SEM) or field emission scanning electron microscopy (FESEM), transmission electron microscopy (TEM), atomic force microscopy (AFM) and X-ray diffraction (XRD) was used for morphology/structure related parameters; while for the permeation related parameters, characterization techniques such as mercury porosimetry, permeation, bubble point technique, permporometry was used. In addition, to test the bending strength that which determines the mechanical strength of ceramic membranes, three point bend test and diametrical compression test are used.

In the current study, the multi-layered ceramic membranes were characterized using scanning electron microscope to check the morphology of the surface, pore-size, and thickness of the membrane layer through cross-section. X-ray diffraction technique was used to find the crystallinity of the prepared membrane and in order to check the accurate pore-size and porosity, mercury porosimetry was used. Diametral compression test was used to find the strength of the membrane.

2.5.1 Scanning Electron Microscope

Scanning Electron Microscope is a very useful technique in characterization of membranes. In order to study the surface topography of membranes, cross-section of membrane, pore-size, surface porosity and pore size distribution, SEM is used.

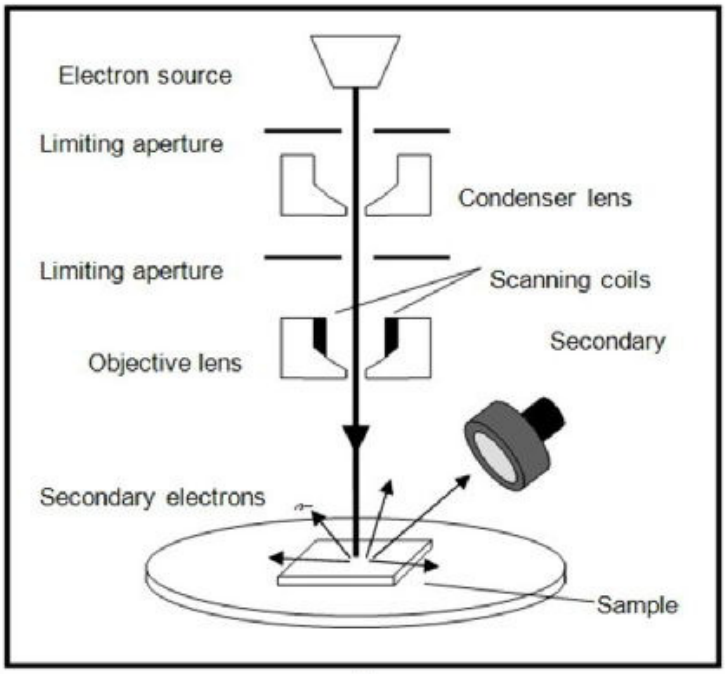

Figure 2.17 Schematic diagram for scanning electron microscope [73].

The working principal of SEM is that an electron gun emits a beam of electrons and this beam travels down to the sample through series of magnetic lenses as shown in Figure 2.17. This beam of electrons helps to scan the surface of the sample and then reflected back to a collector where it collects and displays the scanned image on a cathode ray tube. The sample which is going to be characterized must be electrically conductive. If the sample is non-conductive, a conductive layer must be coated, usually gold is coated to make the surface conductive and then scanning can be done.

2.5.2 X-Ray Diffraction

X-ray diffraction (XRD) is an essential technique for phase identification and crystal structure refinement. It is very often used to examine whether there are any changes in the crystalline structures of membrane materials after being processed into the

membranes. Also, stability of ceramic membranes after long term exposure to a reaction environment is usually checked by XRD. X-ray scattering techniques are a family of non-destructive analytical techniques which reveal information about the crystallographic structure, phases present, and composition. These techniques are based on observing the scattered intensity of an x-ray beam hitting a sample as a function of incident and scattered angle, and wavelength. Bragg's law is then used to compute the crystallographic spacing by using Bragg's law is as follows [77]:

$$n\lambda = 2d\sin(\theta)$$

where:

n is an integer determined by the order given, taken as unity,

λ is the wavelength of x-rays,

d is the spacing between the planes in the atomic lattice, and

θ is the angle between the incident ray and the scattering planes

2.5.3 Mercury Porosimetry

Mercury porosimetry is one of the most popular and fastest methods for determining pore size and pore size distribution in ceramic membranes. It is based on the fact that mercury is a strongly nonwetting liquid on most materials. Therefore, when mercury is forced into a dry membrane with the volume of mercury being determined at each pressure, a cumulative volume of mercury as a function of the applied pressure can be established, as illustrated in Figure 2.18, from which the pore size distribution can be deduced [76].

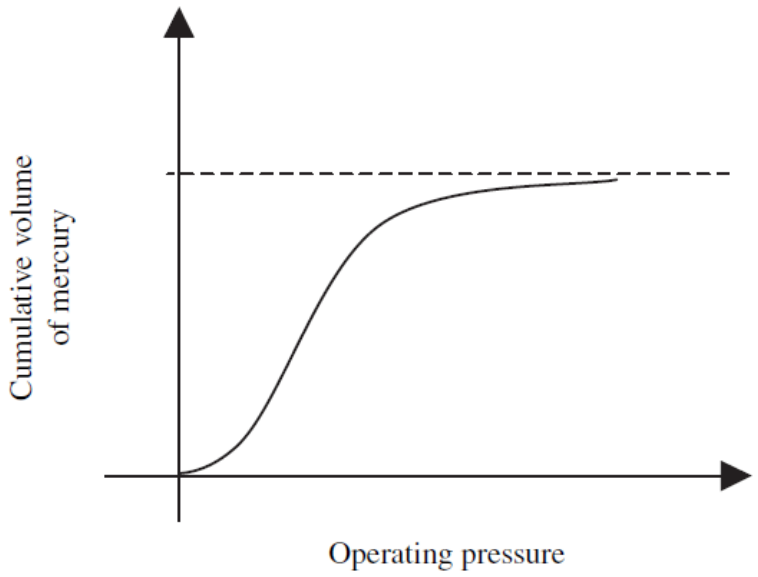

Figure 2.18 Cumulative volume of mercury as a function of the applied pressure [8].

The relationship between the operating pressure and pore size of the membrane can be described by the Laplace equation, if the pore in the membrane is assumed to be cylindrical:

$$r_p = -\frac{2\sigma}{p}\cos\theta$$

Where, P is the applied pressure (gauge), in Pa, σ the surface tension at the mercury/air in N m−1, r_p, the pore radius, in meters and θ, the contact angle.

Based on the above Equation, very high pressures are required for pores in the nanometer range. For example, an operating pressure of 490 MPa is required to measure a ceramic membrane with a pore size of 1.5 nm assuming that the contact angle of the mercury with ceramic materials is at 140º.

CHAPTER 3 EXPERIMENTAL PROCEDURE

3.1 Preparation of macro-porous ceramic support

Alpha-alumina (α-Al_2O_3, from Buehler Co.) powder with average particle size of ~0.3 µm was used to prepare the macro-porous ceramic substrate/support using powder metallurgy route.

3.1.1 Powder Compaction

Alumina powder was uni-axially pressed using different compaction pressures to form the ceramic support green samples using uni-axial hydraulic press.

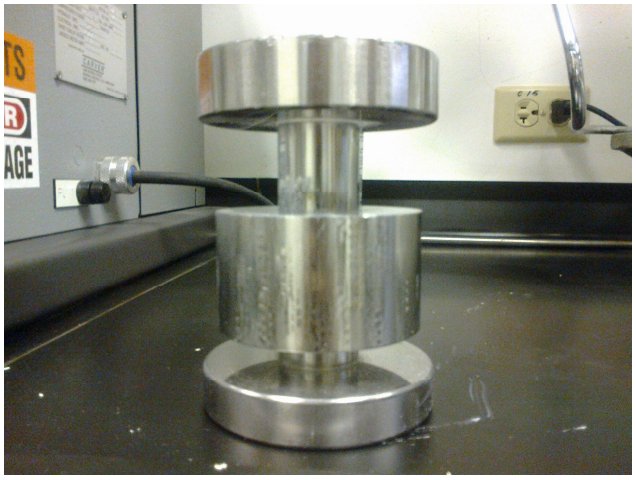

Figure 3.1 Compaction steel die with upper and lower punch

Figure 3.1 shows the 1-inch diameter die with upper and lower punch which was used to prepare the disc shaped samples under the press (Figure 3.2, Carver Auto pellet press).

Figure 3.2 Carver Auto pellet press

The green compacts are of 1-inch diameter and 2-3 mm thickness. Green densities, shown in Table 3.1, were calculated by measuring the weight and physical dimensions of the powder compacts before sintering.

Table 3.1 Green densities of the compacts at different compaction pressures

Compaction Pressure (MPa)	Green Density (g/cm^3)
619.5	1.99
542.1	1.91
464.6	1.88
387.2	1.86
309.8	1.80
232.3	1.76

3.1.2 Sintering

The green compacts were then sintered in a tube furnace as shown in Figure 3.3 (MTI, GSL-1700-60X) in air atmosphere at 1400°C for 2 hours. The utilized ramp up rate was 4°C/min during heating and upon completion of the sintering cycle, the samples were furnace cooled to room temperature by simply switching off the furnace.

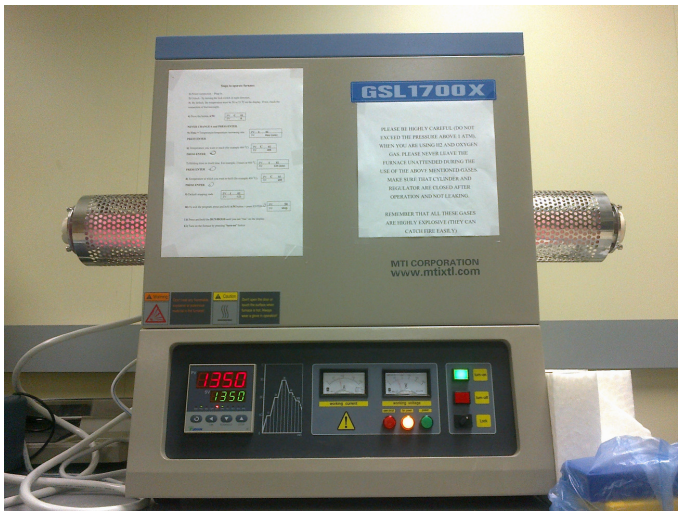

Figure 3.3 MTI high temperature furnace

3.1.3 Porosimetry

To investigate the pore size and pore size distribution of the sintered ceramic structures, mercury porosimetry measurements were performed using Micromeritics Autopore IV 9500 V1.09 Porosimeter. A pore size distribution representing a bulk value for the entire cross-section of the alumina substrate was obtained. The 1-inch ceramic disc was placed in the Porosimetry penetrometer of volume 3.5 cm^3. Then the sample container was placed in a pressure vessel to force the mercury into the pores of the substrate.

3.1.4 Diametral Compression test

The structural integrity of ceramic filters was measured by the diametral compression test performed on the ceramic substrate. There is no standard strength test prescribed by ASTM for ceramic filters in general. Diametral compression test is frequently used to measure the strength of porous ceramics.

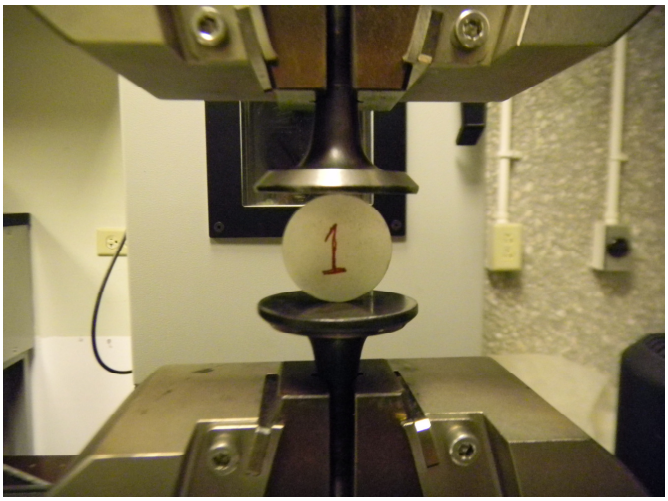

Figure 3.4 Diametral test

It measures the tensile strength of the sample in the direction perpendicular to the loading direction. In this test, a circular disk or hollow ring is diametrally pressed between two flat plates as shown in Figure 3.4. The diametral stress is then calculated as follows [74]:

$$\sigma = \frac{2P}{\pi Dt}$$

Where P is the load, D is the diameter and t is the thickness of the ceramic disk.

3.2 Preparation of mesoporous layer on macroporous support

For the preparation of meso-porous intermediate layer, titania (TiO_2) was selected because of its hydrophilicity, high water flux and chemical stability. Titania was prepared by the most commonly used method called sol-gel dipcoating technique. By using sol-gel technique, a porous structure is obtained upon layer application, drying and calcinations process on the macro-porous support.

3.2.1 Preparation of TiO_2 colloidal sol solution

The colloidal sol solution was prepared by adding 2ml of titanium(IV) iso-propoxide (TTIP) (ALDRICH, 99.99%) to 150ml beaker containing a mixture of isopropanol (Fluka Chemika, 99%) which acts as solvent, and deionized water.

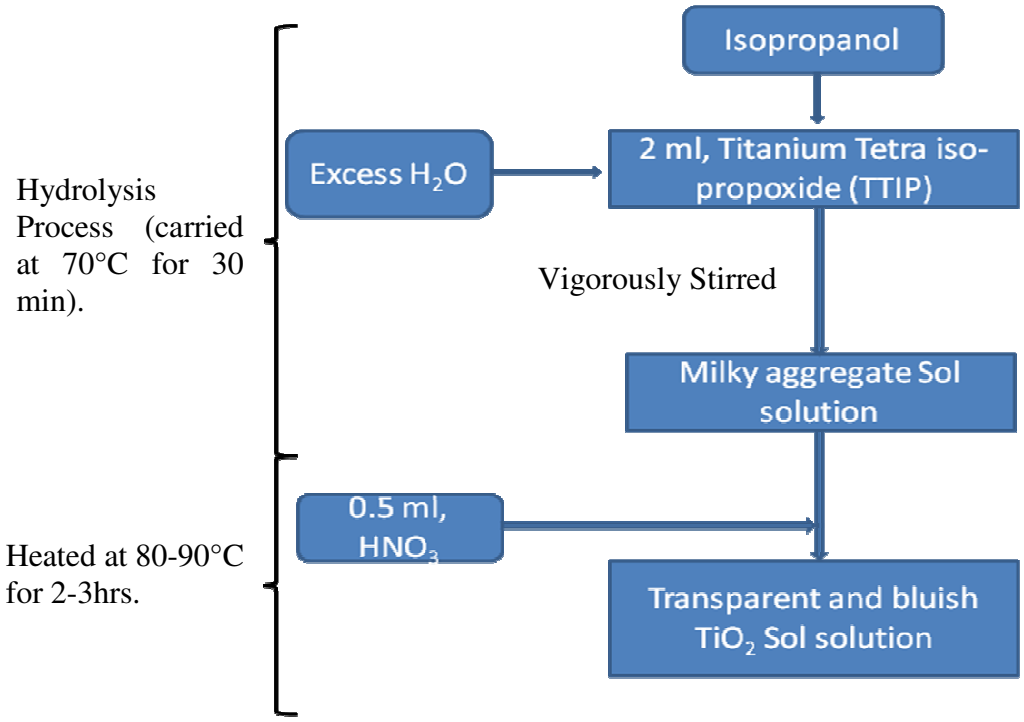

Figure 3.5 Preparation steps of Colloidal TiO_2 sol solution

The process discussed is a modified method from literature. During hydrolysis, excess amount of water was added in the preparation of the colloidal sol in order to get relatively large particle size in the range of 10-50nm when compared to polymeric sol-gel technique. The solution was vigorously stirred using a magnetic stirrer during addition of solvent. The hydrolysis process was carried out at 70^{o}C for 30 min in an oven resulting in a milky aggregate solution. Concentrated nitric acid (0.5ml), which acts as a catalyst, was added drop by drop followed by heating at 70-80^{o}C on a heating plate for 3h yielding in a transparent and bluish solution. In Figure 3.5 it shows complete flow diagram for the preparation of colloidal clear and transparent sol solution.

The resultant colloidal sol solution was dip coated on the prepared disk shaped porous α-alumina substrate (1-inch diameter and 2mm thickness), glass and 316L stainless steel substrates by using two different deposition methods, one is by manual dip coating and the other is by automated dip coating method followed by drying and calcination to check the deposited layer characteristics like homogeneity, uniformity of the surface.

3.2.2 Deposition of titania layer using manual dip-coating technique

Once the titania colloidal sol was prepared, different substrates like alpha alumina (1-inch diameter and 2mm thickness), glass and 316L stainless steel substrates were first polished to make it smooth by 600 size grit size paper and then cleaned in acetone for 10min followed by ethyl alcohol solution for 10min, then rinsed in distilled water for 15min and dried in oven for 3 hr at 60°C.

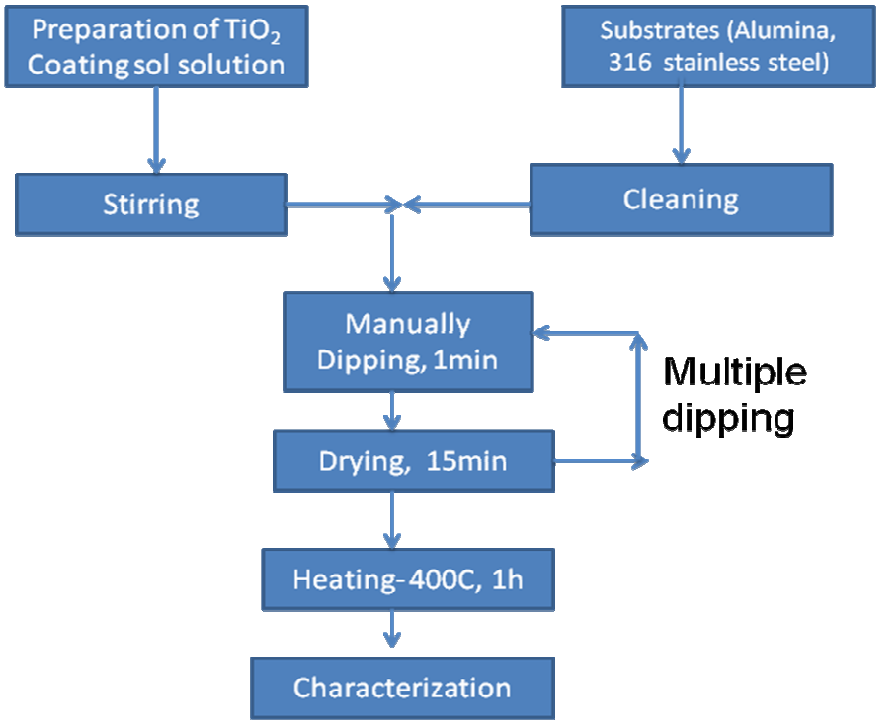

Figure 3.6 Flow diagram for manual dip coating process

The titania layer was then deposited by manually dipping the substrates into the titania sol solution for 1min and dried for 15min in air and then again dipped for multi dipping to get a uniform porous layer and then dried (Figure 3.6). After drying in air the substrates were calcinated in an air oven at 400° C for 1h and then furnace cooled.

3.2.3 Deposition of titania layer using automated dip coating method

The resultant colloidal sol solution was dip coated on the prepared disk shaped porous α-alumina substrate , glass and 316L stainless steel substrates by using a dip coater (MTI, WPTL5- 0.01 Dip Coater).

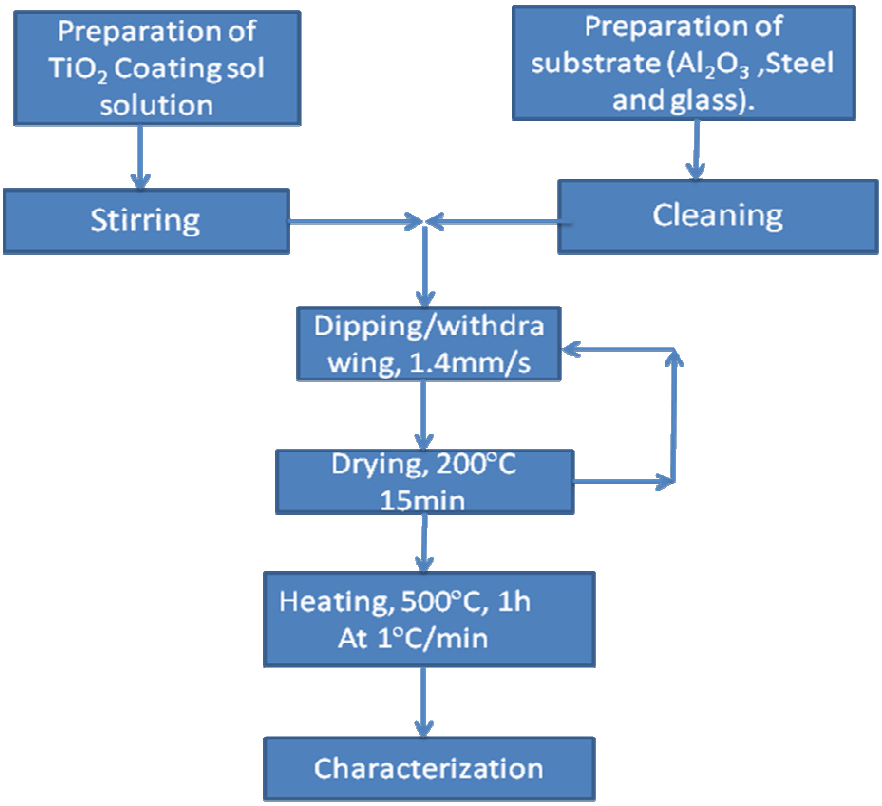

Figure 3.7 Flow diagram for automated dip coating method

Prior to coating, the substrates were first polished (alumina and steel), and then cleaned in acetone for 10min followed by ethyl alcohol solution for 10 min, then rinsed in distilled water for 15min and dried. The TiO_2 layer was deposited by double and triple dipping in the sol solution for 15min, with a constant dipping and withdrawal rate of 1.4 mm/s to control the thickness of the coating. Following the dipping process, the substrates were dried in oven at 200^{o}C for 15min and then heat treated in a tube furnace at 500^{o}C for 1h at a heating and cooling rate 2^{o}C/min [75]. Figure 3.7 gives complete step by step process in a flow diagram performed during automated dip coating technique.

3.3 Preparation of microporous layer on mesoporous TiO_2 layer

For the preparation of micro-porous layer, zeolite-A was used to synthesize the membrane active layer. Two different approaches were used to synthesize the LTA zeolite membrane, (a) multiple synthesis using microwave heating and (b) in-situ aging method. Prior to synthesis of zeolite-A layer, the mesoporous intermediate layer i.e, titania layer supported by macroporous α-alumina substrate of 1 inch diameter was exposed to UV irradiation for 2 hours in a homemade UV lamp box. Because of this UV irradiation, the surface of TiO_2 becomes more hydrophilic, to attract and to bond LTA zeolite gel which results in increase in population of LTA zeolite nuclei on the surface for complete coverage.

The molar ratio of synthesis mixture used for LTA zeolite membrane was as follows: $5SiO_2$: Al_2O_3:$50Na_2O$:$1000H_2O$ [67].The aluminum source was aluminum foil and the silicon source was sodium meta silicate, $Na_2SiO_3.5H_2O$. The synthesis mixture was then prepared by mixing aluminum solution and a silicate solution. The aluminate solution was prepared by dissolving sodium hydroxide (18.3 g) in deionized water (80.28 g). After complete dissolving by stirring continuously aluminum foil (0.5 g) was added slowly into the caustic solution. Similarly, the silicate solution was prepared by dissolving sodium hydroxide (14.63 g) in deionized water (80.28 g) and then adding sodium meta silicate (9.73 g) followed by heating at 40°C until the solution was clear. The silicate solution was added slowly to aluminate solution and mixed it thoroughly by using magnetic stirrer and then it was aged for 1h before using for synthesis.

3.3.1 Synthesis of LTA zeolite membrane using multiple MH synthesis method

During the microwave heating synthesis, the two layered porous disc support (TiO2/Al2O3) was fixed to a poly(difluoromethylene) /PTFE holder as shown in Figure 3.8 and placed in a PTFE reactor vessel. One side of the disc support i.e, uncoated side was protected by a Teflon disc of 1inch diameter. Due to this attachment of support the zeolite layer is formed on the mesoporous titania layer side which has pore size about 80 nm. Then, the synthesis solution was added to the PTFE reactor vessel in which PTFE holder with membrane support disc was placed.

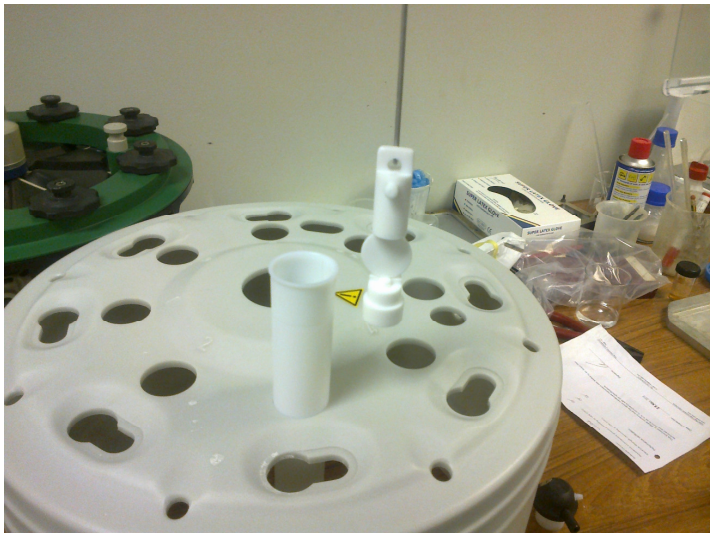

Figure 3.8 Teflon holder with fitted substrate placing in Teflon reactor vessel.

Microwave synthesis was carried out by using the Synthos 3000 Microwave Oven (Anton Paar) as shown in Figure 3.9 & 3.10. The synthesis was performed at 90°C for 15min. In order to get complete coverage (without pinhole) multiple synthesis was carried out step by step after each synthesis.

Figure 3.9 Microwave Oven (synthos 3000, Anton Paar)

After the three consecutive synthesis steps, the membrane disc was washed thoroughly many times with distilled water until the neutral pH was reached. Then the membrane was dried at 90°C in a low-temperature oven overnight.

Figure 3.10 Synthesis reactor vessel for Microwave oven

3.3.2 Synthesis of LTA zeolite using in-situ aging microwave heating synthesis

In this method, after the preparation of synthesis solution, it was aged for 1 h before beginning of in-situ aging MH synthesis. This method has two different steps for preparation of zeolite-A layer. First step is called in-situ aging, which was carried out in an autoclave reactor for hydrothermal synthesis by conventional heating at very low temperature i.e, at 50°C to create nuclei on the surface of the support and in order to provide enough time to cover the surface of the support with nuclei. The membrane support was aged for 7 h in an air oven. The synthesis solution mixture was poured into the autoclave reactor with PTFE liner and along with the PTFE holder which was placed with fitted α-alumina support coated with UV irradiated TiO_2 layer as shown in the Figure 3.11.

Figure 3.11 Autoclave reactor with Teflon tube and Teflon holder fitted with support coated with TiO_2

By varying the aging time, surface and coverage of the nuclei were studied. After studying the aging time during hydrothermal synthesis, the membrane and the synthesis

mixture were then exposed into microwave heating for the second step or so-called crystallization step. The microwave heating was carried out at 90°C at three different synthesis times to study the crystallized surface. During the microwave heating process, an amorphous aqueous aluminosilicate gel was transformed into a crystalline zeolite layer under the action of heat and autogenously pressure. After the MH synthesis, the as-synthesized membrane was washed thoroughly using distilled water and then dried at 100°C in an oven overnight before further characterization works. A complete fabrication process of multi layer in the current study is shown schematically in the Figure 3.12.

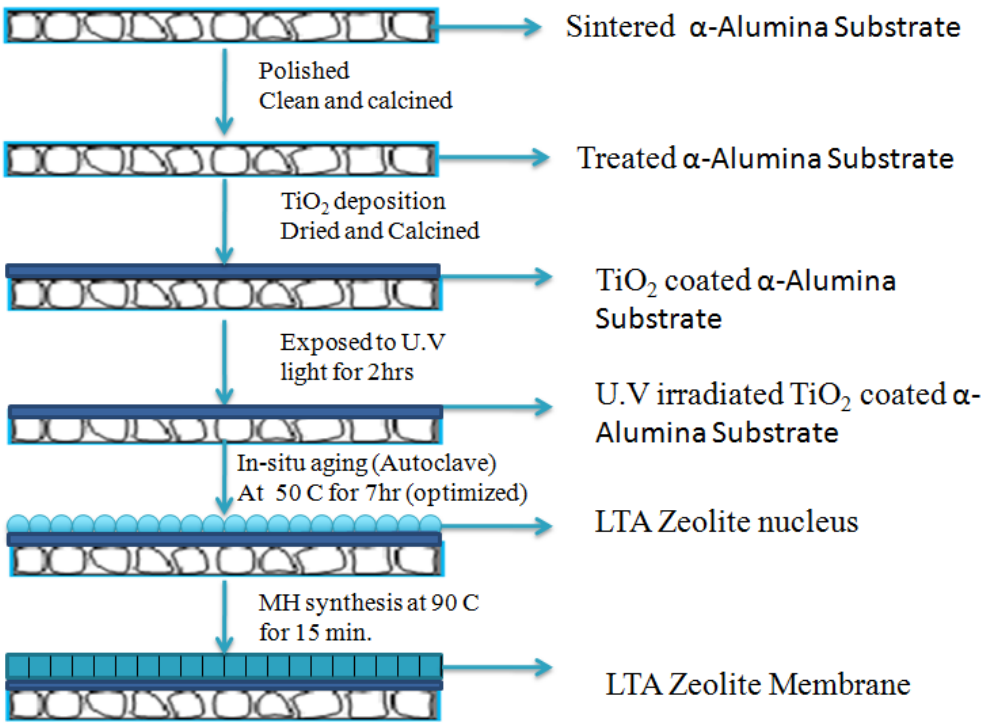

Figure 3.12 Schematic diagram for the fabrication of multi-layered membrane.

3.4 Characterization

The α-alumina substrate and deposited titania and LTA zeolite layer was characterized using scanning electron microscope (SEM-JEOL, JSM-6460LV) equipped with energy dispersive X-ray spectroscopy (EDS), X-ray diffraction (XRD-BRUKER D8 Advance) and Mercury Porosimetry (Micromeritics, AutoPore IV 9520 Series) to study the surface morphology, crystal structure, crystallinity, pore size and surface porosity.

CHAPTER 4 RESULTS AND DISCUSSION

4.1 Preparation of macro-porous support

4.1.1 As-received α-alumina powder

The results related to the characterization of the as-received alumina powder, influence of powder compaction on the green density of the compact and subsequent sintering of the compact are presented underneath.

Figure 4.1 shows SEM images (15kV, Secondary Electron Imaging) of as-received α-alumina powder. The alumina powder is non-agglomerated with an average particle size of 0.3 microns. The variation of particles size observed is very small which is essential to control the pore size of the ceramic support leading to a minimum variation throughout the support layer volume. Figure 4.2 displays the XRD pattern of the as-received powder indicating that this powder is indeed α-alumina type and of high purity (the black pattern belongs to the analyzed powder sample and the red pattern is α-alumina reference taken from the database). Thus, the analysis of the powder as performed by both SEM and XRD techniques confirm that the as-received powder is of high quality and possesses a uniform particle size distribution.

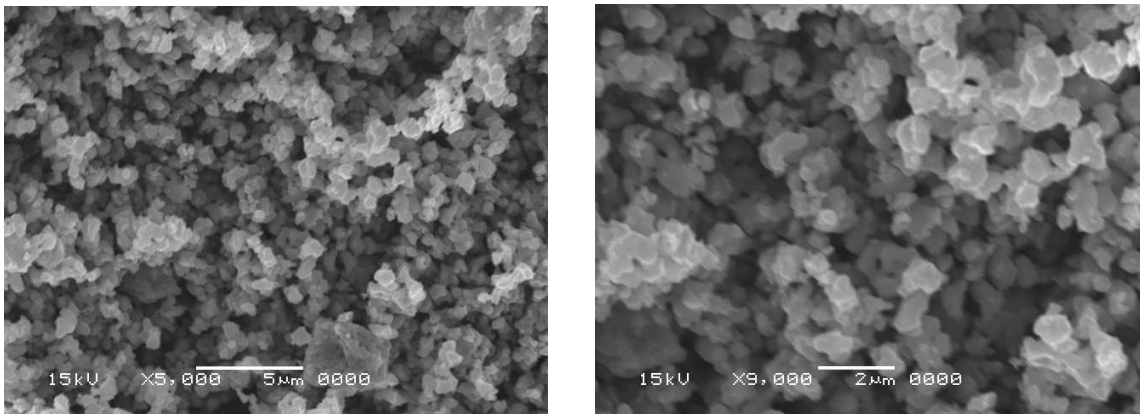

(a) (b)

Figure 4.1 SEM micrographs of as the received α - alumina powder taken at (a) low magnification, (b) higher magnification

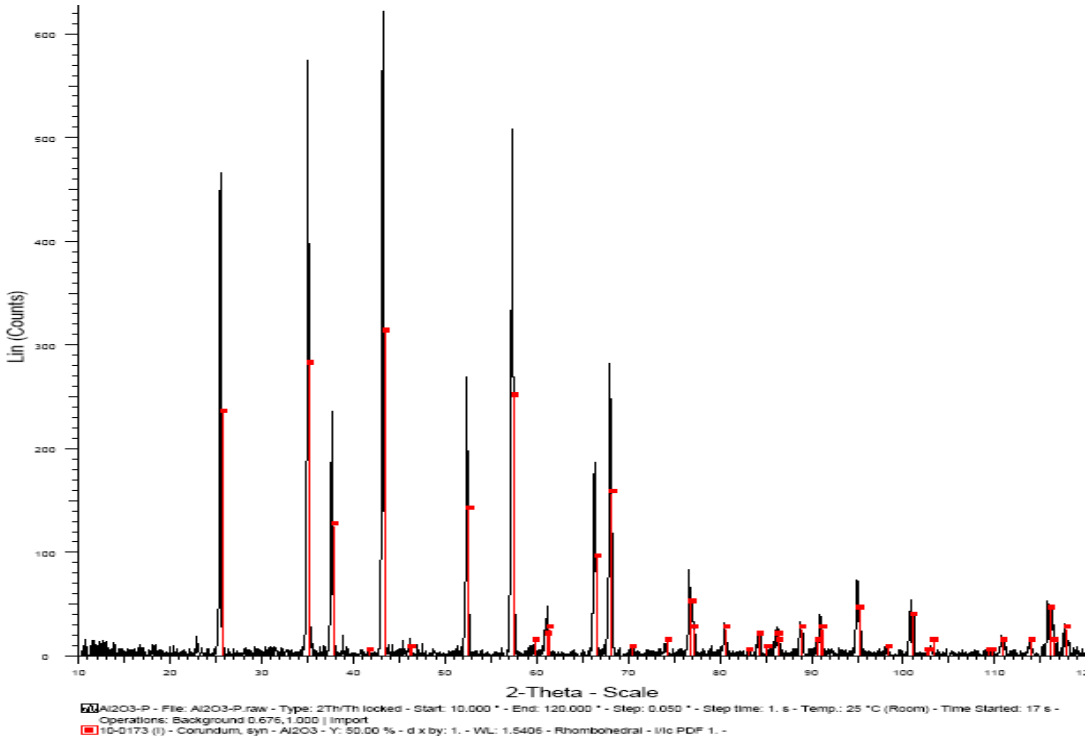

Figure 4.2 XRD pattern of the as-received α-alumina powder

4.1.2 Powder compaction

Figure 4.3 shows the green compact for the alumina powder compacted at a pressure of about 620 MPa. Compaction pressure was varied to achieve a green compact with sufficient strength to be able to perform dimensional measurements, weighing and handling of the green compact prior to sintering. Figure 4.4 displays the variation of the green density with the compaction pressure. As expected, the green density increases with increasing compacting pressure, varying from 1.75 g/cm^3 to 2 g/cm^3 for pressures of 230 MPa to 620 MPa respectively.

Figure 4.3 Green α-alumina compact pressed at 620 MPa

Green density gives an indication of the porosity level in the ceramic substrates and as the green density increases the amount of porosity and pore size generally tends to decrease.

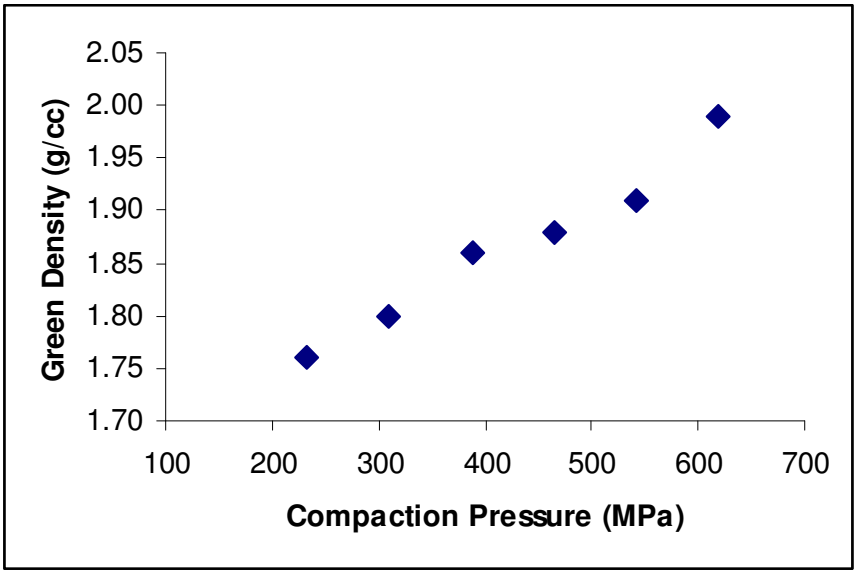

Figure 4.4 Variation of green density with applied compaction pressure

4.1.3 Sintering of the compact

Figure 4.5 shows the alumina support that was compacted at a pressure of 620 MPa and sintered at 1400°C for 2 hours. The sintered alumina support was further characterized using XRD and SEM. The XRD pattern of the sintered sample is shown in Figure 4.6. By comparing the XRD patterns of the as-received alumina powder (Figure 4.2) with that of the sintered sample (Figure 4.6), it is confirmed that no new phase was formed during/after the sintering process. Figure 4.7 shows the corresponding SEM micrographs of the sintered sample shown in Figure 4.5. The main objective of the sintering stage is inducing bonding and adherence of the alumina particles (densification via solid state sintering mechanism) by neck formation, which is crucial for achieving a crack-free filter support. It can be observed from Figure 4.7 that there is good bonding amongst the alumina particles thus providing a good mechanical strength for the ceramic porous support.

Figure 4.5 Sintered α-alumina substrate initially compacted at 620 MPa

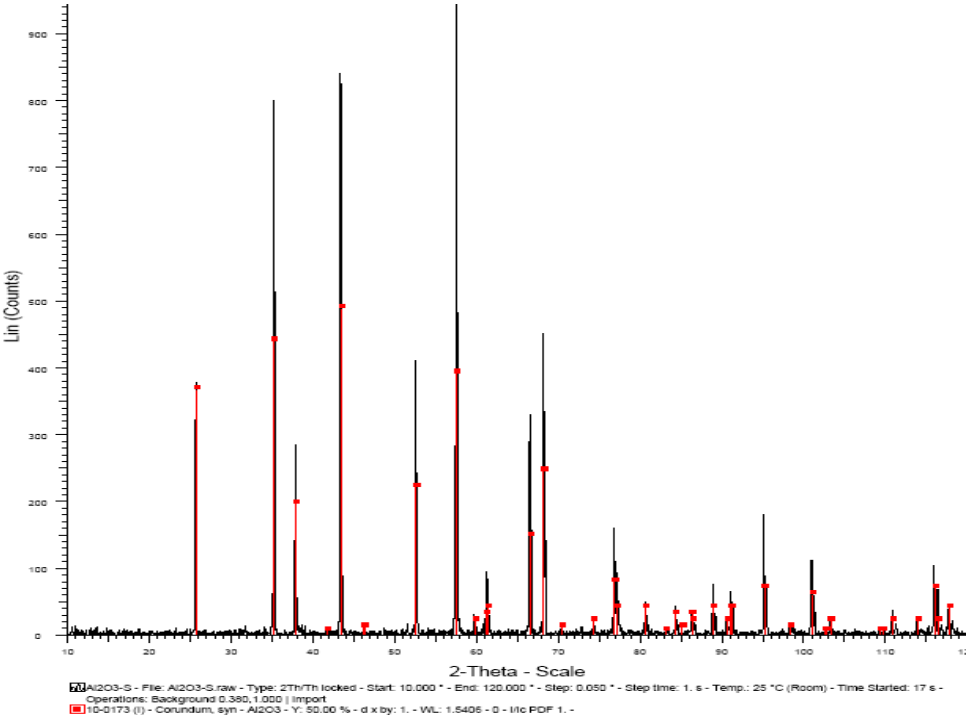

Figure 4.6 XRD pattern of the sintered α-alumina substrate

The pore size, as estimated from the SEM images, ranges from 0.1 to 0.3 µm. However, it is intended to put the layer processed in this study having an average pore size of 0.2 µm on top of the support structure with a larger pore size thus producing a gradient in

porosity. One way to increase the average pore size for the ceramic support is to use larger alumina particles. On the other hand, it is worth mentioning that the microstructure/porosity of porous ceramics can be controlled not only by adjusting the particle size and shape of the initial powders, but also by controlling the compacting pressure as well as the sintering process parameters, mainly temperature and dwell time. This study has lead to the understanding of the relationship between compaction and sintering parameters for a given alumina powder and to optimize the processing parameters of the ceramic support such as initial

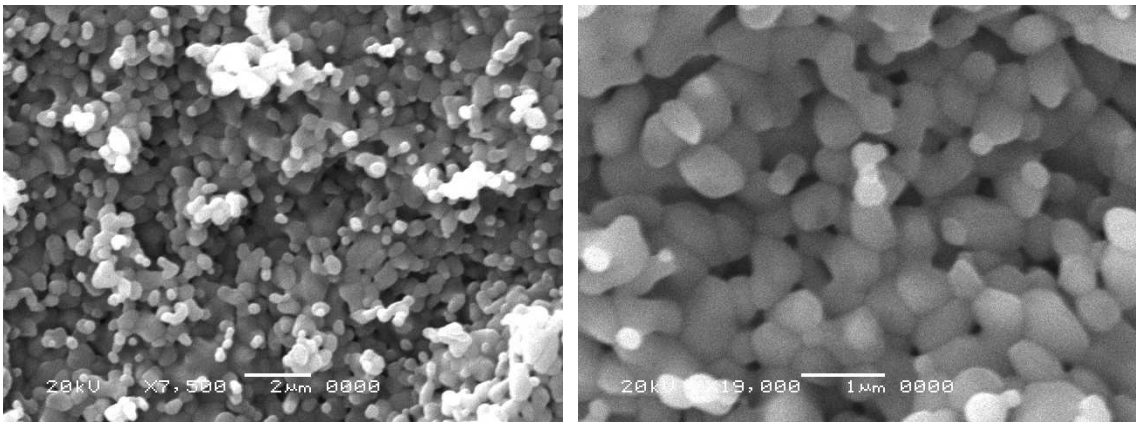

(a) (b)

Figure 4.7 SEM micrographs of the sintered α-alumina substrate at different magnification

particle size, compaction pressure, sintering temperature and time. The other meso and micro porous layers will be deposited onto the support structure using a variety of techniques including sol-gel deposition, dip coating and microwave hydrothermal synthesis for the fabrication of graded macro/meso/micro porous structure; this has been investigated in the second stage of this study.

4.1.4 Strength test

Diametral compression test was performed on alumina discs. Samples used had dimensions of 1-inch diameter and 2-3mm thick (compacted at 375 MPs and sintered at 1400°C for 2 hrs). Samples were polished using SiC grinding paper to make the surfaces flat and parallel, then cleaned using ethanol and deionized water under ultrasonication and subsequently dried. Figure 4.8 shows the polished samples. Instron universal testing machine was used for conducting the tests. Samples are diametrally pressed between flat platens with a crosshead speed of 0.5 mm/min.

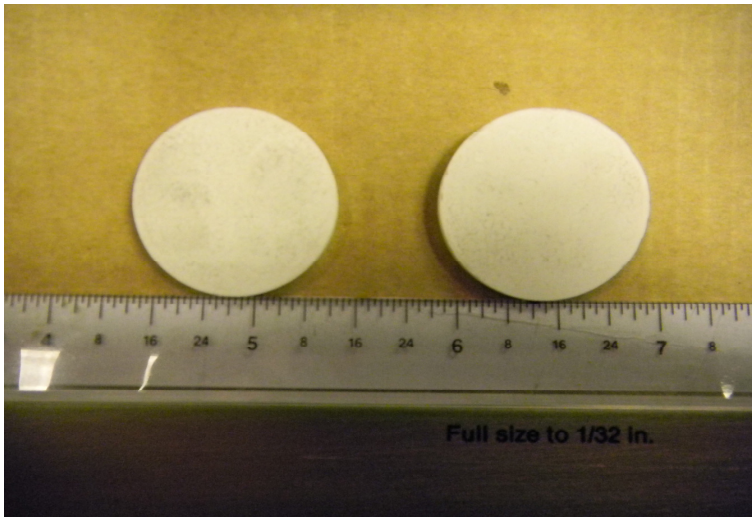

Figure 4.8 Alumina substrates used for structural testing

A fractured sample is shown in Figure 4.9. It can be observed that the sample fractured into two halves indicating that it underwent a tensile failure which is a necessary condition for considering the diametral compression test successful on ceramic structures [74]. Figure 4.10 shows the output of the diametral compression test showing the

variation of compressive stress versus compressive strain. The average strength of the sample tested up to a maximum compressive load of 1263N is 14.87 MPa.

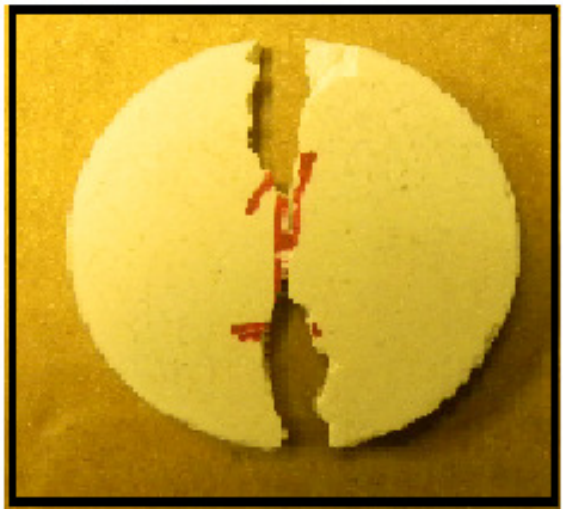

Figure 4.9 Fractured sample after being subjected to diametral compression test

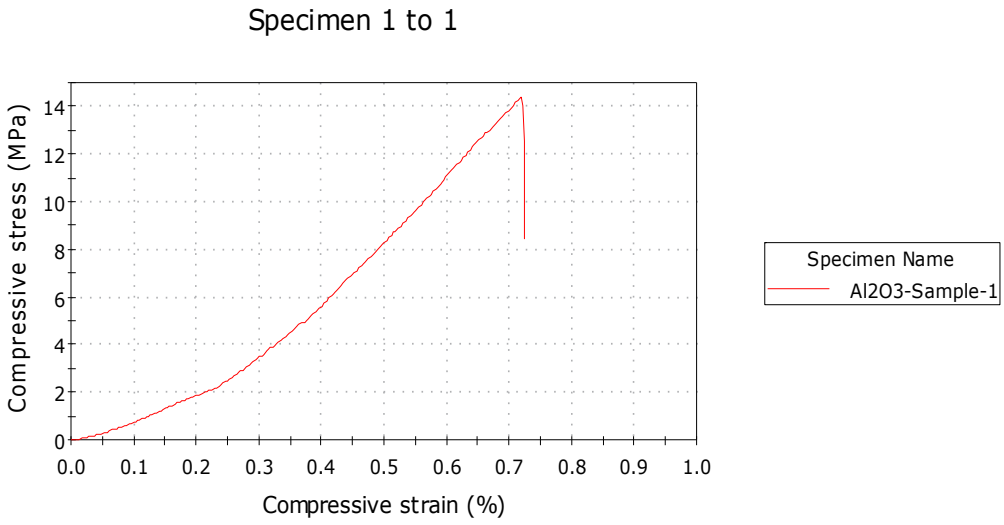

Figure 4.10 Diametral compression test curve

4.2 Deposition of meso-porous TiO_2 layer

For the deposition of defect free titanium dioxide layer, the crucial factors are the integrity of TiO_2 layer and the good adhesion with the α-alumina substrate. Therefore, several experimental tests were performed to investigate the surface morphology of TiO_2 coated on alumina substrate by using two different deposition methods.

4.2.1 SEM analysis for manually and automated coated titania layer

The TiO_2 sol was double and triple coated in order to deposit a layer with good integrity, uniformity and crack free surface. The titanium dioxide thin film was gold coated using ion sputtering machine and examined in SEM to characterize the surface morphology and structure. Figure 4.11 shows scanning electron microscope images of single coating of TiO_2 on alpha alumina substrate for 1min at different magnifications. It is can clearly seen that the TiO_2 layer is formed and is confirmed by EDS but the layer is cracked.

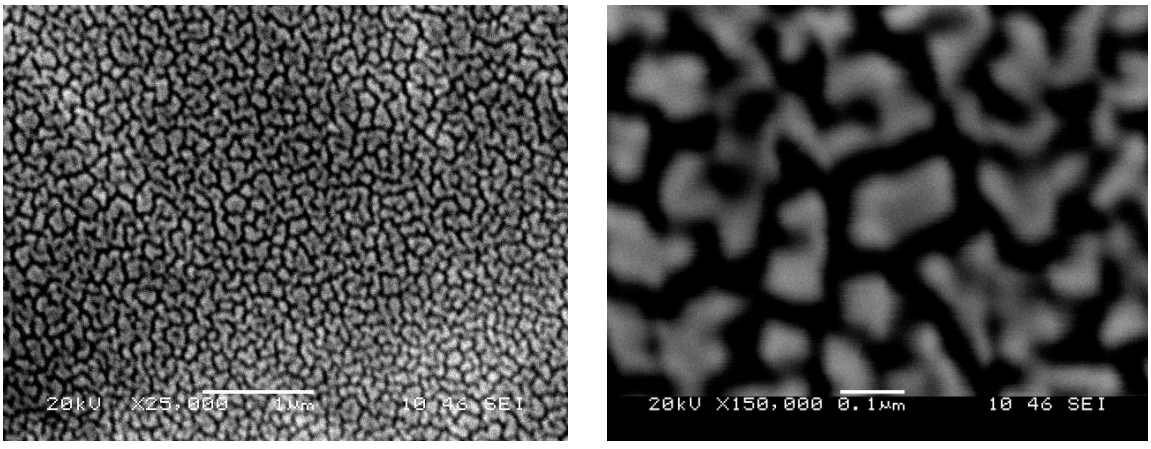

(a) (b)

Figure 4.11 SEM images of TiO2 colloidal sol single coating on alumina substrate at different magnifications (a) × 25,000 (b) ×150,000.

In order to close the crack multiple coating was applied on the alumina substrate and the SEM image can be seen in the Figure 4.12. Though after double coating for 1 min and drying at each step, still it appears cracks on the surface of TiO_2 layer. The reason for this cracking could be either due to uncontrolled heat treatment or drying. As drying is one of the most important factor because in this step large stresses develop due to capillary forces that cannot be relaxed by shrinkage because of existence of rigid support [37]. If this developed stress increases to a certain limit the layer gets cracks and sometimes it peels it off from the support.

Heat treatment is another important parameter. During this heat treatment all the solvents and other residual organic matters and nitrides are removed. The heating and cooling process which develops stresses due the coefficient of thermal expansion, there will be a mismatch between the support and the layer applied which results in cracking or delaminating of the surface. So this has to be controlled by gradually heating and cooling during the sintering process. So in order to get a crack-free and uniform layer heat-treatment, drying, dipping and withdrawal time of the substrate should be controlled. Therefore the automated dipcoating method was tried by controlling the parameters with slow heating and cooling rate.

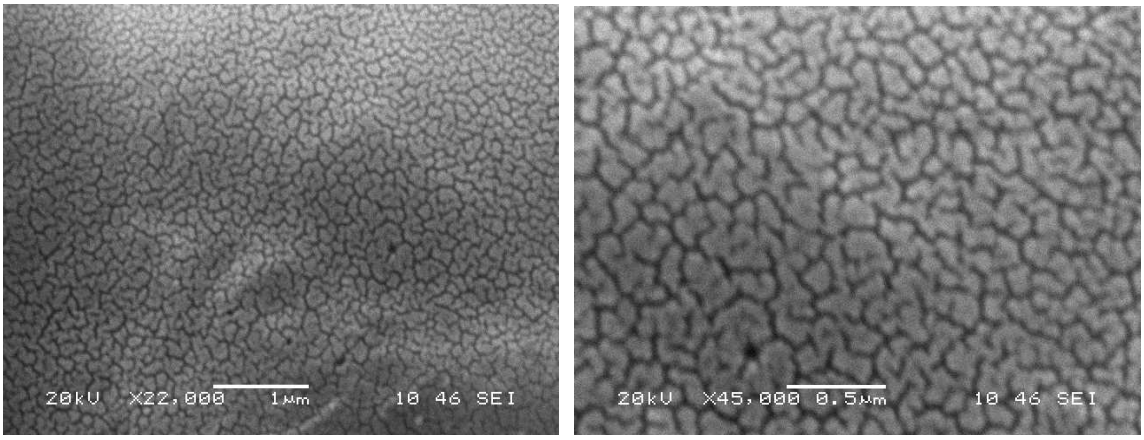

(a) (b)

Figure 4.12 SEM images of TiO_2 colloidal sol double coating on alumina substrate at different magnifications (a) × 22,000 (b) ×45,000.

Figure 4.13 shows the SEM image of a cross-section of the meso-porous TiO_2 layer coated on α-alumina substrate for 15min with the controlled dipping and withdrawal time of 1.4 mm/s and then dried and calcinated at 500°C for 1°C/min heating and cooling rate.

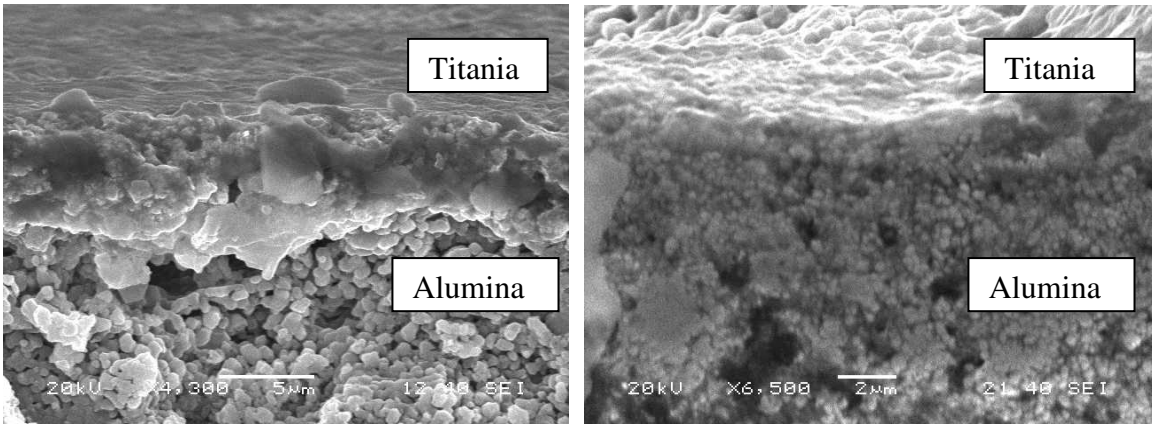

(a) (b)

Figure 4.13 SEM image of cross-section of triple coated titania layer on α-alumina substrate at two different magnification (a) × 4,300 (b) ×6,500.

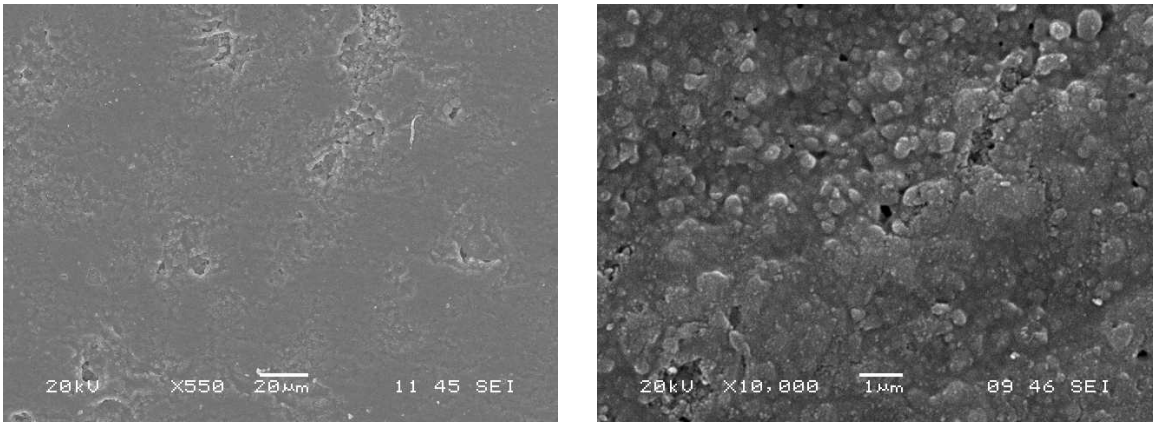

(a) (b)

Figure 4.14 SEM images of TiO_2 triple coating on Al_2O_3 substrate (dipping time 15min, heat treated at 500C, 1h), at magnification (a) × 550 (b) ×10,000 .

The thickness of the meso-porous layer was approximately 1 μm or less, which appears a thick coating due to the porous structure and surface irregularity of α-alumina substrate. From the Figure 4.14 a uniform and homogenous titania layer is seen on the surface of α-alumina substrate.

The TiO_2 coating was also deposited on a glass as well as on 316L stainless steel substrates in order to observe how the multi-coating layers are developed and connected to each other. The titanium dioxide sol solution was coated on the glass and steel substrate. Prior to coating they were cleaned thoroughly using acetone, alcohol and distilled water in order to get rid of any loose particles and contaminants and ultrasonicated for 20mins. Figure 4.15 shows the SEM image of a triple coating TiO_2 layer on glass substrate, which exhibits a crack free and uniform layer similar to that reported by Abdul Hameed [75]. Similarly the TiO_2 sol was double coated on the steel substrate for 15min and heat treated at 500°C for 1h. Figure 4.16 displays SEM images of

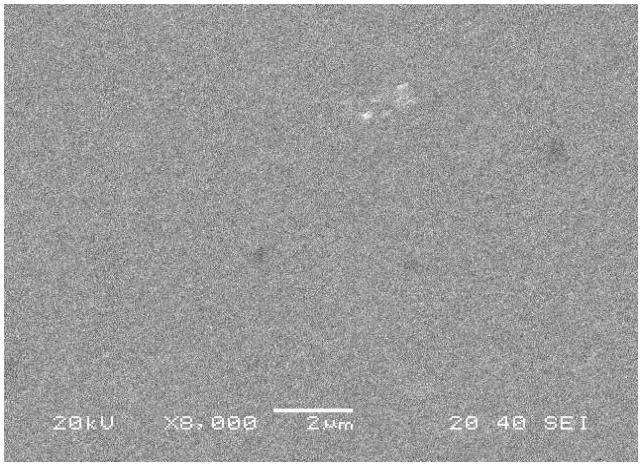

Figure 4.15 SEM image of triple coated TiO_2 film on glass substrate.

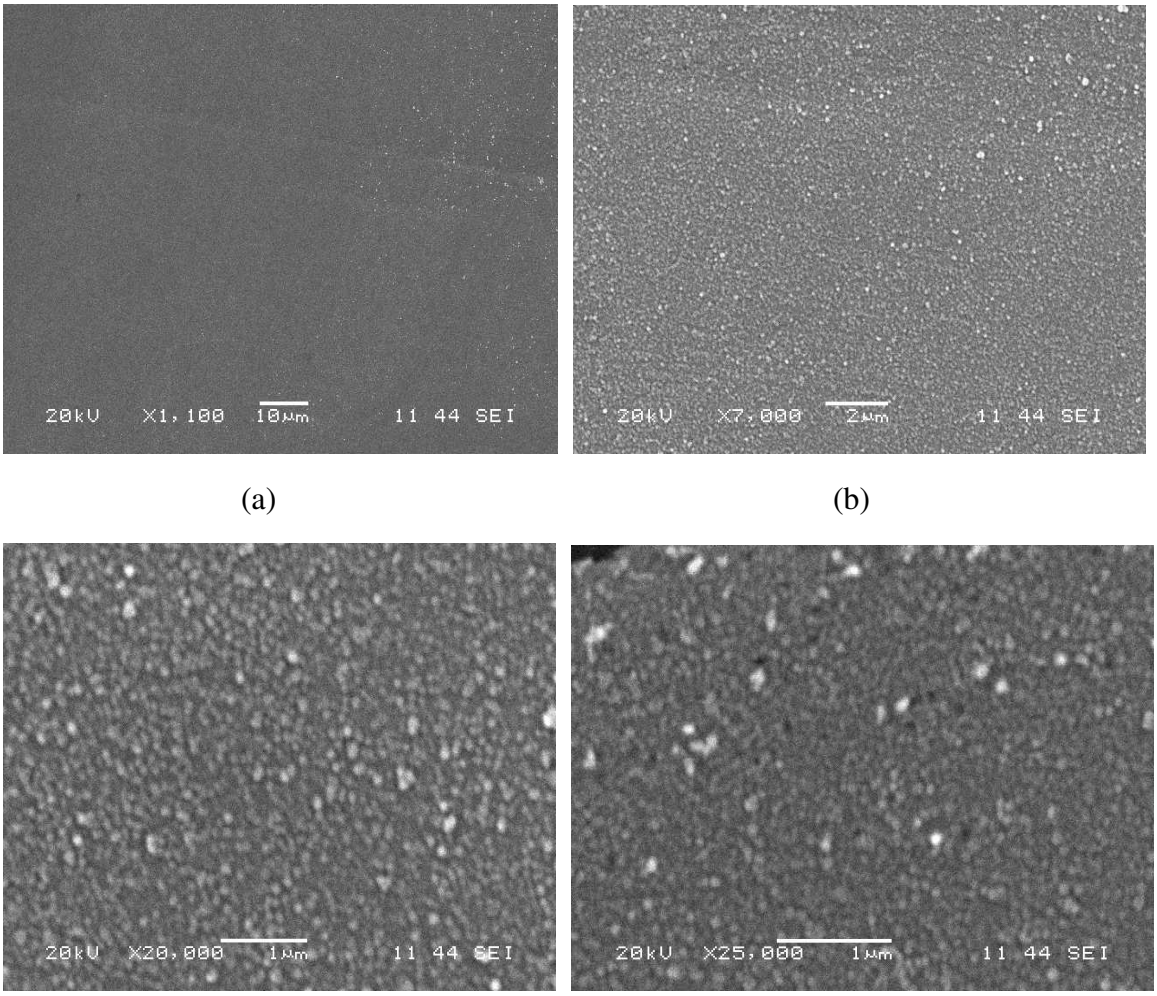

(a) (b)

(c) (d)

Figure 4.16 SEM images of TiO_2 double coated film on 316 stainless steel substrate at different magnifications (a, b, c, d).

porous TiO_2 structure with uniform and crack free surface on 316 stainless steel substrate at two different magnifications.

4.2.2 X-Ray Diffraction results for mesoporous TiO_2 layer

To characterize the crystal structure of titanium dioxide powder and phases of the thin film were observed by X-ray diffraction. The 2θ range was given from 5º to 90º with a step size of 0.05º for 35 min and the diffracted intensity was measured at 0.5º incident angle. The TiO_2 dry powder obtained by using the similar sol-gel process which was used to prepare the TiO_2 layer. The titanium dioxide powder was heat treated at 450°C for 1h and measured by XRD with Cu Kα radiation. Figure.4.17 shows the XRD patterns of the titanium dioxide powder which indicates the crystallized anatase type phase without any other phase.

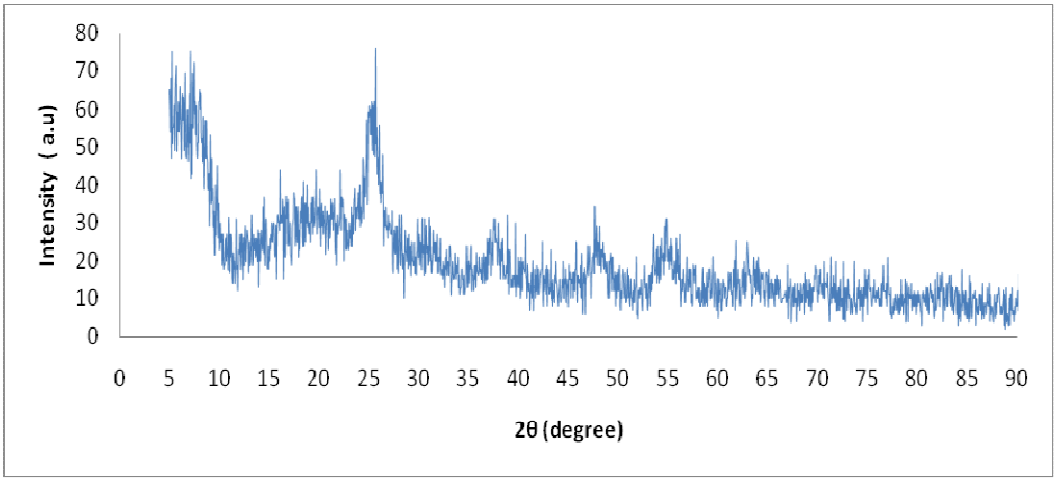

Figure 4.17 XRD pattern of anatase- TiO_2 powder obtained by Sol-Gel method and heat treated at 450°C, 1h.

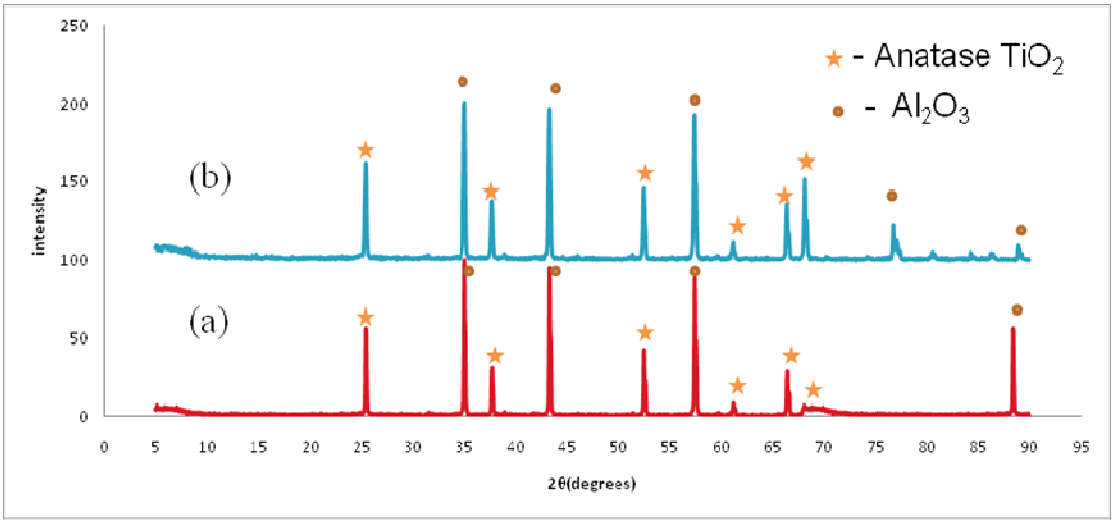

Figure 4.18 XRD patterns of anatase patterns of double (a) and triple (b) coated titania layer on α-alumina substrate

The double and triple coated TiO_2 layer on alumina substrate was very well crystallized and anatase phases are observed at good intensity as shown in figure 4.18. Therefore it confirms that the film was a titania with peaks for the anatase phase for the both double and triple coated TiO_2 layers.

4.3 Porosimetry measurements

Alumina substrate and titania deposited Al_2O_3 substrate were subjected to high pressure mercury intrusion, up to 60,000psi to measure the average pore size and porosity using Autopore IV Mercury Porosimetry. The relation between the minimum pore size diameter and the applied pressure is given by Washburn's equation [76]:

$$D = -4\gamma \cos\theta / P$$

Where γ is the surface tension, D is the diameter of the pore and P is the applied pressure.

The above relationship indicates that the size of the pore into which mercury will intrude is inversely proportional to applied pressure.

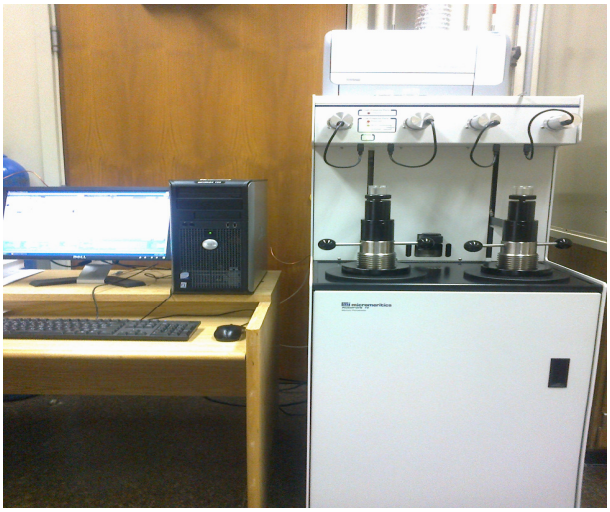

Figure 4.19 Mecruty Porosimeter

The size of the pore can be determined by substituting the pressure values in the equation, as the volume of the mercury that intrudes into the sample due to an increase in pressure from Pi to Pi+1 is equal to the volume of the pores in the associated size range ri to ri+1.

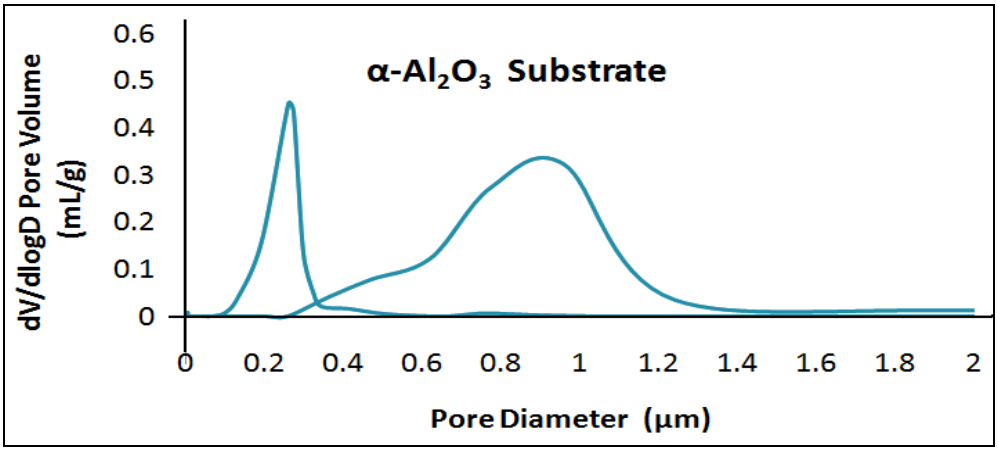

Figure 4.20 Pore size analysis and its distribution of alumina substrate

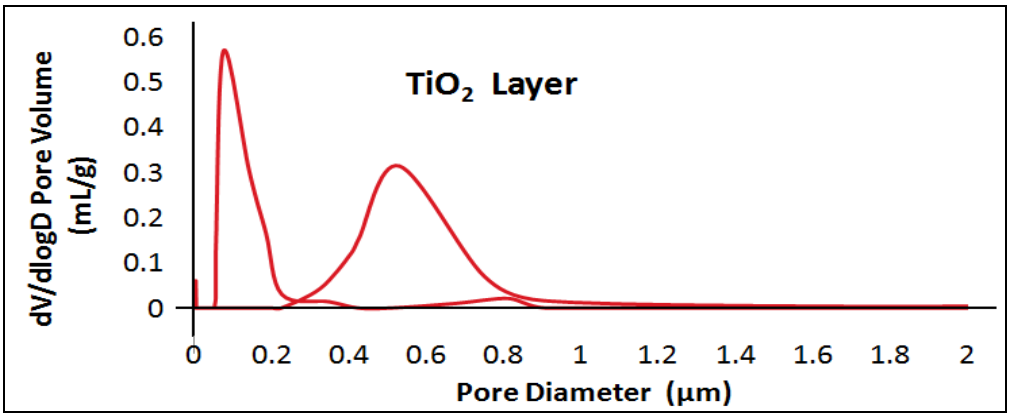

Figure 4.21 Pore size analysis and its distribution of TiO_2 coated alumina substrate

Figure 4.20 and 4.21 shows the graph plotted with pore diameter on x-axis and the pore volume on y-axis. It shows two curves which are the result of intrusion and extrusion of mercury into the sample to find the distribution of pores related to pore volume. During intrusion process in alumina substrate (Figure 4.20) a sharp peak created at the pore diameter of 0.25µm which is the average pore diameter, similar to that obtained from SEM images shown above section (Figure 4.7). The extrusion curve shows a broader peak which shows pore size distribution on the surface with a range of 0.4 to 1.2 µm pore diameter. After depositing the titania layer on the Al_2O_3 substrate the both peaks has been shifted to lower pore diameter side as shown in Figure 4.21. The first peak results in an average pore diameter of 80nm and the second curve which represents the distribution of pores on the surface in a range of 0.2 to 0.7 µm pore diameter. Therefore, by deposition of TiO_2 the average pore diameter has been decreased from 250nm to 80nm approx but the distribution of pores on the surface has been decreased as the area under the curve from Figure 4.21 is lower when compared to alumina substrate. By this decreased pore size it helps to bridge the pore size gap between the substrate and the top or active layer.

4.4 Synthesis of micro-porous LTA Zeolite layer

The mesoporous TiO_2 layer coated on α-alumina substrate plays an effective role in getting defect-free and continuous LTA zeolite layer. This titania mesoporous layer was exposed to UV light for 2h in a closed box. The mechanism what exactly happens after UV irradiations on to mesoporousTiO_2 layer was explained by van den Berg and co-workers.

TiO_2 + Photon energy → e^- + h^+ (step 1)

$O(O)^{2-}$ + $2h^+$ → V(O) + 0.5 O_2 (step 2)

Ti^{4+} + e^- → Ti^{3+} (step 3)

From the above reactions, the step 1 shows that photon energy releases an electron (e^-) from the atomic grid in such a way that the positive hole (h^+) was created on that spot where the electron is missing. When two holes meet an $O(O)^{2-}$ combination(a three-coordinated surface oxygen atom and an neighboring two co-ordinated O^{2-} surface bridging oxygen ion), they come together and form gaseous oxygen and an oxygen vacancy as written in the step-2. In order to keep all charges balanced, Ti^{4+} ions are reduced to Ti^{3+} which is shown in step-3 [70].

The vacancy of oxygen absorbs water molecules, leading to Ti-OH groups at the surface of the mesoporousTiO_2 supported α-alumina substrate and therefore the surface of the support becomes more hydrophilic. This UV irradiated surface helps to attract in-situ grown of LTA zeolite nuclei. It allows the intense interaction between synthesis gel and

the mesoporous titania coated alumina support. In general, the binding of LTA zeolite to support is by means of condensation reactions with support surface OH-groups [69]. Therefore the attachment of LTA zeolite to the support surface increases with increased hydrophilicity.

4.4.1 SEM and XRD Analysis for multiple microwave synthesis

The formationof LTA zeolite membrane using multiple microwave heating synthesis was characterized using scanning electron microscope and X-ray diffraction techniques. The XRD patterns of LTA zeolite membrane synthesized on mesoporous TiO2 coated α-alumina support using multiple microwave heating (MH) synthesis is shown in Figure 4.22. The 2θ range was given from 5º to 80º with a step size of 0.02º for 35min. The diffracted intensity was measured at 0.5º incident angle.

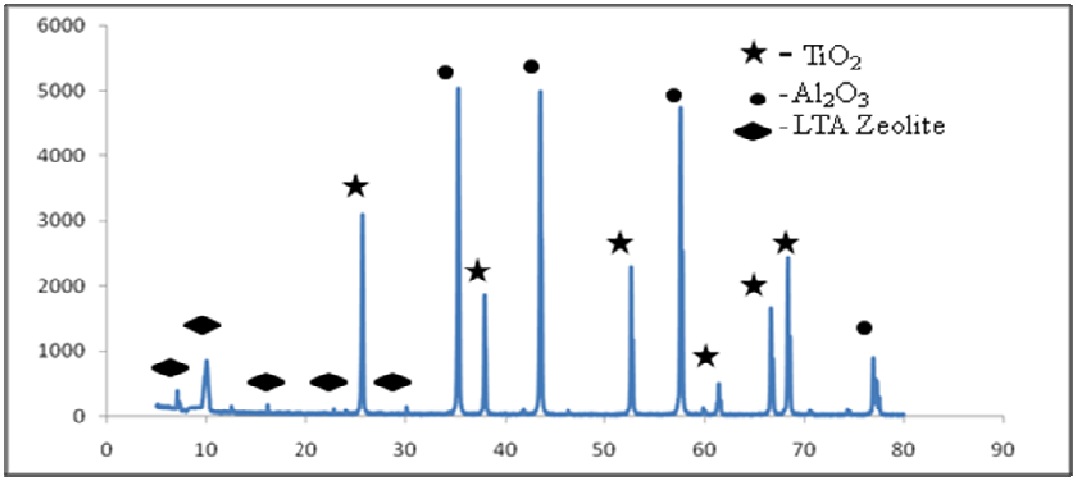

Figure 4.22 XRD patter for prepared LTA zeolites layer by Multiple MH synthesis method

The microwave heating synthesis was repeated consecutively three times at synthesis temperature of 90°C for 15 min. The XRD was measured with Cu Kα radiation. From the Figure 4.22, the diffraction patterns for the obtained membrane are represented by the peaks of alpha-alumina, titania and LTA zeolites. No other phase or diffraction patterns exist.

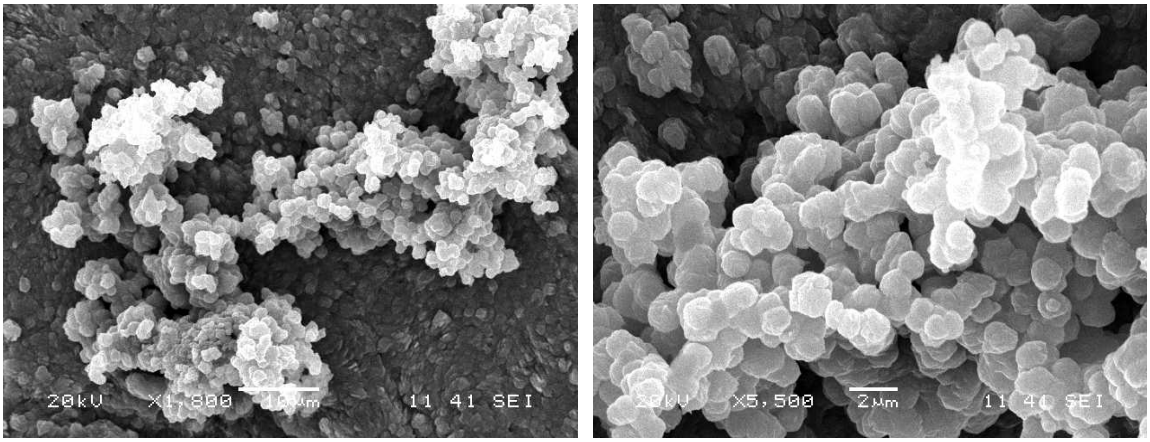

(a) (b)

Figure 4.23 SEM images of LTA zeolite membrane on mesoporous TiO_2 layer using multiple MH synthesis method at different magnification (a) ×1,800 (b) ×5,500.

Though the peaks of LTA zeolite have less intensity which were matched at the same angle represents the presence of LTA zeolite membrane but with less coverage on the surface. The composite (Al_2O_3/TiO_2/LTA) zeolite membrane was further characterized by scanning electron microscope. Figure 4.23 shows the SEM images of LTA zeolite membrane on mesoporous TiO_2 layer coated alpha-alumina substrate using multiple MH synthesis method. The coverage of the LTA zeolite crystals on the substrate was randomly covered at different spots.

During the first synthesis the crystal formed on the surface were again grown and gets attracted at the same spot when the second synthesis is carried out with new synthesis mixture forming the aggregates. Similarly, it happens in the third synthesis. The reason for discontinuous layer on the support surface may be due to insufficient time for the synthesis mixture to form the maximum number of nuclei. During the synthesis, the produced small number of nuclei was coated on the support surface randomly due to which the crystallization takes place at that particular spots resulting in incomplete coverage of zeolite layer on the substrate. Therefore it was difficult to get the full coverage by using direct multiple MH synthesis without aging or not giving proper time to form the nuclei, which was also reported elsewhere [71].

4.4.2 In-situ aging microwave heating synthesis

In this method, the solution mixture (aluminate and silicate) is first aged in an air oven with the UV irradiated titania coated alumina substrate and fitted with a PTFE holder in an autoclave reactor (this process is called “in-situ aging”), then crystallization is carried out using microwave heating. The effect of in-situ aging time and synthesis time on (i) the formation of gel layer; (ii) on the crystallization during the MH synthesis (iii) as well as on the coverage, was investigated by varying synthesis parameters and by comprehensive characterization through scanning electron microscope and X-ray diffraction techniques. Since in the autoclave, the nuclei are not formed simultaneously on the support surface because of low dissolution rate of synthesis gel and slow heating rate. Therefore it needs enough time for the formation of nuclei during aging to get the support surface covered with synthesis gel. To study the effect of in-situ aging time on the coverage of the support surface by synthesis gel, different aging times of 4, 7 and 12

h were studied. Once the required in-situ aging time to cover the surface with the amorphous gel layer is known, then with that optimized in-situ aging time, the microwave heating synthesis was studied by varying the synthesis time for 5, 10 and 15min in order to study the effect of crystallization time on the morphology of the synthesized LTA zeolite layer.

4.4.3 Effect of in-situ aging time

In-situ aging followed by microwave heating synthesis was used to prepare a successful continuous LTA zeolite membrane that which is not obtained if we use directly MH synthesis. In-situ aging helps for nucleation and to accelerate the formation of LTA zeolite under microwave heating. These results are in good agreement with previous report elsewhere that the heterogenous nucleation and growth of LTA zeolite on the support surface can only be boosted by in-situ aging [67].

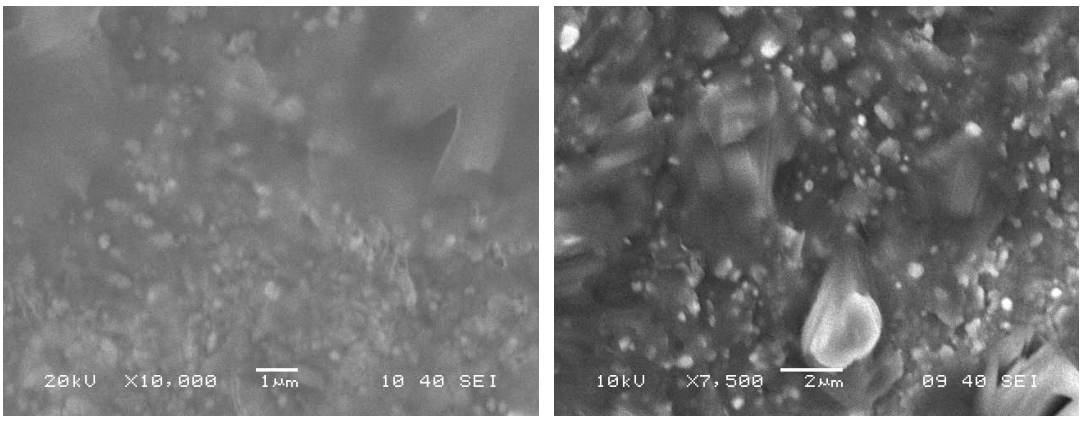

(a) (b)

Figure 4.24 SEM image after 4hrs of in-situ aging on titania/Alumina substrate at different magnification.

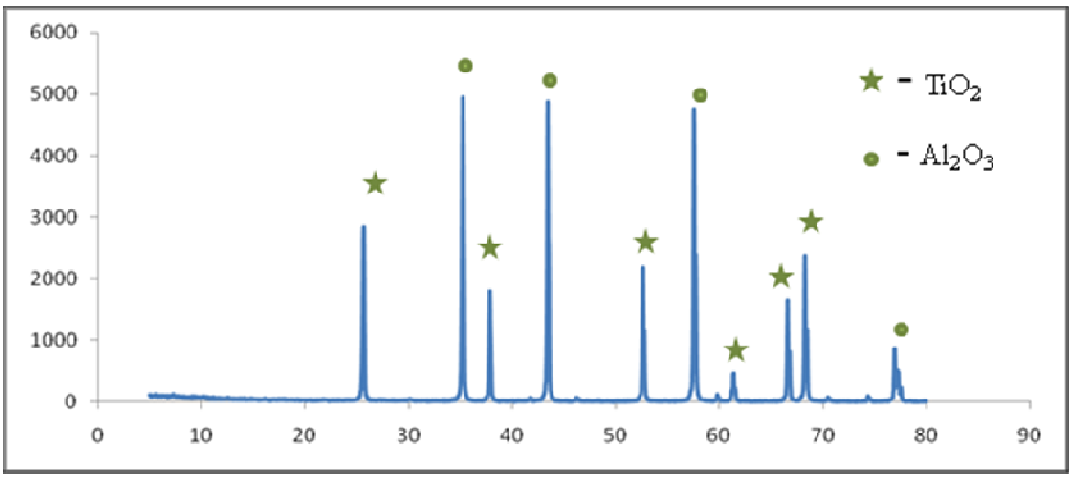

Figure 4.25 XRD pattern after 4hrs of in-situ aging on titania/Alumina substrate

To study the morphology of the LTA zeolite layer produced after suitable in-situ aging time by studing the effect of aging time for 4h, 7h and 12h. Figure 4.24 shows the scanning electron micrograph after 4h of in-situ aging under conventional heating. A thick gel was formed on the support surface along with the amorphous aggregate like spots. This synthesis gel with time gets covered with the amorphous like spots and spread over the surface of the support.

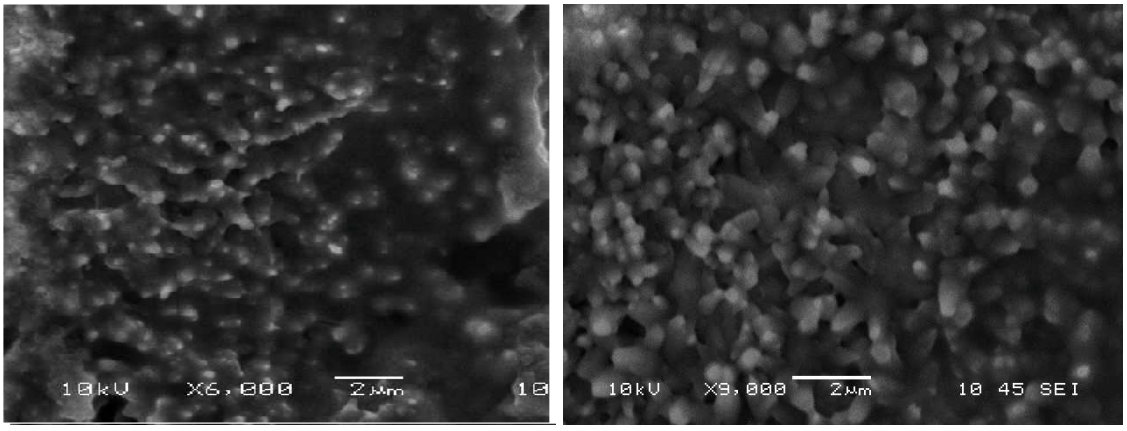

(a) (b)

Figure 4.26 (a,b) SEM images of the gel layer formed on the titania-alumina substrate after in-situ aging for 7hr at 50°C.

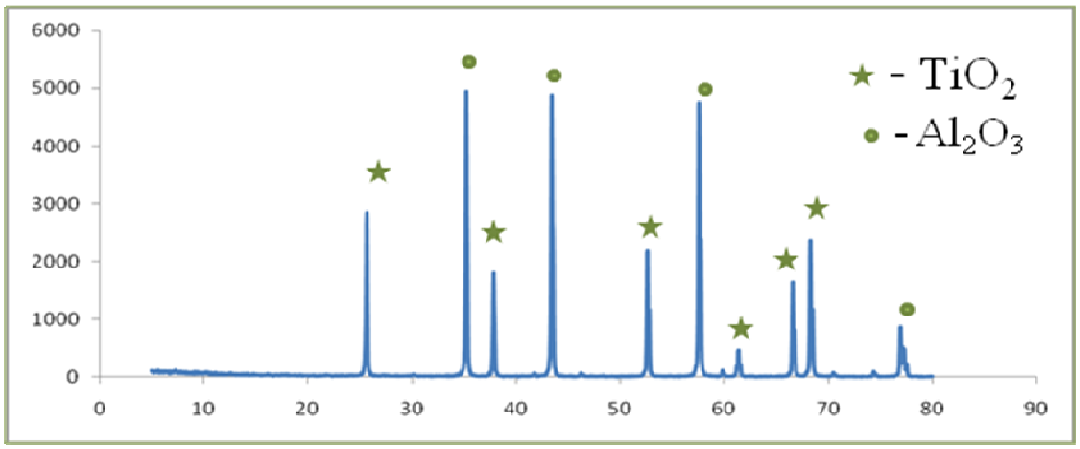

Figure 4.27 XRD patterns of the TiO_2 coated Al_2O_3 support after in-situ aging for 7hr in autoclave reactor at 50°C.

From Figure 4.25, it shows the XRD patterns after 4 h of in-situ aging on mesoporous TiO_2 coated alumina support. There is no LTA zeolite peaks detected other than alumina and titania peaks. This represents that the gel layer formed is amorphous. Figure 4.26 shows the SEM image of the gel layer formed on the titania/alumina substrate after 7hrs of in-situ aging at 50°C. It can be seen that the amorphous gel covering almost the entire substrate's surface with aggregate amorphous spots when compared to the 4 h of aging. This represents that 4h of aging is not enough to get complete nucleation covering the whole support surface. The X-ray diffraction pattern, as shown in Figure 4.27 gives the XRD patterns of the membrane before MH synthesis i.e, after in-situ aging for 7h. The obtained pattern represents only the peaks of alpha-alumina and titania. This shows that the covered synthesis gel nuclei formed on the surface of substrate is amorphous. After that, we tried to age the synthesis solution along with substrate for 12 h to see the effect of long hour aging.

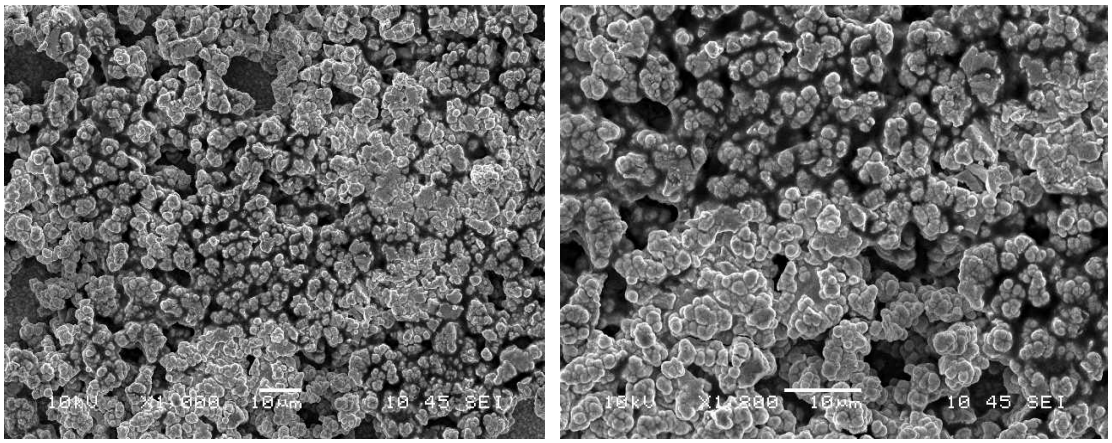

(a) (b)

Figure 4.28 SEM image after 12hrs of in-situ aging on Titania/Alumina support surface at different magnification.

From Figure 4.28 it shows the SEM image after 12hrs of in-situ aging which indicates that the nuclei has grown in to bigger size crstals when compared to aggregate amorphous spots formed at 7hrs of aging time (figure 4.26).

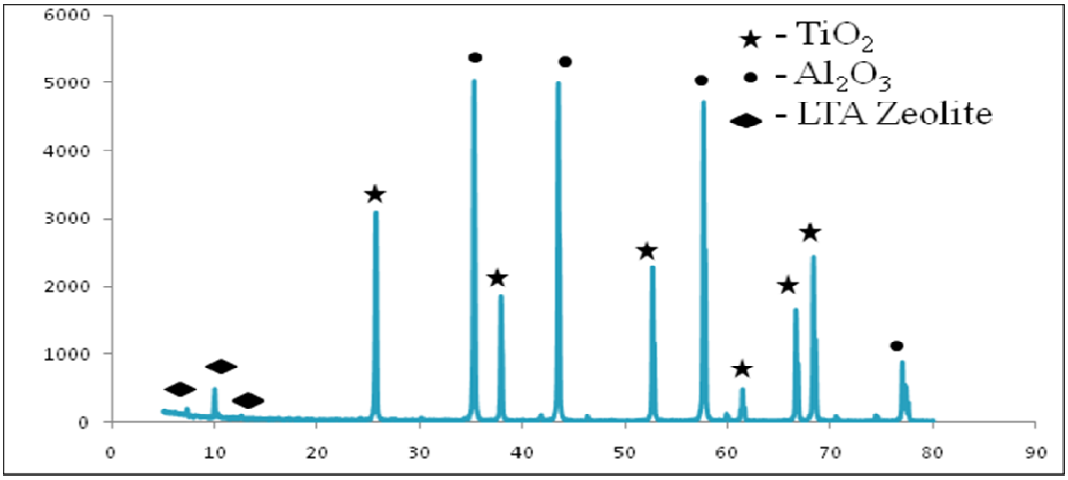

Figure 4.29 XRD pattern after 12hrs of in-situ aging on Titania/Alumina support

This indicates that crytallization has started at some places forming zeolites cyrstals due to long hours of aging. The XRD pattern from the figure 4.32 shows that at 12hrs of

aging time, LTA zeolite peaks was also detected along with the Al_2O_3 and TiO_2 peaks. This represents that for long hours of aging the crystallization starts, turning amorphous synthesis gel to zeolite-A crystals.

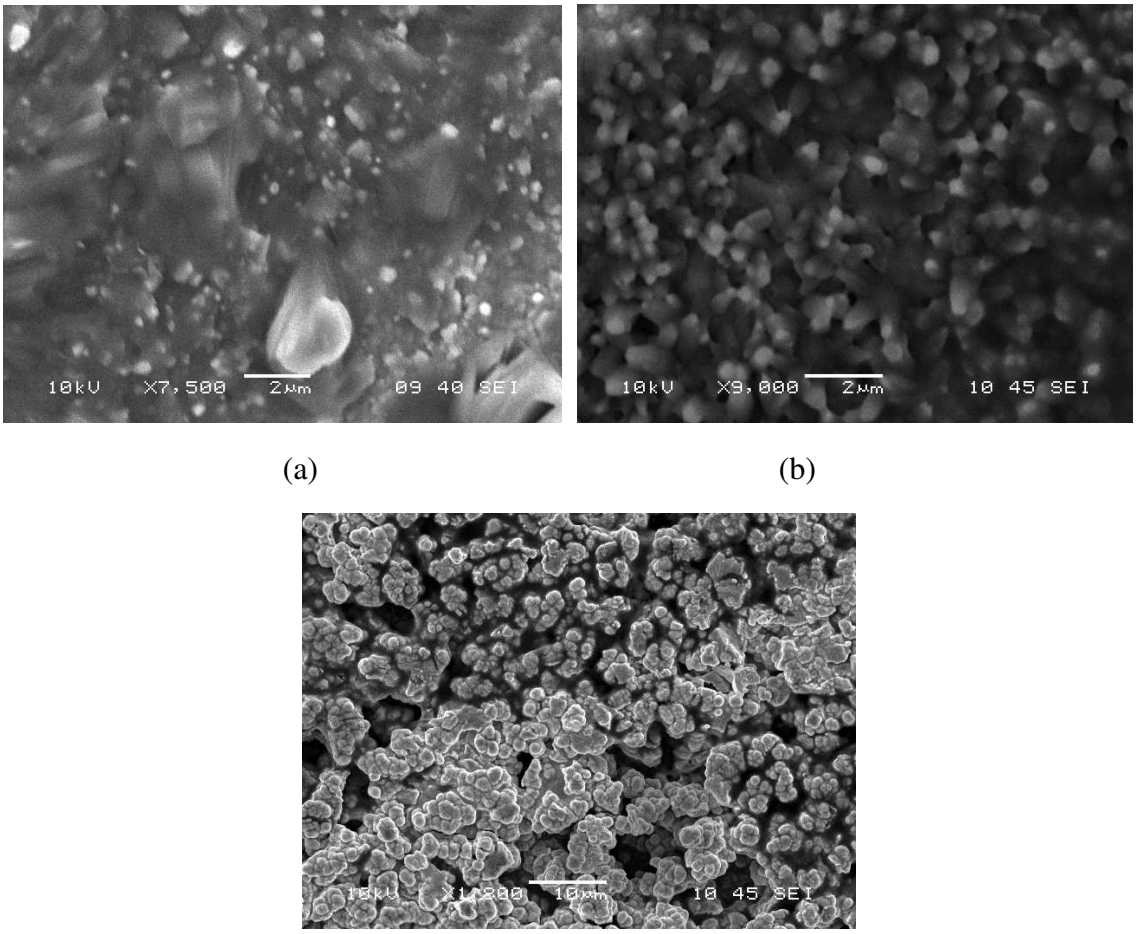

(a) (b)

(c)

Figure 4.30 SEM images of in-situ aging on TiO_2 coated Al_2O_3 substrate after(a) 4hrs, (b) 7hrs, and (c) 12hrs of aging time.

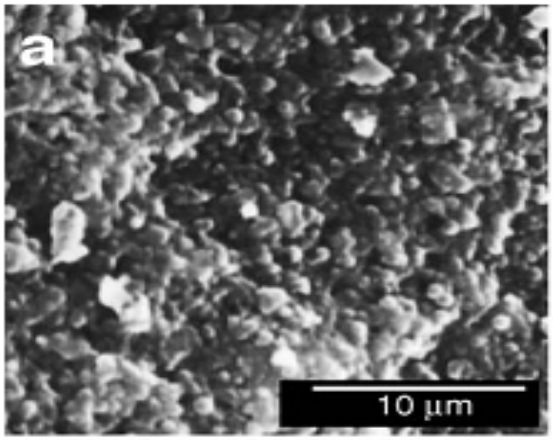

Figure 4.31 SEM images of the as-synthesized membranes prepared by in-situ aging method, 7hr at 50°C

The comparision of all the three conditions at different aging time of 4h, 7 h and 12 h as shown in Figure 4.30, the 7 h in-situ aging time was the best suitable inorder to cover the maximum surface with the aggregate amorphous like spots which was also reported by Li and co-workers as shown in figure 4.31 [67]

4.4.4 Effect of microwave heating synthesis time

After the zeolite nuclei or gel layer with amorphous spots are formed on the titania coated alumina substrate during the in-situ aging at 50°C for 7 h in an air oven, microwave-assisted hydrothermal synthesis was then carried out to crystallize the formed amorphous gel. Therefore, in this case microwave heating time or synthesis time plays an important role on the crystallization and to get a continuous LTA zeolite membrane.

In order to study the effect of synthesis time on continuity and crystallinity of the LTA zeolite layer, the synthesis time was varied to 5 min, 10 min and 15 min at 90°C microwave heating temperature with the controlled in-situ aging time of 7 h at 50°C.

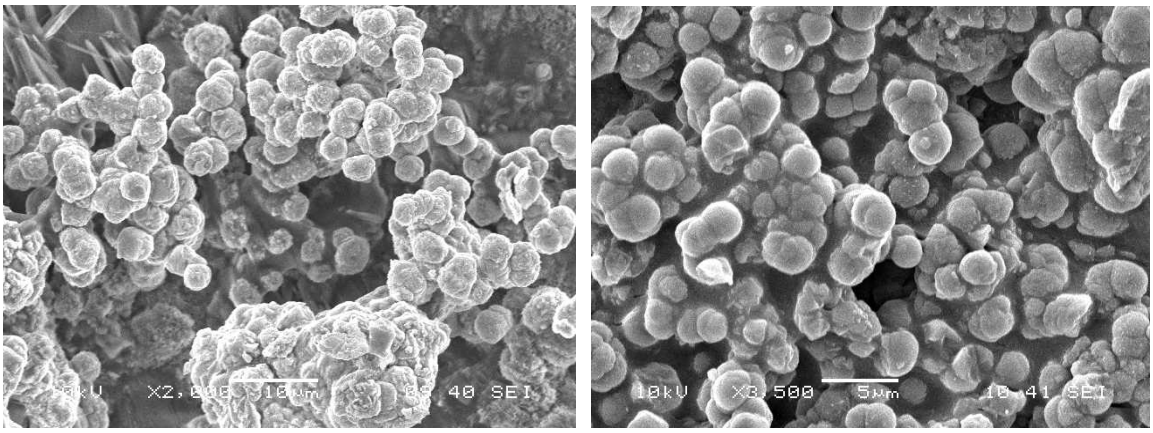

(a) (b)

Figure 4.32 SEM images of LTA zeolite layer formed at different synthesis time using in-situ MH synthesis. (a) 5min (b) 10min synthesis time

From the Figure 4.32(a, b) shows the SEM image of 5min and 10 min synthesis time at 90°C microwave heating temperature. It indicates that spherical shaped crystals are formed on the support surface and the layer is not continuous which corresponds to incomplete crystallization. The XRD pattern in Figure 4.33 shows for 10min of MH synthesis time. The difference between the 5 and 10 min synthesis time from the SEM images is that 10 min synthesis time gives more crystallized zeolite product with time whereas in 5min synthesis time there are few amorphous aggregates along with crystallized LTA zeolite.

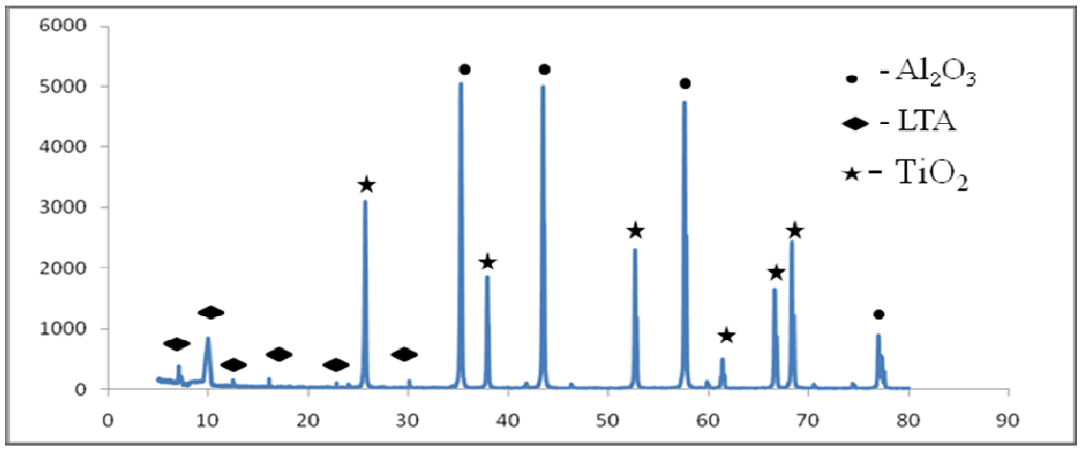

Figure 4.33 XRD images of LTA zeolite layer formed using in-situ aging (for 7hr at 50°C) and 10min of MH synthesis time.

The synthesis for microwave heating to crystallize the amorphous gel layer formed on the substrate was carried out at 90°C for 15min at the ramp up time of 90 s. Figure 4.34 shows the XRD patterns of MH synthesized layer of LTA zeolite on titania coated alumina substrate. The peaks obtained indicates the formation of very good crystalline zeolite peaks along with the peaks of titania and alpha-alumina. By matching the peaks from the literature at the different angles it was confirmed that the formed layer was LTA zeolite layer.

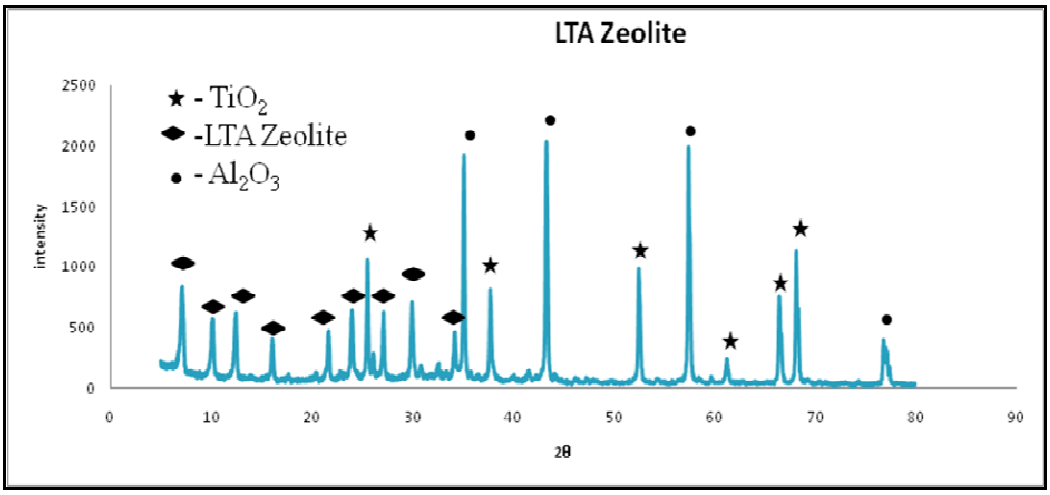

Figure 4.34 XRD patterns of in-situ aging MH synthesized (at 90°C for 15min) layer of LTA zeolite on titania coated alumina substrate

From Figure 4.35 which represents the SEM images of cubic shaped continous and dense layer of LTA zeolite membrane was formed at 90°C and 15min of synthesis time. The crystal size on the support surface is approximately in the range of 1-3 µm. This indicates that sufficient in-situ aging is necessary to form the gel layer on the support surface before the microwave heating synthesis for crystallization. However, the similar experiment was performed by Li et al with 15 min synthesis time and 90°C MH temperature, the LTA zeolite layer obtained on alumina substrate was not continuous as shown in Figure 4.36 [67].

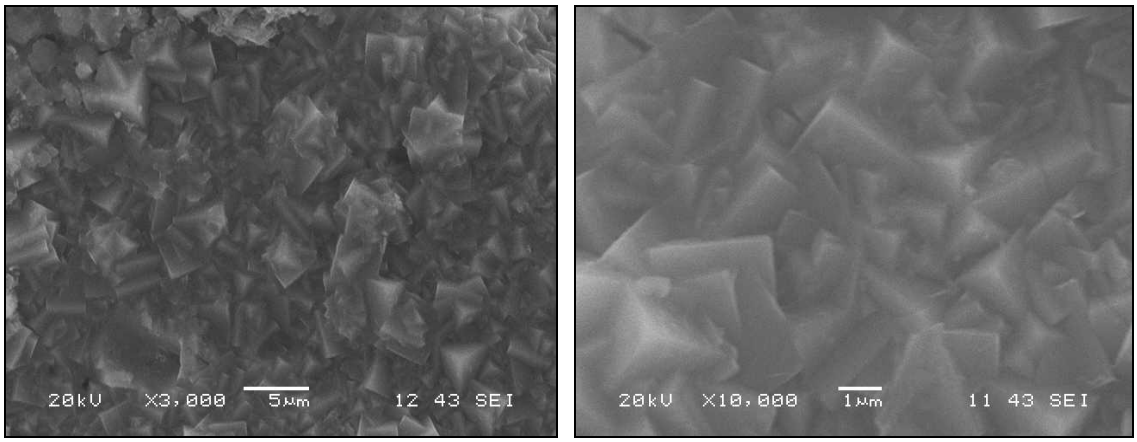

(a) (b)

Figure 4.35 (a&b) SEM images of the continuous and dense layer of LTA zeolite membrane synthesized at 90°C for 15min using in-situ aging MH synthesis method at different magnification.

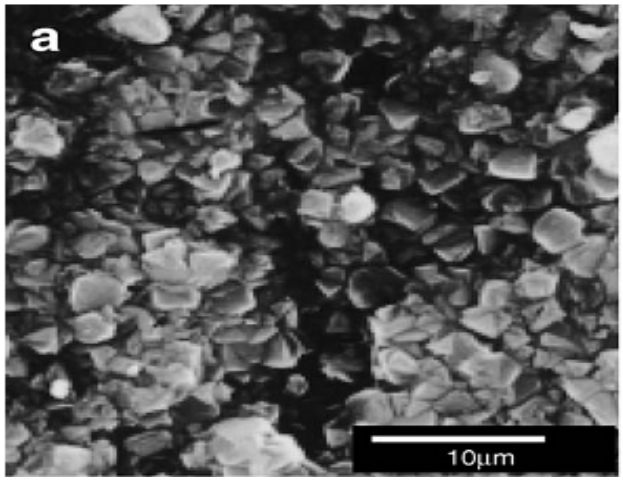

Figure 4.36 SEM image of LTA zeolite layer formed by using in-situ aging MH synthesis at 90°C for 15 min synthesis time [67].

The reason that a continuous LTA zeolite layer was obtained in this work could be due to the deposition of UV irradiated mesoporous titania layer on alumina substrate instead of directly synthesizing the zeolite layer on macroporous alumina substrate. The UV irradiated mesoporous TiO_2 layer played a major role in getting the support surface

hydrophilic by which Ti-OH groups on the surface were increased in number. Thus this enhanced the interaction between the substrate surface and the synthesis gel allowing the attachement of amorphous gel to cover almost the entire substrate's surface. This results in a continuous dense layer of LTA zeolite during microwave heating without any defect. Thus, mesoporous intermediate layer between the alumina support and the top microporous layer is very efficient to get continuous and dense layer of LTA zeolite.

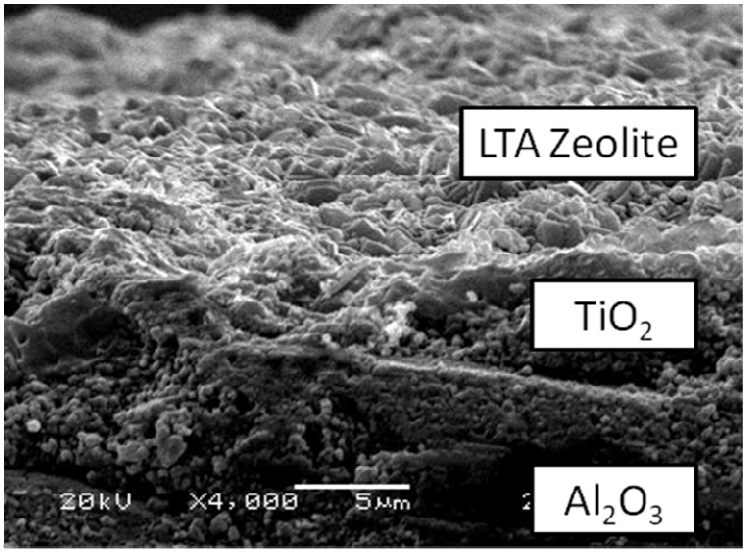

Figure 4.37 SEM images of cross-section of LTA zeolite membrane synthesized at 90°C for 15min using in-situ aging MH synthesis method at different magnification.

The cross-section of the formed multi layered membrane i.e, the macroporous alumina substrate, mesoporous titania layer and the microporous LTA zeolite layer as shown in figure 4.37. The estimated thickness of the microporous zeolite layer on the top of titania coated alumina substrate from the figure was about 1-3 μm. In order to confirm if the formed LTA zeolite layer was dense or with some of the pin holes, the membrane was tested using mercury porosimetry.

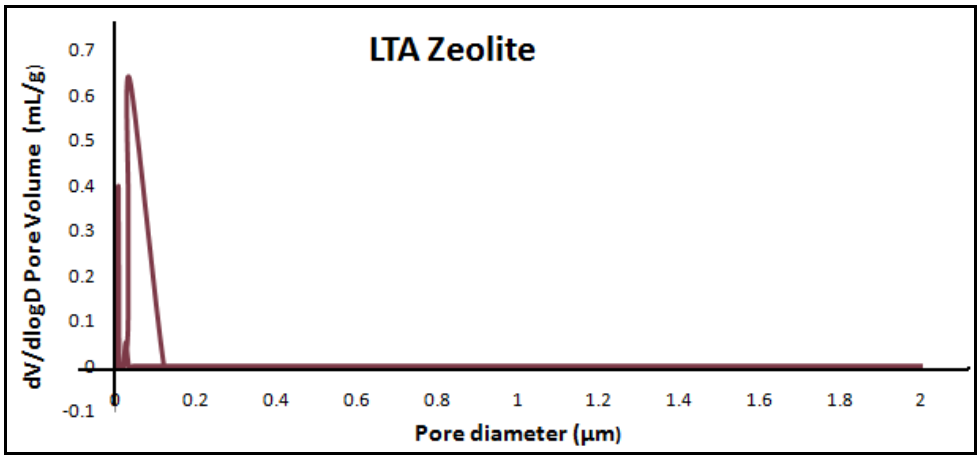

Figure 4.38 Pore size analysis and its distribution of LTA zeolite layer on titania coated alumina substrate.

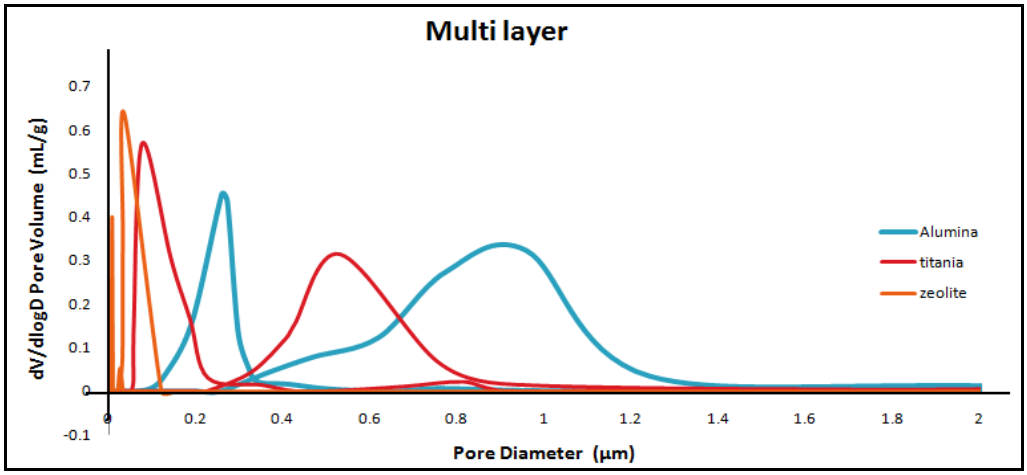

Figure 4.39 Pore size analysis and porosity of multilayer membrane overlapped.

The figure 4.38 shows the mercury porosimetry results with pore diameter on X-axis and pore volume on y-axis. The curve shown is the porosity curve which indicates number of pores formed on the membrane surface. Therefore the porosity from the figure gives the area under the curve which is 1%. Whereas the pore size is around 1 to 2 nm which is indicated by the sharp curve near the y-axis. From the figure 4.39, all the results of macroporous support, mesoporous layer and microporous layer are overlapped. From this

it indicates that the as the layers are deposited on the support surface the curves was shifting to left and extreme left showing the pore size and porosity were reduced and at the microporous layer the pore size obtained was 1 to 2nm and porosity of 1 %.

CHAPTER 5 CONCLUSIONS AND FUTURE SCOPE

The purpose of this study is to fabricate ceramic based multilayer membrane of porous structure with gradient porosity which has the potential to allow selective passage of species during purification process. In the present work, investigation was performed during preparation of the macroporous α-alumina support using powder metallurgy route, meso-porous titania layer using sol-gel dip coating method and microporous LTA zeolite layer by in-situ aging microwave heating synthesis method. The macroporous α-alumina support of 1-inch diameter and 2mm thickness was prepared by powder compaction process followed by sintering resulting in an average pore diameter of 2.5µm and porosity 30% as determined from SEM imaging and later confirmed using mercury porosimetry. The diametral compression strength test was performed on alumina substrate compacted at 620MPa and sintered at 1400ºC, resulting in compression strength of 14.87MPa. For the deposition of mesoporous titania layer with uniform and crack free surface, the parameters like dipping and withdrawal speed, heating rate and drying time were studied and controlled by depositing on different supports (alumina, stainless steel and glass). The deposited layer was dried at 200°C prior to calcination and then heat treated at 500ºC for 1h by controlling the heating and cooling rate at 1ºC/min. The results indicate that the meso-porous titania layer formed on top of the different substrates was uniform, crack free and continuous. The thickness of the deposited mesoporous triple coating titania layer was measured by SEM to be approximately 1µm. The X-ray diffraction analysis revealed that the mesoporous titania layer was crystalline and formed

anatase phase. The pore size analysis performed using mercury porosimetry yielded an average pore size of 80nm with 30% porosity. The microporous LTA zeolite layer for effective filtration was grown on top of mesoporous TiO_2 layer using in-situ aging microwave heating synthesis method. During In-situ aging (autoclave) step, aging time of 7hr at 50ºC was formed most suitable to cover the synthesis gel on the substrate. Microwave heating synthesis time was performed at 90°C for 15 min, crystals of 1-3 µm were grown yielding a continuous, crystalline and dense LTA zeolite. The thickness of the formed zeolite layer was measured to be approximately 2-3 µm by SEM. The pore size of the formed LTA zeolite layer was measured using mercury porosimetry resulting in the range of 0-2 nm approximately, which indicates that there are pin holes available on the formed LTA zeolite layer surface.

For future studies, the thickness and crystal size of LTA zeolite layer should be minimized for effective permeability. Finally, the permeation characteristics of the developed ceramic membranes should be tested using a test flow cell.

References

[1]. T. Younos, Kimberly E. Tulou, “Overview of desalination techniques”, Journal of Contemporary Water Research and Education, Issue-132, 2005(132): p. 3-10.

[2]. M. Soltanieh and William N.Gill, “Review of Reverse-Osmosis Membranes and Transport Models”, Chemical Engineering Communications, 1981. 12(4-6): p. 279-363.

[3]. B. Van der Bruggen, C. Vandecasteele, “Distillation vs. membrane filtration: overview of process evolutions in seawater desalination”, Desalination, 143(3) 2002, P: 207–218.

[4]. Lauren F., Desmond F., “Reverse osmosis desalination: water source, technology and today’s challenges”, Journal of water research, 43(2009) 2317-2348.

[5]. U. Merin, G. Daufin, “Separation Processes using Inorganic membranes in the food industry”, Proceedings of the First international Conference on inorganic membranes, in: Ref. [1], pp. 271-281(1989).

[6]. Erkki levanen, “Alumina membranes-colloidal processing and evolution of functional properties”, PhD thesis, Tampere University of technology, Publication-482, 2004.

[7]. L. Lin, K.C. Rhee & S.S.K, “Bench-Scale membrane degumming of crude vegetable oil: process optimization”, journal of membrane science, 134(1997), P: 101-108.

[8]. KANG Li, Ceramic membranes for separation and reaction-2007, P-306.

[9]. C.D.M Courtinho, M.C. Chiu,"State of art of the application of membrane technology to vegetable oils: A review", Journal of food research international, 42(5-6), P:536-550.

[10]. K.S.Ashaghi, M.Ebrahimi, "Ceramic Ultra and nanofiltration membranes for oil field produced water treatment: A mini review", Open environment journal, 2007, 1(1-8).

[11]. I.Yuji, K.Hiroshi, "Trends in Research and Development of Nanoporous Ceramic Separation Membranes", Science and technology trends, No-32, July-2009.

[12]. El-Dessouky, H.T. and Ettouney, H.M., "Fundamentals of Salt Water Desalination", 2002: Elsevier. 690.

[13]. R.Mallada, M.Menendez,"Inorganic Membranes: Synthesis, Characterization and Applications", Membrane Science and Technology, Elsevier (Text book)-2008.

[14]. H.A. Meinema and R.W.J. Dirrix, "Ceramic Membranes for Gas Separation – Recent Developments and State of the Art" Interceram, Vol. 54 (2005).

[15]. Anita Buekenhoudt, "Stability of Porous Ceramic Membranes", Membrane Science and Technology, Volume 13, 2008, Pages 1-31.

[16]. D.Chaudhary, P.Bishnoi,"Analysis of desalination of water by reverse osmosis", Project report, NIT,Jaipur, May-2010.

[17]. Perry, R.H., Green D.H., “Perry’s Chemical Engineers’ Handbook”, 7th edition, McGraw-Hill, 1997.

[18]. Niina Laitinen, “Development of a ceramic membrane filtration equipment and its applicability for different wastewaters”, Lappeenranta University of Technology, PhD thesis-2002.

[19]. Kritikaki, A. Tsetsekou, “Fabrication of porous alumina ceramics from powder mixtures with sol–gel derived nanometer alumina”, Journal of the European Ceramic Society, Volume 29, (2009) 1603–1611.

[20]. Berna Topuz and Muhsin, “Sol–gel derived mesoporous and microporous alumina membranes”, Journal of Sol-Gel Science and Technology, Volume 56, P: 287-299.

[21]. R. J. R. Uhlhorn, M. H. B. J. Huis, K. Keizer and A. J. Burggraaf “Synthesis of ceramic membranes” Journal of Materials Science, Volume 27(1992), P: 527-537.

[22]. Kanthima Hemra, A. Pavadee,“Development of ceramic membranes for micro and ultrafiltration: Part-1 preparation of Alumina support and alumina membranes for microfiltration”, National metal and materials technology centre, Bangkok.

[23]. G.C.C. Yang, Tubular TiO_2/Al_2O_3 composite membranes: preparation, characterization, and performance C.-J. Li / Desalination 234 (2008) 354–361.

[24]. T.Khalil, J. Bossert, “Preparation, characterization and application of alumina powder produced by advanced preparation techniques” Seventh Conference of Nuclear Sciences & Applications, 2000,Cairo, Egypt.

[25]. Joel S. Hirschhorn, “Intoduction to powder metallurgy”, American Powder Metallurgy Institute (APMI), 1976.

[26]. Gordon Dowson, “Poder Metallurgy: The process and its products”, Adam Hilger series, New York, USA-1990.

[27]. Cheng-Liang Huang, Jun-Jie Wang, “Sintering behavior and microwave dielectric properties of nano alpha-alumina”, Materials Letters, 59 (2005) 3746 – 3749.

[28]. Zhijian Huanga, Masahide Gotoh, “Improving sinterability of ceramics using hybrid microwave heating”, Journal of Materials Processing Technology,(2009), P: 2446–2452.

[29]. Ali Alem, Hossein Sarpoolaky, “Titania ultrafiltration membrane: Preparation, characterization and photocatalytic activity”, Journal of the European Ceramic Society 29 (2009) 629–635.

[30]. Zarina Abdul Wahid, Rafindde Ramli, “Performance of ceramic filters: Influence of particle sizes and sintering temperature”, Solid State Science and Technology, Vol. 17 (2009) 89-103.

[31]. C.Jeffrey.B, G.W.Scherer, “Sol Gel Science: The physics and chemistry of sol-gel processing”, Academic press, Elsevier-1990.

[32]. Leenaars, A. F. M. and Burggraaf, A. J., “The preparation and characterization of alumina membranes with ultra-fine pores”, Journal of Membrane Science, 24 (3): 245–260 (1985).

[33]. A. Ayral, C. Balzer, “Sol-gel derived silica membranes with tailored microporous structures”, Catalysis today, Volume 25, Issues 3-4, 1995, P:219-224.

[34]. Xu. Qunyin, “Physical and chemical factors affecting the synthesis and characteristics of transition metal oxide membranes”, University of Wisconsin, PhD thesis-1991.

[35]. U. Vijayalakshmi and S. Rajeswari, “Preparation and characterization of microcrystalline hydroxyapatite using sol gel method”, Trends Biomater, Artif. Organs, Vol-19(2), PP 57-62(2006).

[36]. Jelena Sekulić ,“Mesoporous and microporous titania membranes”, University of Twente, PhD thesis-2004.

[37]. Sumio sakka, “Sol-gel science and technology”, Kluwer Academic Publishers, Netherland-2003, P-230.

[38]. R.S. Sonawane a, S.G. Hegde ,“Preparation of titanium(IV) oxide thin film photocatalyst by sol–gel dip coating”, Materials Chemistry and Physics 77 (2002) 744–750.

[39]. M. Addamo, V. Augugliaro, “Photocatalytic thin films of TiO_2 formed by a sol–gel process using titanium tetraisopropoxide as the precursor”, Thin Solid Films 516 (2008) 3802–3807.

[40]. A.K. Arof and S.A. Hashim Ali, “Surface Morphology of Anatase TiO_2 Thin Film by Sol-Gel Method”, Materials Science Forum, Vol- 517, P: 135-140.

[41]. A. Nakaruk, C.Y. Lin., D. S. Perera, “Effect of annealing temperature on titania thin films prepared by spin coating”, Journal of Sol-Gel Science and Technology (2010) 55:328–334.

[42]. K.-N.P. Kumar, “Nanostructured ceramic membranes”, PhD Thesis, University of Twente,1993, pp 96-99.

[43]. G.W. Scherer, “Sintering of sol-gel films”, Journal of Sol-Gel. Sci. Tech. 8 (1997) 353-363.

[44]. Tim Van Gestel, Carlo Vandecasteele, “Alumina and titania multilayer membranes for nanofiltration: preparation, characterization and chemical stability”, Journal of Membrane Science 207 (2002) 73–89.

[45]. P. Puhlfürß, A. Voigt, R. Weber, M. Morbé, “Microporous TiO2 membranes with a cut off <500 Da”, J. Membr. Sci. 174, 1 (2000) 123-133.

[46]. Ali Alem, Hossein Sarpoolaky, “Sol–gel preparation of titania multilayer membrane for photocatalytic applications”, Ceramics International, Volume 35-2009, Pages 1837-1843.

[47]. N. Agoudjil, T. Benkacem, “Synthesis of porous titanium dioxide membranes”, Desalination, 206 (2007) 531–537.

[48]. Neeranut K., Santi Kulprathipanja “Synthesis of NaA Zeolite Membranes: Comparative Study of Microwave, Autoclave, and Electrophoretic Techniques”,Thailand-2008.

[49]. C. Baerlocher, L.B. McCusker, and D.H. Olson., "Atlas of Zeolite Framework Types. Elsevier, 6th revised edition, 2007.

[50]. Maesen, T. , Jiří Čejka, Herman van Bekkum, Avelino Corma (2007). The zeolite scene–An Overview, in: Introduction to zeolite science and practice, (Ed.), (1- 9), Elsevier, Hungary.

[51]. Santi Kulprathipanja, "Zeolites in Industrial Separation and Catalysis", Wiley,2010.

[52]. J.D. Sherman, "Synthetic zeolites and other microporous oxide molecular sieves", Proceedings of the National Academy of Sciences of the United States of America, 96(7):3471–3478, 1999.

[53]. J. van den Bergh,W. Zhu, J. Groen, F. Kapteijn, "Natural gas purification with a DDR zeolite membrane, permeation modelling withMaxwell- Stefan equations", Studies in Surface Science and Catalysis, 170A:1021–1027, 2007.

[54]. J. Coronas and J. Santamaria, "State-of-the-art in zeolite membrane reactors. Topics in Catalysis", 29(1-2): 29–44, 2004.

[55]. Liangxiong Li, Ning Liu, "Enhanced Water Permeation of Reverse Osmosis through MFI-Type Zeolite Membranes with High Aluminum Contents", Ind. Eng. Chem. Res. 2007, 46, 1584 1589.

[56]. Wei Liu , "High Surface Area Inorganic Membrane Module", Pacific Northwest National Laboratory, Richland, WA 99352.

[57]. Jelan Kuhn, “Zeolite Membranes:Ozone Detemplation, Modeling, and Performance Characterization”, PhD thesis, Delft University of Technology, the Netherlands, May 2009.

[58]. Colin S. Cundy, Paul A. Cox, “The hydrothermal synthesis of zeolites: Precursors, intermediates and reaction mechanism”, Microporous and Mesoporous Materials, 82 (2005) 1–78.

[59]. Chu, P.; Dwyer, F. G. & Vartuli, J. C. (1998) “Crystallization method employing microwave radiation”, US Patent, 4778666, (October 1988).

[60]. Zhi Lin cheng, Zi Sheng chao, Hui Lin wan,“Synthesis of Compact NaA Zeolite Membrane by Microwave Heating Method”, Chinese Chemical Letters, Vol. 14, No. 8, pp 874 – 877, 2003.

[61]. Zhi-Lin Cheng, Zan Liu, “Microwave-heating Synthesis and Gas Separation Performance of NaA Zeolite Membrane”, Chinese Journal of Chemistry Volume 23, Issue 1, pages 28–31, January, 2005.

[62]. Srinivasan, A. & Grutzeck, M. W, “The adsorption of SO_2 by zeolites synthesized from fly ash”, Environmental Science & Technology, 33, 9, (May 1999) 1464-1469, 0013-936X.

[63]. Panzarella, B.; Tompsett, G, “In Situ SAXS/WAXS of zeolite microwave synthesis: NaY, NaA, and Beta zeolites”, Chem.phys. , 8, 3, (February 2007) 357-369, 1439-4235

[64]. Ann elezabeth taylor, “Microwave synthesis and occlusion reactions of zeolites”, PhD thesis, University of Birmingham, 2007.

[65]. A. Arafat, “Microwave preparation of zeolite Y and ZSM-5”, Zeolites Volume 13, Issue 3, March 1993, Pages 162-165.

[66]. Cundy, C. S., “Microwave techniques in the synthesis and modification of zeolite catalysts: A review”, Collection of Czechoslovak Chemical Communications, 63, 11, (November 1998) 1699-1723, 0010-0765.

[67]. Yanshuo Li , Hongliang Chen, “Microwave synthesis of LTA zeolite membranes without seeding”, Journal of Membrane Science 277 (2006) 230–239.

[68]. Aisheng Huang, and Jürgen ,“Application of Microwave Heating on the Facile Synthesis of Porous Molecular Sieve Membranes”, Institute of Physical Chemistry and Electrochemistry, Leibniz University of Hannover, Germany.

[69]. Van den Berg a, L. Gora a, J.C. Jansen, “Zeolite A membranes synthesized on a UV-irradiated TiO2 coated metal support: the high pervaporation performance”, Journal of Membrane Science 224 (2003) 29–37.

[70]. Nandini Das, Debtosh Kundu, Minati Chatterjee, “The effect of intermediate layer on synthesis and gas permeation properties of NaA zeolite membrane”, J. Coat. Technol. Res., 7 (3) 383–390, 2010.

[71]. W.S. Yang, X.C. Xu, J. Liu, L.W. Lin, “Synthesis of zeolite membranes by microwave heating”, CN, Patent, B01D 71/02, C01B 39/00.

[72]. Yanshuo Li, Weishen Yang,“Microwave synthesis of zeolite membranes: A review”, Journal of Membrane Science 316 (2008) 3–17.

[73]. Kourosh Kalantar-zadeh, B.F., Nanotechnology-Enabled Sensor: Springer; 1 edition (October 31, 2007).

[74]. David C. Cranmer, "Mechanical testing methodology for ceramic design and reliability", Published by CRC Press; 1 edition (February 1, 1998).

[75]. M. Abdul Hamid, “Preparation of TiO2 thin film by sol-gel dip coating method”, Malaysian Journal of Chemistry, 2003, 086-091.

[76]. Paul A.Webb,"An introduction to physical characterization of materials by mercury intrusion porosimetry with emphasis on reduction and presentation of experimental data", Micromeritics Instrument Corp, Georgia, January 2001.

[77]. William D. Callister, Jr. "Materials science and engineering an introduction" Seventh ed., John Wiley & Sons, Inc., New York, 2007.

Vita

Name: Mirza Aqeel Baig

Nationality: Indian

Present address: P.O. Box: 8577, King Fahd University of Petroleum and Minerals, Dhahran 31261, Kingdom of Saudi Arabia.

Telephone: 009665-3585-2292 (Present)

Education: Received Bachelor of Technology degree in Mechanical Engineering from Jawaharlal Nehru Technological University, Hyderabad, India in 2008.

Joined Mechanical Engineering Department of King Fahd University of Petroleum and Minerals, Dhahran as Research Assistant in February 2009.

E-mail: mirzaaqeel15@gmail.com, mirza_aqeel15@yahoo.co.in